Modifying Acetylation in Skeletal Muscle to Improve Health- and Life- Span

By

SURAJ J. PATHAK
DISSERTATION

Submitted in partial satisfaction of the requirements for the degree of

Doctor of Philosophy

in

Molecular, Cellular, and Integrative Physiology

in the

OFFICE OF GRADUATE STUDIES

of the

UNIVERSITY OF CALIFORNIA

DAVIS

Approved:

Keith Baar

Karen Ryan

Jon Ramsey

Committee in Charge

2023

Declaration

I declare that this thesis is my own unaided work. It is being submitted for the degree of Doctor of Philosophy at the University of California, Davis.

It has not been submitted for any degree or examination at any another University.

Acknowledgements

First and foremost, I would like to thank my entire family for always believing in me and supporting me. To my mother and father for sacrificing so much to provide me with the privileges I possess today—a position I will never take for granted. To my brother Sagar, who has been my best friend and role model since I was young enough to retain memories, for being my biggest supporter, always being there for me, and reminding me that “champions keep playing until they get it right.” To my sister-in-law Saloni, for showing me the importance of being compassionate towards others—something you do every day, and something I try to embody. To my four-legged son, Almo, for pulling me away from work and reminding me to enjoy the simple pleasures we so often take for granted. And to my four-legged sister Winter, for being a constant reminder that those you love will always walk alongside you.

Secondly, to all my cousins that taught me to find happiness no matter the circumstance and for their unwavering love and support. The fellas in TCD, for being the family that I chose, checking in on me, and for dealing with me—which is no small task. To all of my lab mates and The Bin, for making the work environment more enjoyable than I could have ever imagined and keeping a smile on my face. And to all of the undergraduate students that helped me with data collection, and to whom I had the pleasure of mentoring, it was and always will be my pleasure to have been a part of your journey.

Lastly, thanks to all of my mentors; my past, present, and future accomplishments would be unachievable without you. To my major professor, Dr. Keith Baar, for trusting me to join his lab, always treating his students as equals, for being a friend, and embodying his motto of “performing world class research in a family environment.” To Dr. Jon Ramsey and his entire team for helping me out more times than I can count, and for being among the best people I have ever had the pleasure of knowing. And Dr. Karen Ryan, for making it a priority to go over

this body of work, providing crucial feedback, and playing an essential role in getting this dissertation across the finish line.

In totality, this work is dedicated to those that are devoted to making a difference.

Table of Contents

Abstract: Manipulating Skeletal Muscle Acetylation to Enhance Healthspan and Lifespan

Human aging is marked by a progressive loss of skeletal muscle mass and cognitive function—two primary determinants of healthspan and lifespan. Even though there are many studies characterizing this association, the mechanisms underlying this relationship remain unclear. In contrast to aging, endurance exercise has been shown to improve skeletal muscle mass and function and slow age-related cognitive decline [1,2]. Further, animals bred for low levels of physical activity show impaired muscle and neurocognitive function [3]. The main adaptations seen with endurance exercise training are heightened fat oxidation, and increased mitochondrial mass and activity downstream of a transcriptional co-factor called the peroxisome-proliferator activates receptor 1α (PGC-1α), which is regulated by acetylation [4,5]. Roberts et al (2017) demonstrated that the use of a ketogenic diet (KD), increased protein acetylation and activated PGC-1α in muscle concomitant with improved markers of skeletal muscle strength, mitochondrial mass and activity, endurance, neurocognitive function, and extended lifespan 13.6% in mice [6]. Along with enhanced healthspan and lifespan, mice on a KD demonstrated improved muscle mitochondrial biogenesis, muscle mass, and oxidative fiber cross-sectional area; all things associated with endurance exercise training [7]. However, the molecular mechanisms underlying the benefits seen with increases in either exercise or a KD on skeletal muscle and neurocognitive function remains largely unexplored. Our global hypothesis for this body of work was that increasing protein acetylation plays a central role in improving skeletal muscle mass and function, mitochondrial biogenesis, and neurocognitive function. In the present work, we identify novel mechanisms that underlie the ability of skeletal muscle to

increase muscle mass and function and describe the role of skeletal muscle mitochondria in augmenting cognitive performance in response to manipulation of acetylation either through natural compounds, pharmaceuticals, or a KD. Our approach to understand how acetylation both with and without a KD enhances healthspan, and lifespan was 4-fold: 1) Determine the effect of a cocktail of natural products, selected to inhibit the NAD-dependent deacetylase Sirtuin 1 (SIRT1) in rats following ablation of the gastrocnemius and soleus muscles (Functional Overload—FO), on the resulting increase in plantaris muscle fiber cross sectional area, 2) Establish how the class II histone deacetylase (HDAC) inhibitor, scriptaid, affects skeletal muscle and neurocognitive function, and 3) Determine whether a 2-month KD alters skeletal muscle function, mitochondrial mass, and cognitive behavior in middle-aged female mice,

Muscle mass and strength are important aspects of human health. Low levels of muscle mass and strength are directly correlated with lifespan. In Chapter 2, we optimized a cocktail of naturally occurring compounds (epicatechin, epicatechin-gallate, and celestrol) that were believed to inhibit sirtuin 1. This work shows that optimal inhibition of SIRT1 increases global protein acetylation (Figure 2.3C), and the increase in fiber cross sectional area (fCSA) in response to FO 61.5% more than vehicle dosed counterparts (Figure 2.2H). One proposed limit to skeletal muscle hypertrophy in both mice and man is the capacity for protein synthesis (i.e., ribosome mass)[8–10]. In response to an optimal dose of the SIRT1 inhibitor cocktail, ribosomal RNA (which comprises ~80% of the total RNA) relative to muscle mass decreased in the optimal group (Figure 2.4B). This was supported by lower markers of ribosome biogenesis (ITS1 and 5’ETS RNA levels) indicating that the benefit of the cocktail is not the result of increased

translational machinery (Figure 2.4C&D). One possible explanation for the apparent increase in hypertrophy could be an increase in translational efficiency secondary to acetylation of ribosomes [11]. In support of this, immunoprecipitation of ribosomal subunits showed greater associated acetylated lysine levels in the optimal group when compared to control animals (Figure 2.6A-C).

Though a long term KD has been shown to help maintain oxidative fCSA and improve muscle and cognitive metrics, there is still uncertainty surrounding the mechanism underlying the changes caused by a KD [6,7]. To address this gap in knowledge, in Chapter 3 we employed an isocaloric (11.2 kcal/day) KD in 23-month-old mice (Table 3.2) together with concomitant injection of either the class II HDAC inhibitor scriptaid (SCRIPT) or a vehicle (VEH) control. Our findings demonstrated that a one-month KD intervention increases mitochondrial mass (Figure 3.2D) and improved grip strength (Figure 3.1G) in skeletal muscle preferentially while not affecting fCSA (Figure 3.4A&B). As an explanation for the significant improvement on grip strength in the KD fed animals, we are the first to report that an acute KD increases dystrophin protein levels (Figure 3.4F). These data indicate that KD muscle is better able to laterally transmit force and prevent contraction induced muscle damage than their CD fed counterparts. To understand to what degree a short-term KD started late in life influences cognitive behavior the Y-Maze, Novel Object Recognition, and Open Field assays were conducted (Figure 3.1H, 3.1J&K). We report no changes between the CD and KD fed animals. These findings indicate that an acute KD first effects skeletal muscle biochemistry and functionality prior to that of neurocognitive function. Interestingly, all of the biochemical and functional benefits seen with an acute KD were

blunted when paired with SCRIPT treatment. This blunting of adaptation coincides with KD SCRIPT animals' inability to produce adequate ketones in the fasted state. This finding implies that ketone production may be a crucial component of maintaining skeletal muscle adaptation and functionality in aged female mice.

Even though positive effects of a KD had been demonstrated in old and diseased male mice, whether the diet could benefit females was uncertain. To test the hypothesis that female mice would thrive on a KD, in Chapter 4 middle-aged female mice were put on a two-month isocaloric KD (Table 4.1) and upon collection, skeletal muscle and liver mitochondrial mass and biogenesis, cognitive function, and serum were analyzed. Our results show that a two-month KD is sufficient to improve mitochondrial mass (Figure 4.4A) and PGC-1α protein level in the total and nuclear muscle fractions (Figure 4.4C&E) of skeletal muscle. PGC-1α being responsible for the expression of kynurenine aminotransferases (KAT) in muscle [12], enzymes that convert a potential neurotoxin kynurenine (KYN) into kynurenic acid (KYNA) that cannot enter the brain, therefore we measured KAT protein levels in muscle after a 2-month KD. Two KAT proteins, KAT1 and KAT4 increased in the GTN muscle (Figure 4G&I). The increase in muscle KAT proteins was associated with a significant decrease in circulating KYN and strong trend for KYNA to increase (Figure 4F&G). The increase in KAT protein and decrease in circulating KYN were associated with improvements in Barnes maze and rearing assays, indicating greater spatial learning and memory capacity along with decreased anxiousness (Figure 4J&K). We are the first to propose a mechanism that connects muscle metabolism to brain function in response to a dietary intervention.

Within this dissertation, I discuss mechanisms whereby altering acetylation in skeletal muscle improves translational efficiency resulting in greater load-induced skeletal muscle hypertrophy; however, acetylation is not sufficient to induce mitochondrial biogenesis or improve cognitive function.

Chapter 1: An Introduction to the Effect of Ketogenic Diets on Aging Skeletal Muscle Mass and Performance

This chapter was previously published as:

Pathak, S.J., and K Baar. Ketogenic Diets and Mitochondrial Function: Benefits for Aging but not for Athletes. **Exercise and Sports Science Reviews.** 2023 Jan 1;51(1):27-33.

Abstract

As humans age, we lose skeletal muscle mass even in the absence of disease (sarcopenia) increasing the risk of death. Low mitochondrial mass and activity contributes to sarcopenia. It is our hypothesis that, a ketogenic diet improves mitochondrial mass and function when they have declined due to aging or disease, but not in athletes where mitochondrial quality is high.

Key Points

> A ketogenic diet (KD) increases longevity 13.6% in mice.

> A KD increases mitochondrial mass and activity as well as measures of muscle strength (grip force), and endurance (wire hang) in aged individuals.

> A ketogenic diet activates the peroxisome proliferator-activated receptor (PPAR) family of transcription factors resulting in an increase in the enzymes necessary to transport and oxidize fatty acids as a fuel.

> The PPARs also increase pyruvate dehydrogenase kinases that prevent carbohydrate oxidation, resulting in impaired glucose utilization and impaired elite performance.

Introduction

Humans progressively lose skeletal muscle mass with age in the absence of disease (sarcopenia). Sarcopenia increases the risk of all-cause mortality and is a reliable indicator of frailty and poor prognosis in clinical settings [13]. In 2000, it was estimated that the direct cost of sarcopenia in America was $18.5 billion annually with this number rapidly increasing [14] — highlighting the importance of maintaining muscle mass as we age. This loss of muscle mass with advancing age is accompanied by a preferential loss of type IIa fiber area when compared to type I and type IIb fiber types [15]. This is an important distinction as type IIa fibers produce greater force over time, and strength is the main component in predicting all-cause mortality [16]. One way to ensure the preservation of skeletal muscle mass and strength with age is exercise; however, many are unable or unwilling to exercise at the intensity needed to achieve the physiological adaptations needed to maintain an enriched quality of life.

One of many physiological factors that can initiate or accentuate sarcopenia is a decline in mitochondrial mass and/or activity within skeletal muscle [17]. Beyond sarcopenia, mitochondrial health plays a role in a variety of skeletal muscle-based diseases. One of the major consequences of aging is a decline in mitochondrial bioenergetics, independent of changes in fat free mass [18]. Studies using muscle biopsies from young healthy individuals show an age related decline in mitochondrial mass, O_2 consumption, mitochondrial quality control, and oxidative phosphorylation (OxPhos) activity [19–22]. These data suggest that the age-related changes in mitochondrial function are due to a decrease in both the quantity and quality of the mitochondria. Therefore, it is paramount to maintain mitochondrial health and activity as we age. In 2017, Roberts and

colleagues studied the effect of a ketogenic diet (KD) on lifespan and health span [6]; specifically measuring muscle and brain function in mice as a function of age and diet. In this context, a KD increased lifespan 13.6% with a concomitant increase in skeletal muscle mitochondrial mass and enzyme activity, as well as measures of muscle strength (grip strength) and endurance (4-limb wire hang). As in mice, a KD in humans increases mitochondrial function [23], suggesting that the metabolic shift required during a KD drives an increase in mitochondrial mass and function in skeletal muscle.

Since oxidative energy production (mitochondrial mass) is key to VO_{2max} and endurance performance, high fat diets have been proposed as a tool to increase athletic performance. However, the improved muscle function in old animals on a KD has not translated into improved performance for elite athletes. In fact, numerous studies have shown that there is either no benefit or possibly an impairment of elite performance on a KD.

It is our working hypothesis that a ketogenic diet improves mitochondrial mass and function only when mitochondrial quality has declined due to aging or disease, but in athletes where mitochondrial quality is already high a ketogenic diet does not improve mitochondrial mass and activity further. In this chapter, I discuss the evidence for and against this hypothesis and how these effects of a ketogenic diet (KD) are mediated at a molecular level.

Effect of KD on Skeletal Muscle:

Metabolism

Production of ketone bodies such as acetoacetate (AcAc) and β-hydroxybutyrate (βHB), via ketogenesis in the liver is an evolutionary conserved process that plays a significant

role in mammalian survival under the stress of limited food availability. Ketones bodies (KBs) are lipid derived molecules that are primarily produced in the liver in response to a scarcity of glucose. In response to a KD, fasting, or prolonged physical exercise, ketone bodies are distributed to skeletal muscle which, on average, comprises 41.3% and 33.1% of body mass in adult men and women, respectively [24]. Ketone bodies, namely βHB, are imported into skeletal muscle mitochondria via monocarboxylate transporters (MCT), and oxidized into AcAc via D-β-hydroxybutyrate dehydrogenase (BDH) rapidly generating two molecules of acetyl-CoA [25]. Together with the increase in βHB, skeletal muscle also becomes more reliant on fatty acids in the generation of ATP, resulting in a dramatic shift in metabolism (Figure 1.1).

A consequence of a KD, the production of ketones via ketolysis in the liver, and the rapid generation of acetyl-CoA is an abundance of intracellular acetyl-CoA. The increase in acetyl-CoA likely explains the rapid increase in acetylated lysine levels seen upon diet administration [6]. Acetylation is a post translational modification that affects both histones and other cellular proteins. Acetylation of histones removes the positive charge inherent in lysine residues diminishing the electrostatic affinity between histone proteins and DNA; promoting a more open chromatin structure that is permissive to gene transcription [26–28]. Acetylation of other cellular proteins alters their stability, activity, localization within the cell, and affinity to binding partners [4] in a way that mimics the effect of phosphorylation. Similar to a KD, an Increase in protein acetylation is seen following exercise [29,30] – another stimulus that increases fat oxidation [31], and mitochondrial mass and activity [32]. However, the relationship between acetylation and

increases in mitochondrial biogenesis and activity in skeletal muscle remains largely unexplored.

A diet low in carbohydrates (CHOs) that does not produce ketosis, or a strict ketogenic diet, results in fat adaptation and together with elevated levels of acetyl-CoA leads to greater activity of the peroxisome proliferator-activated receptor (PPAR) family of transcription factors. Higher PPAR activity increases key enzymes of fat oxidation [7,33,34] such as lipoprotein lipase (LPL), fatty acid binding protein (FABP), cluster of differentiation 36 (CD36) and stearoyl-Coenzyme A desaturase (SCD)-1 [35,36]. This stimulation of fatty acid oxidation through PPAR upregulation comes at the expense of glucose oxidation. PPAR∂, the most active PPAR isoform in skeletal muscle [37,38], also increases pyruvate dehydrogenase kinase-4 (PDK4) expression. PDK4 serves to inactivate pyruvate dehydrogenase (PDH), a key enzyme in the conversion of pyruvate into acetyl-CoA during entry into the mitochondria to compensate for the increased acetyl-CoA coming from fatty acid oxidation and βHB [39]. Stellingwerff and colleagues showed that individuals cycling at 70% of VO_{2max} in a fat adapted state showed significantly lower PDH activity and a concomitant increase in fat oxidation during exercise [40]. Thus, elevated free fatty acid oxidation is driven by an increase in PPARs activity that upregulates fatty acid transport and oxidation enzymes and decreases the oxidation of CHO resulting in a shift to fat as the primary fuel in skeletal muscle (Figure 1.1).

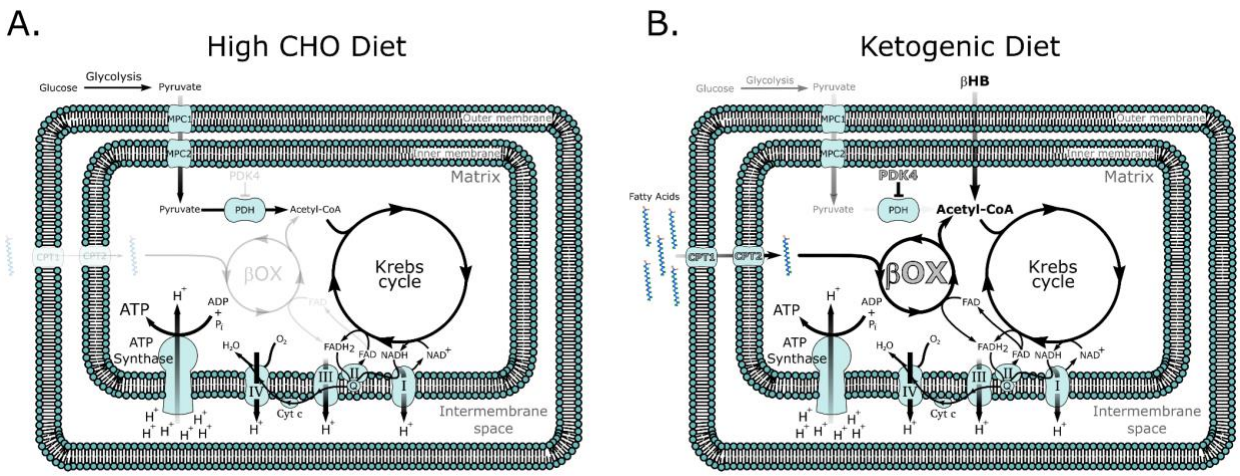

Collectively, a KD increases levels of circulating fatty acids and KBs resulting in an increase in fat oxidation, acetyl-CoA generation, and acetylated lysine levels. With this shift in metabolism there is a beneficial effect on transcriptional availability of DNA, stability/localization/affinity of cellular proteins, and PPAR activity.

Mitochondria Mass and Function

As previously mentioned there is a growing amount of evidence suggesting a KD is able to increase mitochondrial biogenesis and activity within skeletal muscle, resulting in greater muscle function with age [6,7]. A KD increases the expression of the master mitochondrial biogenesis regulator PGC-1α (peroxisome proliferator activated receptor gamma) and proteins from each complex of the ETC [7]. Interestingly, markers of mitochondrial mass and enzymatic activity increase in a tissue specific manner with only skeletal muscle showing a significantly greater mitochondrial:nuclear DNA (mtDNA:nDNA) ratio and improved complex I and IV activity when compared to their control diet fed counterparts, even after 14 months on diet. By contrast, brain and liver tissue showed no change or a decrease in mtDNA:nDNA ratio and limited improvements in activity [41]. The increase in muscle mitochondrial mass and activity

upon adoption of a KD occurs concomitantly with elevated levels of acetylated lysine protein levels. Manipulating acetylation in muscle using the histone deacetylase (HDAC) inhibitor, scriptaid, can also increase mitochondrial mass, lipid oxidation, and fatigue resistance [42]. Having established in the previous section that a similar physiological response is seen following exercise, the increase in mitochondrial biogenesis in muscle observed with a KD may result from the activation of MEF2, a vital transcription factor in the control of PGC-1α expression, and specifically increased transcription of the exercise-inducible form of PGC-1α, PGC-1α2/3 [43]. In C2C12 cells, dosing with 5mM of AcAc resulted in an ~4-fold increase in MEF2A binding capacity to transcriptional promoter regions [44]. HDAC acetylation and activation of MEF2 could also be a direct effect of the primary ketone, βHB [45]. Though the mechanism of action of βHB's inhibition of class I HDACs has yet to be confirmed, the proposed mechanism of action is via competitive inhibition of HDAC catalytic sites. For the structurally similar butyrate, which differs from βHB only by its 3'carbon oxidation state, the carboxylic acid group binds to the catalytic zinc at the bottom of the HDACs active site effectively suppressing it's activity [46]. Additionally, upon increased fat oxidation in response to a KD, a rise in the phosphorylation of AMP-activated protein kinase at the threonine 172 ($AMPK^{Thr172}$) site is observed [47,48]. $AMPK^{Thr172}$ is then free to phosphorylate HDACs promoting the release of MEF2 and an increase in PGC-1α2/3 expression [49]. Further, acetoacetate increases p38 mitogen activated protein kinase (p38 MAPK) activity [50]. When activated, p38 MAPK phosphorylates and activates PGC-1α protein [51] and promotes PGC1α2/3 expression through its target protein ATF2 (activating transcription factor 2). Lastly, the tumor suppressor p53 is a regulator of mitochondrial integrity, function, content, and

biogenesis [52–57]. Interestingly, acetylation of p53, which rises ~10-fold on the KD [6], is fundamental for its activity, complex assembly and thereby, its cellular responses [58]. Specifically, p53 is colocalized to the mitochondria where it acts to stabilize mtDNA expression preventing DNA damage [59]—a hallmark of aging [60]. When p53 is knocked out, there is a significant decline in mitochondrial content, mitochondrial aerobic capacity, and mtDNA depletion [54,61]. Within the nuclear genome, p53 encourages mitochondrial biogenesis via upregulation of mitochondrial transcription factor A (Tfam), nuclear respiratory factor-1 (NRF1) and cytochrome C oxidase [57,62–64]. However, it is important to note that there have been contrasting reports of p53 and its influence on mitochondrial content and enzymatic activity. Specifically, in 2017 Stocks and colleagues used a muscle specific KO of p53 to show that p53 was not required for mitochondrial biogenesis, morphology, or enzymatic activity [65]. These data suggest that a KD has multiple, possibly redundant ways, through which it can increase mitochondrial mass and activity in skeletal muscle.

Within the realm of mitochondrial quality control, there is still much to be investigated concerning the effect of a KD on skeletal muscle. A progressive decline in muscle function and quality is hypothesized to result from an accumulation of damaged or dysfunctional mitochondria [66]. The accumulation of damaged or dysfunctional mitochondria is prevented through mitochondrial-specific autophagy (mitophagy). Since mitophagy is increased when AMPK is activated [67] and mTORC1 (mechanistic target of rapamycin complex 1) activity is inhibited [68], exactly what is observed in muscle during a KD, there is strong support for the hypothesis that KD increases mitophagy in skeletal muscle. However, to date there is little published evidence showing the effects of a KD

on in skeletal muscle mitophagy. Understanding how this important aspect of mitochondrial quality control is modulated in response to a KD will provide key insight to the field.

In order to maintain a healthy mitochondrial network and population, mitochondria must also undergo continuous cycles of fission and fusion [69].Though exercise can promote mitochondrial fission and fusion [70] there is limited evidence in the literature as to whether a KD might cause similar effects. In 2012, Sebastián and colleagues demonstrated that expression of mitochondrial fusion protein 2, Mitofusin 2 (Mfn2) was required for adaptation to a high fat diet [71]. Subsequently in 2015, Mishra and colleagues showed that mitochondrial dynamics were regulated in a fiber type specific manner; with type IIa fibers requiring both Mitofusin1 (Mfn1) and Mitofusin2 (Mfn2) for mitochondrial elongation and fusion [72]. With a preferential preservation of type IIa fibers on a KD [7], this preservation may play a crucial role in the maintenance of healthy skeletal muscle mitochondria. In cultured cells, βHB stimulates mitochondrial elongation [73] and dampens irregularities in mitochondrial morphology in skeletal muscle [74]. Together, these data indicate that in response to a KD there is an increase in fatty acid mobilization, mitochondrial biogenesis and activity that is accompanied by improved mitochondrial dynamics in skeletal muscle.

Muscle Mass, Function, and Fiber Type

The importance of maintaining skeletal muscle mass and function through age is paramount since it is a strong predictor of mortality, and of our ability to respond/receive/tolerate disease burden or standard of care therapies [75]. Nakao and colleagues suggested that a KD can induce severe skeletal muscle atrophy in female mice [76]. However, it is important to note that the KD feed used in this study was likely completely unpalatable and led to starvation in their cohort. When a palatable KD has been used, muscle mass and function are preserved or improved depending on the length of the study [6,41,77]. In our hands, we have demonstrated that a KD results in a protective effect on skeletal muscle in an aged mouse model and significantly increases its performance on measures of strength (grip strength) and endurance (4-limb wire hang) when compared to their control diet fed counterparts [6]. One reason for this is the preservation of type IIa (fast-oxidative) fibers at the expense of IIb (fast-glycolytic) fibers (Figure 1.2). This shift in fiber type has been theorized to take place due to: 1) the shift in metabolism leading to a preferential atrophy of fibers that can't generate sufficient energy aerobically (IIb (fast-glycolytic) fibers); 2) improved protein quality control; or 3) the ability of a KD to increase the rate of reinnervation through axonal sprouting of IIa nerves, since reinnervation normally diminishes with aging [78]. The preservation of type IIa fibers with a KD is important since type IIa fibers are preferentially lost with advanced age resulting in the loss of skeletal muscle mass and function in humans [79]. Beyond aging, in a rat model of Duchenne's muscular dystrophy (DMD) a medium chain triglyceride based ketogenic diet showed impressive benefits in skeletal muscle quality, mass, and grip strength [77]. A possible explanation for these beneficial changes in

muscle function is the ~6-fold increase in acetylation of histone acetyltransferase p300 in KD fed mice [6]. Acetylation of p300 on the 17 lysine residues within its regulatory domain stimulates acetyltransferase activity and interaction with other proteins [80–82]. A skeletal muscle-specific knockout of p300 results in rapid decreases grip strength and rotarod performance leading to death, even with minimal changes in fiber cross sectional area CSA [83]. making p300 an attractive candidate for future studies regarding the KD and muscle function.

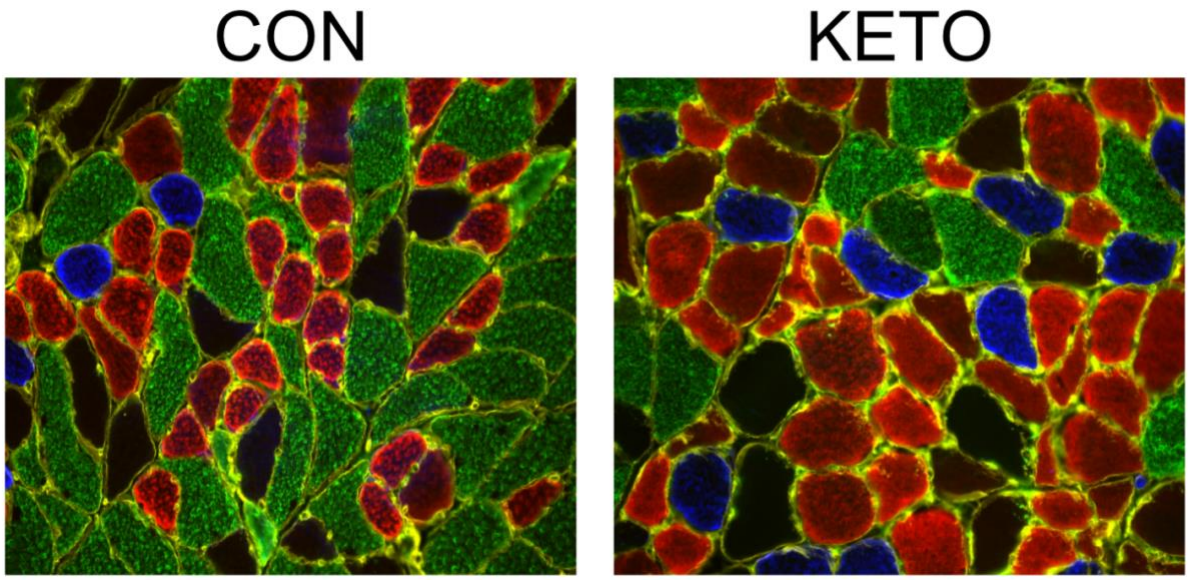

The cellular basis for changes in muscle fiber cross-sectional area is a shift in balance between muscle protein synthesis and muscle protein breakdown. A KD does little to alter the increase skeletal muscle mass in response to resistance exercise [84,85]. This can potentially be explained by a KD causing a decrease in myofibrillar fractional synthetic rates [7]. The impaired rate of protein synthesis can be explained, in part by a ~3-fold increase in phosphorylation of eIF2α^{ser51}, which over 30 years ago was shown to

inhibit the initiation of translation [86]. This decrease in translation initiation would be expected to dramatically slow protein synthesis rates which, while bad for muscle hypertrophy, could promote better protein quality control, decreasing misfolding and ER stress. It is also possible that the decrease in translation initiation can be partially overcome by an increase in acetylation of the ribosome. Acetylation of ribosomes effectively stabilizes them, increasing their translational efficiency and creating better quality control of protein as has been shown to be true in rat liver [11].

Since muscle mass reflects the balance between myofibrillar protein synthesis and degradation it is also important to understand how a KD affects breakdown. In 2018, Thomsen and colleagues demonstrated that βHB induces anticatabolic effects during LPS induced weight loss resulting in a 70% reduction in phenylalanine efflux from muscle in 10 healthy men [87]. This, coupled with blunted proteosome activity seen on a KD [7] suggests that there is less protein degradation in muscle on a KD. However, in our studies the decrease in degradation on a KD is only observed in older animals, suggesting that a KD may have a bigger effect on degradation when breakdown is increased by age or disease rather than in young healthy muscle.

Altogether, a KD presents a promising strategy to mitigate the age- or disease-related decline in skeletal muscle mass and function through the preservation of type IIa fibers, increased quality control of protein synthesis, and its anticatabolic effects.

Effect of KD on Elite Athletic Performance

As described above, a KD can improve muscle size, strength, and mitochondrial mass and activity. Since muscle strength and endurance are an essential component of athletic performance, many athletes, coaches, and sports scientists have hypothesized

that a KD would increase performance. However, the data to date indicates that there is either no additional benefit or an impairment in elite performance when athletes train on a KD [88–92]. Chief among these studies are Prof. Burke and colleague's Supernova studies that demonstrated that a KD impairs elite athletic performance. In this outstanding series of studies, the authors found an 8.5% decrease in race walking performance and impaired markers of bone health in elite race walkers [91,93]. To put this into perspective, an 8.5% reduction in performance in the 2020 Olympic 20km or 50km race walk final would result in a last place finish when compared to the top time. These performance deficiencies can be explained by the long-standing concept of substrate utilization in response to varying degrees of exercise intensity [94]. The most likely mechanism for this decrease in performance is the decrease in PDH activity following fat adaptation [40]. As discussed above, fat adaptation, or a long term KD, leads to the activation of PPARs and the subsequent increase in PDK4 [39]. The rise in PDK4 results in the phosphorylation and inhibition of PDH, decreasing the capacity to oxidize CHO and increasing the reliance on fat as a fuel. The generation of ATP from fat oxidation normally declines as exercise intensity increases [94] and this has been attributed to the inability to efficiently transport fatty acids into the mitochondria during higher levels of exercise intensity (greater than ~65% VO_{2max}) [95,96]. Even if fatty acid transport was not limiting, athletes on a KD would require significantly more oxygen to perform at the same amount of work when compared with athletes on a carbohydrate based diet [91]. Since economy, the volume of oxygen needed to maintain a specific power or speed, is directly related to performance, this would suggest that a KD would limit high end performance. However, this is not to say that a KD cannot be useful to the elite athletic

population. There have been reports that submaximal exercise performance (<60% VO_2 max) can be improved in runners on a KD [97]. Separately, semi-professional soccer players that adhered to a 30-day KD, benefited from significant decrease in body fat, visceral adipose tissue and waist circumference, without changes in muscle strength [98]. This implies that, athletes that would like to lose weight without losing muscle strength may benefit from adopting a KD during the offseason to improve lean mass:body weight ratio.

Another rapidly developing area is the use of ketone esters (KE) such as 1,3-butanediol acetoacetate diester, (*R*)-3-hydroxybutyl (*R*)-3-hydroxybutyl, (*R*)-1,3-hydroxybutyl (*R*)-3-hydroxybutyrate and ketone salts (KS) β-hydroxybutyrate-mineral salt to improve performance [99–105]. Currently, the suitability of ketone supplements for elite athletes on a high carbohydrate diet is equivocal. Cox and colleagues reported that supplementation with (*R*)-1,3-hydroxybutyl (*R*)-3-hydroxybutyrate, together with carbohydrate ingestion, increased cycling time trial performance after 1 hour of fatiguing exercise [99] while studies by Rodger et.al and Leckey et.al contradict this report [105,106]. It is important to note that the contradicting studies used a β-hydroxybutyrate-mineral salt and 1,3-butanediol acetoacetate diester, respectively. This indicates that different forms of dietary ketones may modulate the effectiveness of KEs, and this is an area of study that has yet to be properly explored.

Conclusion

With limited strategies to mitigate the age-related loss of skeletal muscle, a ketogenic diet and its concomitant increase in fatty acid uptake and oxidation and acetylation levels remains an exciting area of research. With the ability to maintain muscle mass

and function together with increased mitochondrial biogenesis and quality control as we age, it will be important to elucidate further the mechanisms of action driving these beneficial changes. Since the behavioral change necessitated by a KD is significant, the role of other agents (KEs or HDAC inhibitors) that can mimic a KD without the need for drastic changes in behavior must also be explored. However, even though it is already clear that KDs have been successful at improving muscle size and function in disease and aging animal models, a KD fails to improve elite athletic performance likely because the key molecular change that underlies the health benefits (PPAR activation) is the same thing that decreases performance. Until this paradox is addressed, we are unlikely to see KDs in elite athletes during competition.

Figure Legends

Figure 1.1. Mitochondrial metabolism on (A) a high carbohydrate (CHO) versus (B) a ketogenic diet**.** Note that on a high CHO diet acetyl-CoA is primarily synthesized from pyruvate generated from the breakdown of glucose in the cytoplasm. By contrast, on a ketogenic diet β-hydroxybutyrate (βHB) can directly enter the mitochondria and be converted into acetyl-CoA. The increased oxidation of fatty acids also activates PPAR transcription factors resulting in the upregulation (in grey with black outline) of key PPAR target genes such as fatty acid transporters (carnitine palmitoyl transferase (CPT)1 and 2), enzymes of β-oxidation, as well as pyruvate dehydrogenase kinase (PDK) 4, driving fatty acid oxidation and inhibiting CHO oxidation, respectively.

Figure 1.2. Skeletal muscle morphology in mice following 14 months on a control (CON) or ketogenic (KETO) diet. Muscle sections from 26-month-old mice were stained for type I (blue), IIa (red), Iix (black), and Iib (green) myosin heavy chain. Note the increase in oxidative (blue and red) fiber number and size and the concomitant decrease in glycolytic (green) fibers. Adapted from [7].

Chapter 2: Increasing Muscle Hypertrophy with a Natural Product Designed to Inhibit SIRT1

This chapter is currently in revision at Scientific Reports as:

Pathak, S, M. Wallace, S. Athalye, S. Schenk, H.T. Langer, and K. Baar. Increasing Muscle Hypertrophy with a Natural Product Designed to Inhibit SIRT1

Abstract

We have previously identified a series of molecular brakes that slow muscle growth. One potential molecular brake is SIRT1, which is activated by a negative caloric balance. In this work, we identified natural product inhibitors of SIRT1 and tested their effects on load-induced increases in muscle fiber cross-sectional area (fCSA) using an incomplete factorial design. Supplying varying amounts of three natural products during two-week overload resulted in increases in fCSA that varied from -2 to 113%. Using these data, we produced a model that predicted the optimal combination and concentration of each natural product and then validated this model in a separate cohort of animals. Following two-week overload, fCSA in the optimal group increased 62%, whereas in the placebo fCSA increased only 3%. The greater increase in fCSA was associated with decreased ribosomal RNA synthesis, and a trend for lower total RNA/mg muscle. Despite the lower ribosome biogenesis, the increase in protein synthesis was similar, suggesting that the natural product cocktail may be increasing ribosomal efficiency rather than capacity. These data suggest that inhibition of SIRT1, together with exercise, may be useful in increasing muscle fCSA.

Introduction

Muscle mass and strength are important aspects of human health, since the rate of mortality of individuals correlates with both low muscle mass [107] and strength [108,109]. Low muscle mass and function also limits post-surgery recovery and mobility [110], and increases the impact or risk of diseases such as diabetes, cardiovascular disease, and cancer [111]. Thus, improving muscle mass and strength is a vital part of life- and health-span (8).

Muscle mass and strength are also important components of human aesthetics and performance. Indeed, each year, tens of billions of dollars are spent on supplements that are purported to result in increases in muscle mass and strength [112]. Many of these products are of dubious scientific value, since wide scale screens for products that result in *bona fide* improvements in muscle mass and strength are rare. One clinically validated way to increase muscle mass gains as a result of training is to combine strength training with protein supplementation [113]. However, very few scientifically validated nutraceutical approaches to increase muscle mass in response to training have been reported.

Sirtuin1 (SIRT1) is an NAD^+-dependent deacetylase that is activated in muscle in response to changes in cellular energy flux. Metabolic stress during calorie restriction (6) and endurance exercise (3) are known to directly activate SIRT1. Since calorie restriction and endurance exercise are thought to slow muscle growth (1,7), we hypothesized that SIRT1 inhibits muscle growth. Protein acetylation has also been linked with muscle growth. The ribosomal S6 protein kinase (S6K1), whose

phosphorylation and activity has previously been shown to be associated with increased muscle protein synthesis and muscle hypertrophy [114], can be acetylated by the acetyl transferase p300 and deacetylated by SIRT1 [115]. Beyond S6K1, almost every protein within the ribosome has at least one acetylated lysine [116]. Given that lysine acetylation can regulate numerous aspects of cellular homeostasis beyond its well-described role in epigenetics and gene transcription, it is possible that acetylation contributes to the regulation of protein synthesis. Since loading and nutrition result in transient increases in myofibrillar protein synthesis [117,118], which is thought to play an important role in muscle growth [119], here we sought to determine whether increasing acetylation within muscle could augment the increase in muscle fiber cross-sectional area in response to a hypertrophic stimulus.

Our approach to addressing this objective to was to increase protein acetylation by reducing SIRT1 deacetylase activity. For this, we first sought to identify natural products that could inhibit SIRT1 deacetylase activity. Second, we sought to determine whether these natural products could augment muscle hypertrophy when combined in the optimal manner. Overall, our hypothesis was that a novel nutritional supplement that inhibits SIRT1 deacetylase activity could augment the increase in muscle fiber cross-sectional area in response to an overload stimulus.

Results

SIRT1 Inhibitor Screen

The high-throughput screen of 800 natural products identified 45 compounds that inhibited SIRT1 >65% at a concentration of 50μM. Of these, many showed a dose-dependent effect on SIRT1, with 35 compounds showing at least 20% inhibition at 5μM (data not shown). Of the 35 inhibitors identified, 3 were already used extensively in human foods (Table 1) and came from 3 distinct chemical classes (one each quinone-methide, polyphenol, and flavonoid). These compounds (Celastrol, Epigallocatechin-3-Monogallate, and Epicatechin Monogallate) were selected to study effects on adaptive muscle hypertrophy in rats.

Table 1. Percent inhibition of SIRT1 deacetylase activity for the 3 compounds used in current study

Compound Name	5μM	50μM	Class
Celastrol	101	100	Quinone-Methide
Epigallocatechin-3-Monogallate	72	99	Polyphenol
Epicatechin Monogallate	66	99	Flavinoid

List of specific inhibitors of SIRT1 and the percent inhibition at 5 or 50μM

DOE Model Generation

The three compounds identified above were entered into a Box-Behnken incomplete factorial design to quickly assess any interactions between the different products. Thirteen rats received different combinations of the three products (ranging from 0-2mg/kg/day epicatechin; 0-10 mg/kg/day epigallocatechin-3-gallate; and 0-500μg/kg/day celastrol), while five controls received the middle amount of each product (1mg/kg/day

epicatechin; 5mg/kg/day epigallocatechin-3-gallate; and 250μg/kg/day celastrol)to determine biological variability (Table 2).

Table 2. Inhibitor compounds and the dose used during the validation study

Compound Name	Optimal Dose	Average Dose	Least Dose
Celastrol	0.5	0.2	0.435
Epigallocatechin-3-Monogallate	20	14	6
Epicatechin Monogallate	0.7	0.7	1.3

Doses of epigallocatechin-3-monogallate and epicatechin monogallate (mg/kg/day) and celastrol (μg/kg/day) for each inhibitor cocktail used in the validation study.

Fourteen days of overload resulted in changes in muscle fiber cross-sectional area that ranged from -4.3% to 115.8% depending on the treatment (Figure 2.1A), with the controls averaging 66.8±6.9%. From these data, response surface plots indicated that the epigallocatechin-3-gallate could modulate the effect of the other two products and a model predicting the optimal combination and concentration of each product was produced (Figure 2.1B).

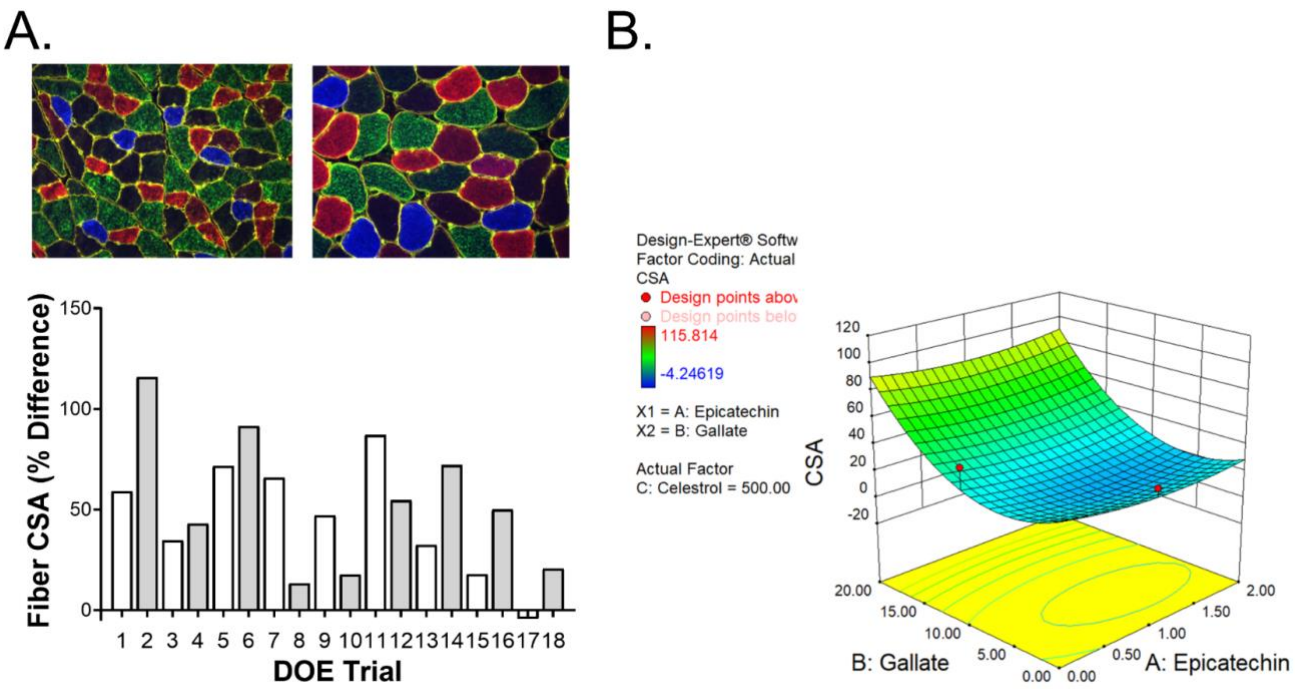

Model Validation

To validate the model, an independent group of rats underwent synergist ablation and were gavaged daily (beginning 5pm the night of surgery) with either a saline control or the predicted optimal, least effective, or a combination of the three products predicted to produce an increase in fiber CSA between the other two groups. The dose of each product for each group is outlined in Table 2. Following 14 days of overload and treatment, the animals were sacrificed, and body, heart, liver and muscle weights were determined (Figure 2.2A-D). There were no statistical differences between the untreated and treated groups for body, heart, or liver mass, suggesting that the treatment did not result in any acute toxicity. Both the moderate and optimal groups showed a significant increase in muscle mass relative to the control treated rats. Analysis of muscle fiber CSA demonstrated that the control legs showed similar distribution of fiber CSA regardless of treatment. There was a right shift in fiber CSA with overload that was greatest in the optimal group. The mean fiber CSA of the SHAM legs for all groups were 1847±114.6, 1945±132.5, 1883±114.6, and 1730±60.0 μm^2 for the control, least, moderate, and optimal groups, respectively, whereas the overloaded legs showed averages of 1901±108.3, 2348.1±172.8, 2306.5±119.7, and 2800±145.9 μm^2, for the respective groups (Figure 2.2G). To test the predictive power of the Box-Behnken model, the predicted change in fiber CSA was plotted against the measured value for each of the groups. The resulting line had an r^2 value of 0.9586 validating the ability of the model to predict changes in muscle hypertrophy (Figure 2.2H).

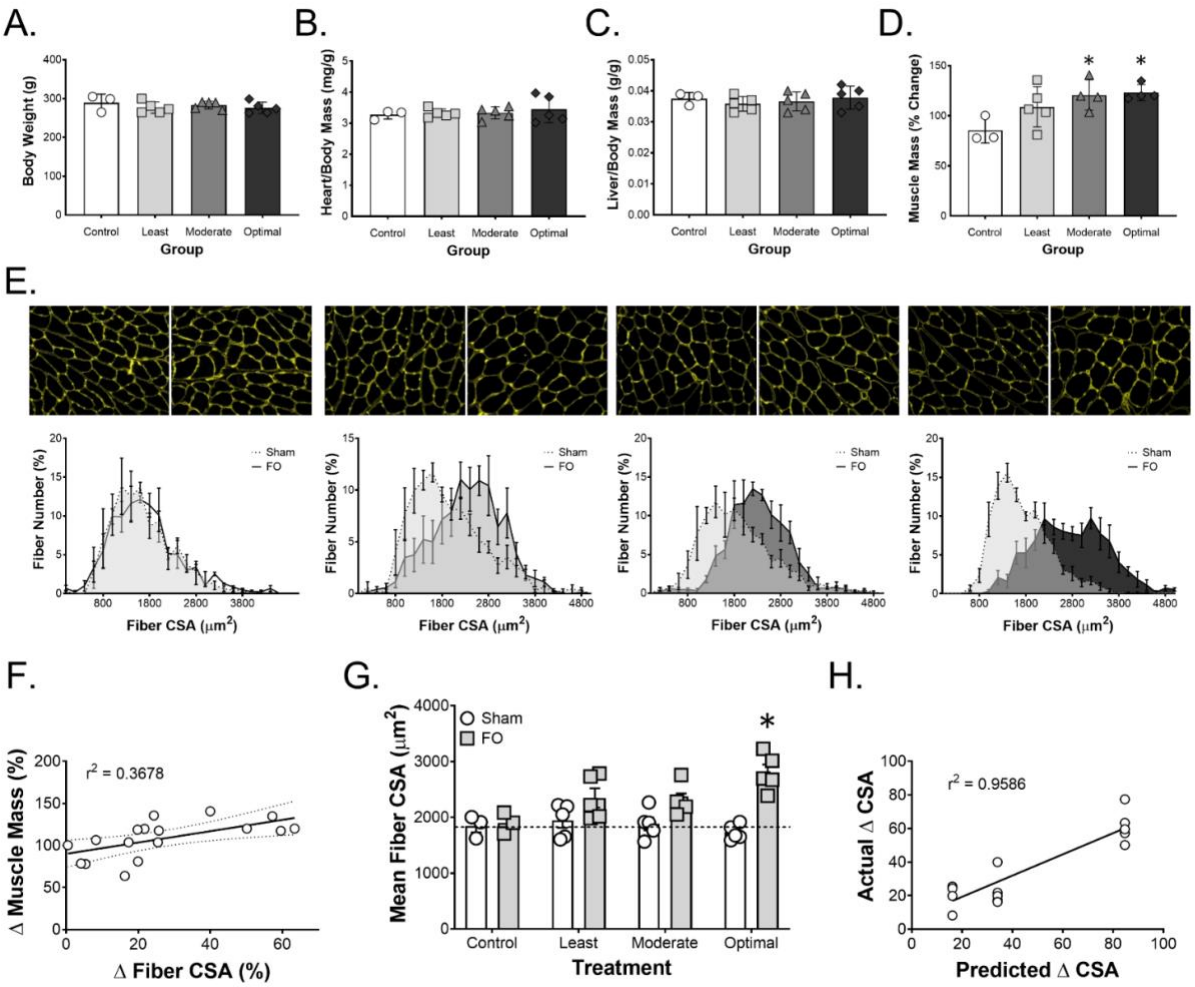

SIRT1 Levels and Activity

Since the treatment was meant to inhibit SIRT1, the levels of SIRT1 and a gauge of its enzyme activity (p53 acetylation) was determined (Figure 2.3A). As observed previously [120], the levels of SIRT1 increased significantly following overload in the control group (~2-fold) and SIRT1 levels were even higher in both the control and overloaded limbs following treatment with the SIRT1 inhibitors. As a measure of SIRT1 activity, we determined the levels of acetylation of p53 at lysine 382 (Figure 2.3B). As has been reported for other SIRT1 inhibitors [121], overload together with treatment with the natural product cocktails increased p53 acetylation at this residue; however, there was no

difference in p53 acetylation with the different doses. Lastly, to determine whether the natural product cocktail altered global protein acetylation, total acetylated proteins were measured and there was no statistical difference in total acetylated proteins with any of the treatments at the two-week time point (Figure 2.3C).

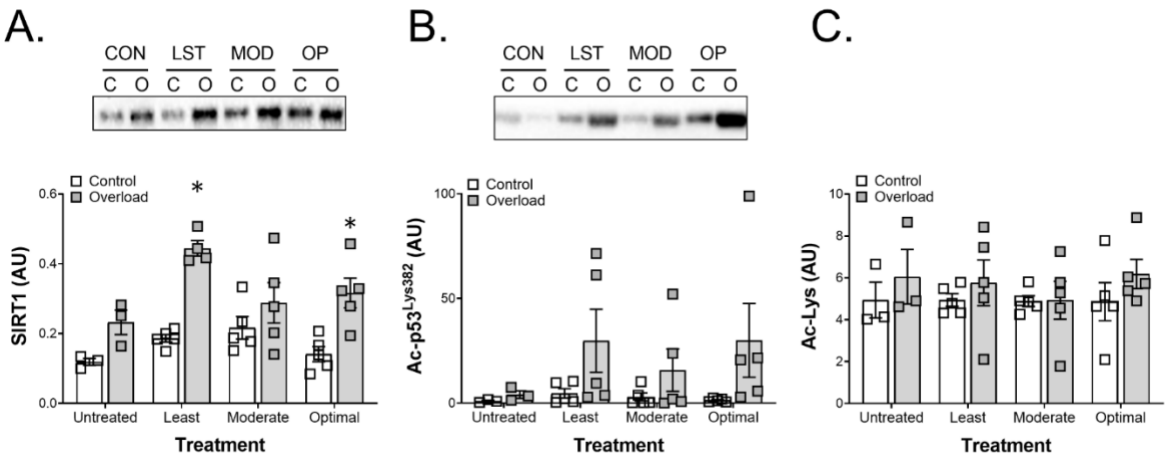

Protein Synthetic Response

To begin to understand the mechanism through which the natural products were increasing muscle fiber CSA, the rate of protein synthesis was determined by SuNSeT. Even though there was a trend for baseline protein synthesis to increase with the natural product cocktail, the increase in protein synthesis with overload was similar across all treatment groups (Figure 2.4A). Since ribosome mass is thought to control protein synthesis in extreme states, such as during overload [9], we next determined total RNA and the rate of ribosome biogenesis. Contrary to our hypothesis, total RNA tended to decrease from control to optimal treatment (Figure 2.4B). Further, when the rate of ribosomal RNA synthesis was determined by measuring the expression of the internal

transcribed spacer 1 (ITS1) and 5′ external transcribed spacer (5′ETS), the expression of these markers of ribosomal biogenesis decreased from control, to least, to moderate, to optimal where the 5'ETS value was significantly lower than the control treated muscles (Figure 2.4C and D). To determine whether the increased growth in the natural product groups was the result of greater Akt-mTORC1 signaling, the phosphorylation of Akt, S6K1 and eEF2 were determined. There was a tendency for Akt phosphorylation to increase with overload and decrease in the natural products (Figure 2.4E); however, neither of these effects reached significance. As reported previously, S6K1 phosphorylation was higher in the overloaded leg (Figure 2.4F). Contrary to expectation, there was a trend for overload-induced S6K1 phosphorylation to decrease from control towards the optimal natural product combination; however, the activity of S6K1

(determined through eEF2 phosphorylation) was no different in any of the overloaded groups (Figure 2.4G).

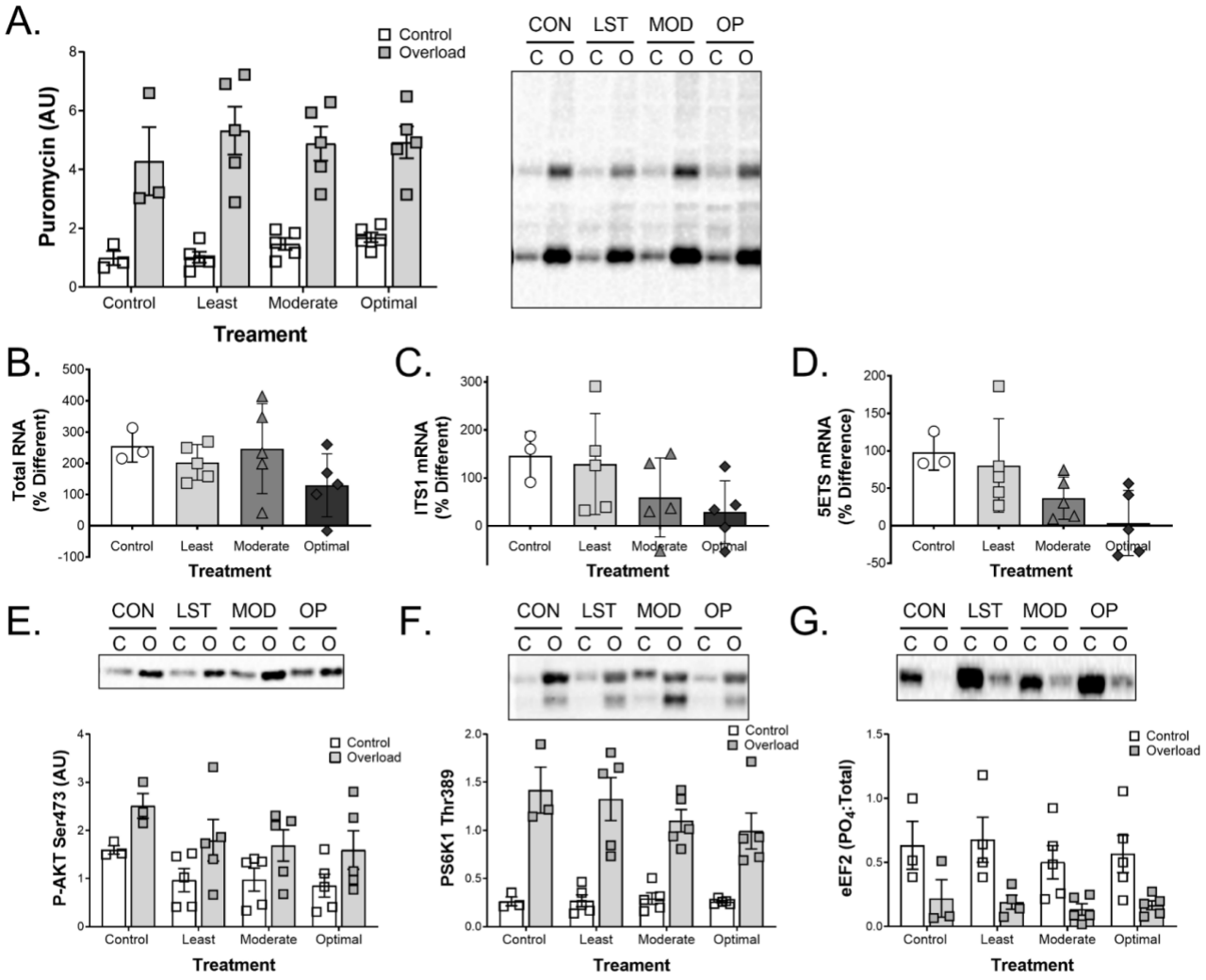

<u>Markers of Protein Turnover/Degradation</u>

Since there was no effect of the natural products on protein synthesis, a quick measure of markers of protein turnover was made by measuring the expression of MuRF and MafBx. As has been reported previously, MuRF and MafBx expression tended to

increase with overload and were not affected by the natural product treatment (Figure 2.5).

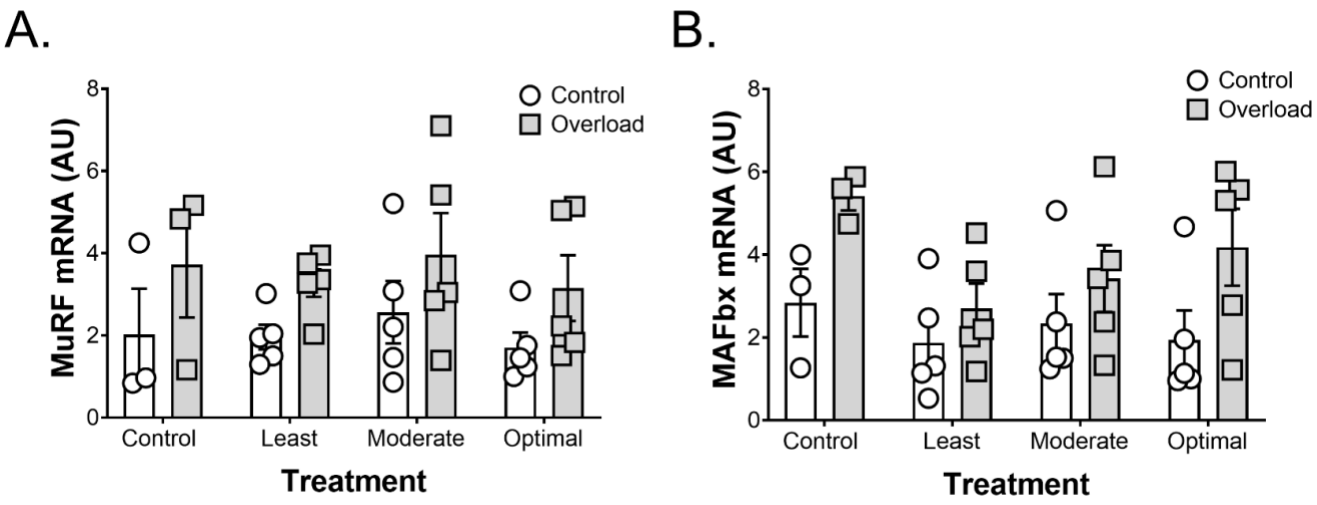

Ribosomal Protein Acetylation

The ribosomal proteins are regulated by acetylation. Since SIRT1 is a deacetylase, the acetylation of proteins representative of the small and large ribosomal subunits was determined following immunoprecipitation. With optimization of the natural product cocktail, there was a trend for the acetylation of the ribosomal proteins to increase (Figure 2.6A and B). By contrast, S6K1 acetylation tended to decrease with optimization of the natural product cocktail (Figure 2.6C).

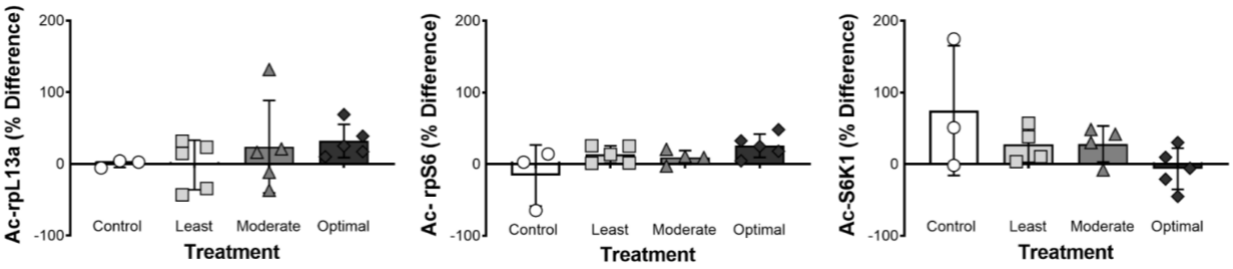

Discussion

Here we show that several natural products have the ability to inhibit SIRT1 in an *in vitro* activity assay. Combining three of these natural products that are generally recognized as safe (GRAS), a Food and Drug Administration designation that a chemical added to food is considered safe by experts, and therefore exempt from the Federal Food, Drug, and Cosmetic Act food additive tolerance requirements, in the optimal manner results in a significant increase in muscle fiber hypertrophy following 14 days of overload. The significant increase in muscle fiber CSA was not the result of an increase in ribosomal mass. In fact, the optimal group showed significantly less 5'ETS and a strong trend towards lower ITS1 levels and total RNA, suggesting fewer ribosomes than the control muscles. The acetylation of ribosomal proteins tended to increase suggesting that the increase in myofibrillar protein could be the result of an increase in ribosomal efficiency rather than capacity. Importantly, the natural product cocktail did not alter body mass or the weight of the heart and liver suggesting that it has limited toxicity and together with exercise may be useful in growing or maintaining muscle mass.

We have previously identified SIRT1 as one of a series of molecular breaks that limit the growth of muscle in response to extreme stimuli, such as synergist ablation [120]. We hypothesized that the activation of SIRT1 would result in the deacetylation of TAF68, a component of the SL-1 transcription factor that drives the expression of the 47S ribosomal RNA [122]. Deacetylation of TAF68 has previously been shown to inhibit rRNA transcription and therefore ribosome mass. Since ribosome mass is thought to limit growth following synergist ablation [9,123], we hypothesized that blocking SIRT1 would decrease TAF68 acetylation, increase the expression of rRNA, increase the capacity for

protein synthesis, and allow greater skeletal muscle hypertrophy in response to overload. With this background, we sought to determine whether SIRT1 could be inhibited by natural products and produce an improvement in growth.

Using the NatProd Collection, 800 pure natural products and their derivatives, derived from plant, animal, and microbial sources, we identified 45 compounds that inhibited the activity of SIRT1 towards p53 by greater than 65% at a concentration of 50μM and 35 compounds that inhibited SIRT1 by at least 20% inhibition at 5μM. This represents a unique list of compounds, many of which are polyphenols, including quinones and flavonoids that inhibit SIRT1. The fact that the majority of the compounds that inhibited SIRT1 were polyphenols suggests that regulation of SIRT1 may be one reason that polyphenols have a significant impact on human health and disease prevention [124]. We chose to focus on three of these polyphenols, epicatechin, epigallocatechin-3-gallate, and celastrol because they had a history of use in human medical trials without complication [125–127] and have different chemical structures that might mean different degrees of digestion, absorption, delivery, and activity in muscle following ingestion. Using an incomplete factorial design, we treated animals with different concentrations and combinations of natural products to create a model as to how each natural product contributes to the increase in muscle CSA following overload. Response surface plots were used to determine the relative importance of each component and their interaction with the other natural products in the cocktail (Figure 2.1B). To validate the model, we chose three different combinations of the natural products based on their predicted effect on muscle fiber CSA following overload. An independent cohort of rats (n=5 per treatment) underwent synergist ablation and then received a daily gavage containing of

one of the three combinations of natural products, or the placebo control. The fact that the model prediction for the increase in fiber CSA was proportional to the measured change in CSA (r^2 = 0.9586), suggests that the model was valid and that the predicted combination of epicatechin, epigallocatechin-3-gallate, and celastrol was optimal for muscle hypertrophy.

The optimal combination of epicatechin, epigallocatechin-3-gallate, and celastrol increased mean fiber CSA 61.5% compared with ~4% in the control group. This finding is striking for two reasons. First, as seen in Figure 2.2F, the increase in muscle mass following overload was not proportional to the mean increase in fiber CSA. In fact, the mass of the muscle appeared to have to increase by ~80% before an increase in the mean fiber CSA was observed. However, we did not observe a significant increase in fiber number over that period (data not shown). These data suggest that the majority of the increase in muscle mass that occurs following 14 days of functional overload is not due to an increase in average fiber CSA. In the plantaris muscle, there are regions of very big fibers and other regions of relatively small fibers. It is possible that the regional difference in fiber CSA negate any obvious effect on mean fiber area following overload. However, it is also possible that the muscle is growing in other ways. Following the removal of the soleus and gastrocnemius muscles, the ankle of the rat is held in a more dorsiflexed position, which would be expected to increase the resting length of the plantaris. We have preliminary data that indicates that one result of the shift in ankle position is that the plantaris muscle increases in length by approximately 10%. Others have recently made a similar suggestion in mice [128]. These data suggest that the plantaris muscle is increasing in mass as a result of functional overload in part through

the addition of sarcomeres in series. However, this hypothesis needs to be more thoroughly evaluated.

The finding that the optimal group had a 61.5% increase in mean fiber CSA compared with ~4% in the control group is also striking for the magnitude of the difference in hypertrophy with the natural product cocktail. Other treatments that augment muscle hypertrophy, such as consuming leucine rich protein, have an effect size of ~5% [113]. These data suggest that the mechanism underlying the effect of the natural product cocktail is distinct and likely rate limiting in load-induced skeletal muscle hypertrophy.

One proposed limit to skeletal muscle hypertrophy in both mice and man is the capacity for protein synthesis; i.e. ribosome mass [8,9,123]. To determine whether ribosome mass was increased in the animals fed the natural product cocktail we determined total RNA relative to muscle mass. Contrary to our hypothesis, total RNA tended to increase less with the natural product cocktail than in the vehicle controls. In support of this observation, the rRNA spacers (ITS1 and 5'ETS) showed the same pattern, with the change in 5'ETS being statistically lower than controls. These data suggest that even though the natural product cocktail increased hypertrophy, the improvement was not the result of an increase in translational capacity. Alternatively, the natural product cocktail may have resulted in an early (3-7 days) increase in ribosome mass that returned to baseline sooner. Further experiments are necessary to determine whether this is a difference in dynamics or absolute change in total RNA.

One possible explanation for the apparent increase in muscle protein without a concomitant rise in ribosome mass is an increase in translational efficiency. While there is a paucity of recent work on the role of acetylation of the ribosomal proteins and

translational efficiency, early work showed that following hepatectomy, when protein synthesis rates increase to regenerate the tissue, the acetylation of the ribosomal proteins precedes the protein synthetic response [129]. This suggests that acetylation of the ribosomal proteins may increase translational efficiency. Choudhary and colleagues identified 75 ribosomal proteins that were acetylated at a minimum of 136 locations [116]. For the mitochondrial ribosome, proteins MRPL10 and 19 are deacetylated by the mitochondrial sirtuin SIRT3 [130]. When SIRT3 is overexpressed, MRPL10 and 19 become deacetylated and this corresponds with a decrease in protein synthesis. When a catalytically inactive SIRT3 is used there is no change in acetylation or protein synthesis. Further, when SIRT3 is targeted with shRNA, acetylation and protein synthesis both increase [130]. Lastly, ribosomes isolated from the liver of SIRT3 knockout mice show more protein synthesis per unit of ribosomal protein [130]. Together, these data suggest that sirtuins can deacetylate ribosomal proteins and this corresponds with a decrease in translational efficiency. Consistent with these data, we show that our putative SIRT1 inhibiting natural product cocktail tends to increase the acetylation of two ribosomal proteins and this is associated with a greater change in protein synthesis (similar increases in puromycin) relative to total RNA or ribosomal biogenesis (5'ETS), suggesting improved translational efficiency.

Beyond the acetylation of ribosomal proteins, the cell size regulator S6K1 can also be acetylated [131,132] and this decreases its ability to be phosphorylated by mTORC1 [115], and its ability to phosphorylate ribosomal protein s6 in mesangial cells [115,133]. The deacetylation of S6K1 can be catalyzed by either SIRT1 or 2 [115]. Therefore, inhibition of SIRT1 would be expected to increase S6K1 acetylation and decrease Thr389

phosphorylation. Interestingly, in muscles treated for 14 days with presumed inhibitors of SIRT1, we observed a tendency for S6K1 acetylation and phosphorylation to both decrease. when trying to rectify our data with the existing literature, it is important to note that the effect of SIRT1 on S6K1 acetylation was performed in culture following 3 hours of treatment with the sirtuin inhibitor nicotinamide [115]. It is also important to note that much of the *in vitro* study looked specifically at S6K1 acetylation at lysines 427, 484, 485, and 493. By contrast, the current work looked at total acetylation of S6K1 following immunoprecipitation. It is possible that longer periods of sirtuin inhibition in the presence of a growth stress would lead to the acetylation of 427, 484, 485, and 493 but deacetylation at other sites, resulting in the net deacetylation that was observed in the current study. Further work is needed to better understand the specific residues acetylated in S6K1 and their role in the regulation of protein synthesis.

Using an *in vitro* assay, we have identified several natural products that can inhibit SIRT1 activity. By combining three of these inhibitors *in vivo* we were able to develop a model for how different combinations contributed to muscle hypertrophy following overload. When validating the model, we discovered that the optimal combination of natural products could significantly increase muscle hypertrophy in response to loading even though it significantly decreased ribosome biogenesis and tended to decrease the rise in ribosome mass that occurs with overload. This suggests that the natural product described here may increase ribosome efficiency, possibly by increasing the acetylation of ribosomal proteins, resulting in greater skeletal muscle hypertrophy.

Methods

All methods were carried out in accordance with relevant guidelines and regulations.

SIRT1 inhibitor screen.

The NatProd Collection library (MicroSource Discovery Systems, Inc. Gaylordsville, CT) in ten source plates was screened at two doses (5 μM and 50 μM final in the reaction mixture, duplicate for each dose). The inhibitory activity of the compounds was assessed in duplicate against 2ng/μL purified human SIRT1 using 3μM p53 as a substrate. The assay was a mobility shift assay based on charge differences before and after electrophoretic separation of product from fluorescently labeled substrate read using a Caliper EZ Reader (Perkin Elmer, Boston, MA). All reactions took place in the presence of excess nicotinamide adenine dinucleotide and the known SIRT1 inhibitor suramin was used as a control.

Box-Behnken model generation.

Three of the inhibitors identified in the natural product screen were selected based on their previous use in humans and complementary chemical structures. These inhibitors were then used to create an incomplete multifactorial design Box-Behnken model using Design-Expert® software. The three-factor design with one central point required 12 animals. Five more animals received the central dose of all three natural products to determine the biological variability of the intervention.

Synergist ablation.

All animal procedures were approved by the Institutional Animal Care and Use Committee at the University of California, Davis and are reported in accordance with ARRIVE guidelines. Eighteen rats were used for both the DOE and validation

experiments. The animals were anesthetized using 2.5% isoflurane, the distal hindlimb shaved and prepared for aseptic surgery. The whole soleus and bottom two thirds of the gastrocnemius were removed at the Achilles tendon, 38hospng the plantaris (PLN) muscle and innervating nerve intact. The overlying fascia and skin were sutured closed, and the animals were moved to a temperature regulated area for recovery. The left leg served as a contralateral control. Animals were monitored daily to ensure they returned to normal activity and did not suffer any stress from the procedure. Animals were orally gavaged on a daily basis (just prior to lights out), in accordance with their respective treatment group.

Muscle Collection.

Following the 14th day of treatment, animals were anesthetized, and the overloaded and contralateral PLN muscles, hearts, and livers were collected. Upon removal, PLN muscles were trimmed conservatively, weighed and then pinned at resting length on cork, snap-frozen in liquid nitrogen cooled isopentane and stored at -80˚C until further processing.

Histology.

PLN muscles were blocked in a cryostat on corks using Tissue Tek O.C.T. Compound (Sakura), and 10μm sections were mounted onto slides for CSA quantification. Slides were prepped for histological analysis by being blocked in 5% normal goat serum (NGS) in PBST w/1% tween, and incubated in primary antibodies for type I, Iia, Iib fibers, and/or laminin over night at 4˚C. The next day, slides were washed with PBST w/0.1% Tween and incubated in HRP conjugated secondary antibodies for 60 minutes, washed

again and mounted using Prolong Gold (no Dapi). Four random images were taken of each respective muscle section for CSA quantification using Fiji.

Validation experiment.

Following synergist ablation, animals were randomly assigned to one of four treatment groups, control (n=3), Least (n=5), Moderate (n=5), and Optimal (n=5). Least, moderate, and optimal refer to the best (optimal) and worst (least) combination of the natural products relative to the predicted effect on muscle fiber CSA. The Moderate group was predicted to have an effect of fiber CSA between that of the Optimal and Least groups. The control group received phosphate buffered saline (PBS), whereas the least, moderate, and optimal groups received different combinations and concentrations of the three SIRT1 inhibitors as a single cocktail dissolved in PBS (Table 2). All treatments were administered via oral gavage just prior to lights out for 14 days; the first gavage was given at 5pm on the day the surgery took place.

mRNA Isolation, reverse transcription, and qPCR.

Following blocking, PLN muscles were powdered using a hammer and pestle. Total RNA was extracted from weighed powdered muscle tissue using RNAzol in accordance with the manufacturer's protocol. RNA was quantified using Biotek Epoch Microplate Reader via absorbance (Biotek,Winooski, VT), and the RNA/mg muscle was calculated by dividing total RNA in the sample by the mass of muscle powder used. 1.5µg of total RNA was then converted into cDNA using MultiScribe reverse transcriptase and oligo (DT) primers. cDNA was diluted 1:10 before conducting qPCR. qPCR was performed using CFX384 Touch Real-Time PCR Detection System (Bio-Rad, Hercules, CA), along with Quantified Mastermix and Bio-Rad Sybr Green Mix solution and Bio-Rad 384 well

PCR plates. PCR reactions were performed in accordance with the manufacturer's instructions with the following primers: rITS-1 (fwd-TCCGTTTTCTCGCTCTTCCC- ; rev-CCGGAGAGATCACGTACCAC-), r5E1TS (fwd-ACGCACGCCTTCCCAGAGG-; rev-CGCGTCTCGCCTGGTCTCTTG-). Gene expression was calculated using a delta delta threshold cycle method [134] and GAPDH (fwd-TGGAAAGCTGTGGCGTGAT- ; rev-TGCTTCACCACCTTCTTGAT-) was used as the housekeeping gene. The absolute C_T of GAPDH was unchanged by either overload or treatment.

Tissue homogenization and western blotting.

Two scoops of muscle powder were incubated in 250 µL of sucrose lysis buffer [1M Tris, pH 7.5, 1M sucrose, 1mM EDTA, 1mM EGTA, 1% Triton X-100, and protease inhibitor complex]. The solution was set on a shaker for 60 minutes at 4˚C, spun down at 8,000g for 10 minutes, supernatants were transferred to new Eppendorf tubes and protein concentrations were then determined using a DC protein assay (Bio-Rad, Hercules, CA). 750 µg of protein was diluted in 4X Laemmli sample buffer (LSB) and boiled for 5 minutes. 10µL of protein sample was loaded onto a Criterion TGX Stain-Free Precast Gel and run for 45 minutes at a constant voltage of 200V. Proteins were then transferred to an Immobilon-P PVDF membrane, after it was activated in methanol and normalized in transfer buffer, at a constant voltage of 100V for 60 minutes. Membranes were blocked in 1% Fish Skin Gelatin (FSG) in TBST (Tris-buffered saline w/ 0.1% Tween) and incubated overnight at 4˚C with the appropriate primary antibody diluted in either TBST or 1% FSG at 1:1,000. The next day, membranes were washed three times with TBST for 5 minutes, and successively incubated at room temperature with peroxidase-

conjugated secondary antibodies in a 0.5% Nonfat Milk TBST solution at 1:5,000. Bound antibodies were detected using a chemiluminescence HRP substrate detection solution (Millipore, Watford, UK). Band quantification was determined using BioRad Image Lab Software.

Immunoprecipitations.

Muscle powder was homogenized, and protein quantified as above and 500µg protein was placed into a tube containing 25µL of antibody loaded Protein G-Dyna beads were aliquoted into an Eppendorf tube and prepped for immunoprecipitation using the instructed protocol (Thermo Scientific, Protein G-Dyna Beads). Antibodies for pulldown were used at a concentration of 1:100, and the final solution was submerged in a 30µL of 1X LSB, boiled for 5 minutes and stored at -80˚C. 6µL of sample was loaded per well onto a Criterion TGX Stain-Free Precast Gel and carried forward with the western blotting protocol above.

Antibodies.

Primary antibodies for western blotting and immunoprecipitation were diluted to a concentration of 1:1000. Antibodies were from Cell Signaling Technology (Danvers, MA, United States)- total eEF2 (CS-2332S), p-53 (CS-2524S), 41hosphor-eEF2 (CS-2331S), SIRT1 (CS-947S), Ac-Lys (CS9441S), 41hosphor-S6 (CS-5364S), Ac-p53 (CS-252S), P-AKT (Ser473) (CS-4060S), Cytochrome-C (CS-4280S); Santa Cruz Biotechnology (Santa Cruz, CA, United States)- rps6 (SC-13007), rpL13a (SC-390131), Dystrophin (SC-465954); Abcam (Cambridge, UK)- Total OxPhos (ab110413); and Millipore- puromycin (MABE343).

Statistics.

Data were analyzed using one-way or two-way ANOVA (loading x inhibition) using GraphPad Prism software (GraphPad Software, Inc., La Jolla, CA). Tukey's post hoc analysis was used to determine differences when interactions existed. Statistical significance was set at $p < 0.05$. All data are presented as mean ± standard error mean (SEM).

Acknowledgements

The work was supported by a research grant by Advanced Muscle Technologies (KB) and a grant from the National Institute of Arthritis, Musculoskeletal and Skin Diseases (AR069775R21) to SS and KB.

Author Contributions

K.B., S.S. contributed to conceptualization of the study. S.J.P., M.W., S.A, and H.T.L., contributed to the data collection. S.J.P., M.W., S.S and K.B., carried out the formal analysis. S.J.P., S.S., and K.B contributed the manuscript. All authors approved the final manuscript.

Data Availability Statement:

Raw Data were generated at UC Davis. All raw data are available from KB on request.

Competing Interests

The inhibition of SIRT1 and enhanced muscle hypertrophy (U.S. patent number 9,480,675) and the natural product cocktail described in this manuscript (U.S. patent number 11,312,695) have been patented. Both patents have been licensed by Advanced Muscle Technologies (AMT). AMT provided funds for the studies described in this manuscript, paid KB as a consultant, and provided shares to SS and KB. SP, MW, SA, and HTL have no conflicts to disclose.

Figure Legends

Figure 2.1. Development of a Box-Behnken model of natural products versus muscle cross-sectional area. Eighteen separate combinations and concentrations of the three natural products were established using an incomplete factorial design. Thirteen of the combinations were unique, whereas five were identical in order to determine the biological variability in the system. (A) Mean change in fiber cross-sectional area for each of the 18 different treatment groups following 14 days of overload. (B) Response surface plot for the relationship between CSA and the amount of epicatechin and epigallocatechin-3-gallate at a constant level of celastrol (500μg/kg/day).

Figure 2.2. Validation of the Box-Behnken model of the relationship between natural products and muscle fiber cross-sectional area. (A) Body weight, (B) heart weight/body weight, (C) liver weight/body weight, (D) muscle mass following 14 days of overload with different levels of natural products. (E) Distributions of fiber cross-sectional area changes in the control, least effective, moderately effective, and most effective combination of natural products, from left to right. (F) Relationship between muscle fiber CSA and muscle mass following 14 days of overload. Note that mass increases ~80% before a measurable change in mean fiber CSA occurs. (G) Mean fiber CSA as a function of overload and treatment. (H) Relationship between the prediction of the change in fiber CSA from the Box-Behnken model and the actual measured change in fiber CSA following 14 days of overload. Data are means ± SEM for n = 5 animals per treatment group. * indicates a significant difference from control muscle.

Figure 2.3. SIRT1 levels and acetylation with overload and natural product treatment. (A) Levels of SIRT1 protein following overload and natural product treatment. (B)

Acetylation of p53 at K382 with both overload and treatment with natural products. Note the greater increase in p53 acetylation with the natural product treatment. However, the variability in each group precludes statistical significance. Finally, (C) shows the level of acetylation of lysines in the whole muscle homogenate. Data are means ± SEM for n = 5 animals per treatment group with every point shown. * indicates a significant difference from control muscle.

Figure 2.4. Protein synthesis and ribosomal markers with overload and natural product treatment. (A) Protein synthesis as estimated by SUnSET. Both the blot and quantified data are shown. Estimates of ribosomal mass were made by measuring (B) total RNA (~80% of which is ribosomal RNA), (B) the internal transcribed spacer 1 (ITS1), and (C) the 5′ external transcribed spacer (5′ETS). To get an idea of Akt-mTORC1 signaling, (D) Akt Ser473, (E) S6K1 Thr389, and (F) eEF2 phosphorylation were measured. Data are means ± SEM for n = 5 animals per treatment group with every point shown. * indicates a significant difference from control muscle.

Figure 2.5. Markers of protein turnover with overload and natural product treatment. (A) MuRF and (B) MaFBx mRNA were measured. Data are means ± SEM for n = 5 animals per treatment group with every point shown. * indicates a significant difference from control muscle.

Figure 2.6. Acetylation of ribosomal proteins and regulators with overload and natural product treatment. To get an estimate of ribosomal acetylation, representative proteins from the large (A) L13A and small (S6) ribosomal subunits were blotted following immunoprecipitation with an acetyl-lysine antibody. (C) Levels of S6K1 acetylation were also determined in the same manner. Note the opposite pattern of the two measures.

Data are means ± SEM for n = 5 animals per treatment group with every point shown. * Indicates a significant difference from control muscle.

Chapter 3: Class IIa Histone Deacetylase Inhibitor and an Acute Ketogenic Diet's Effect on Skeletal Muscle of Old Female Mice

This chapter has been submitted to Cell Reports as:
Pathak, S.J., E.S. Elessawy, E. Ponce, R. Crone, J. Rutkowsky, J.J. Ramsey, and K. Baar. Class IIa Histone Deacetylase Inhibitor and an Acute Ketogenic Diet's Effect on Skeletal Muscle of Old Female Mice

Abstract

The primary determinants of nursing home placement are a decline in skeletal muscle and cognitive function. We have previously shown a ketogenic diet (KD) maintains skeletal muscle cross sectional area and function concomitant with improved cognitive function in both old-age male and middle-aged female mice. However, the mechanism underlying these adaptations remains unknown. The greatest physiological change seen with a KD is an increase in acetylated histone and non-histone protein levels. Here we aimed to understand the effects of an acute 28-day KD started at 23 months of age ± treatment with histone deacetylase inhibitor, scriptaid (SCRIPT), on skeletal muscle and neurocognitive function. At 24 months of age cognitive and motor behavior tests were performed and skeletal muscle was collected. 28 days on a KD failed to improve cognitive function, while makers of strength (forelimb grip strength) were significantly increased. This improvement in strength performance was associated with significantly higher dystrophin protein rather than changes in fiber cross-section. When a KD was paired with SCRIPT, there was a blunting of ketone production, namely β-hydroxybutyrate (BHB) in the fasted state. Accompanying the lack of fasted BHB production in the KD SCRIPT animals the beneficial biochemical changes were also lost. This provides potentially crucial insight highlighting the importance of BHB production on skeletal muscle and brain function on an acute KD.

Introduction

Over the last decade, interest in the potential therapeutic benefits of a ketogenic diet (KD) has grown. Currently, there is little known about the mechanisms underlying the benefits of KDs. Previous reports have demonstrated that interventions that shift metabolism towards fat oxidation and ketone production like a KD [6], time restricted feeding [135], intermittent fasting [136], and caloric restriction [137] increase longevity. Interestingly, these dietary interventions have a molecular signature akin to endurance exercise, another stimulus that increases the capacity for fatty acid oxidation and circulating ketones [138,139]. As the reliance on fatty acid oxidation increases, more acetyl-CoA is derived from fat and the need for glucose oxidation is reduced.

A KD, where fats are high and carbohydrates are limited, results in both a shift in metabolism towards fatty acids and the production of ketone bodies such as β-hydroxybutyrate (BHB) in the liver. Importantly, in rodents simply limiting carbohydrates with a low carb high fat diet (LCHF) fails to increase BHB levels, or improve skeletal muscle mitochondrial mass and function, or neurocognitive function [6]. This suggests that increasing fatty acid oxidation is not sufficient to improve muscle and brain function. With the rise in circulating BHB achieved with a KD, there is an increase in both acetylated histone and nonhistone proteins, whereas a LCHF has limited effect on protein acetylation [6]. As with a KD, protein and histone acetylation increases following endurance exercise [5]. Previous work in young male mice has shown, that the class IIa histone deacetylase inhibitor ($HDAC_i$), scriptaid, administered at $1mg/kg \bullet bw^{-1}$, disrupts the class IIa HDAC corepressor complex and, like exercise or a KD, leads to acute histone acetylation. When repeated daily for a month, scriptaid treatment increased lipid

oxidation, time-to-fatigue, and mitochondrial mass [42]. Similar to scriptaid administration, BHB inhibits class I and IIa HDACs both in vivo and in vitro [140,141]. Together, these data suggest that ketosis may affect skeletal muscle in a way that may serve as an exercise mimetic. However, to what extent protein acetylation contributes to the ability of the KD to increase mitochondrial biogenesis or fat oxidation has yet to be determined.

Beyond mitochondrial biogenesis, there is a growing body of literature that demonstrates a KD improves skeletal muscle function and helps maintain healthy muscle across different species, sexes, and disease states [6,77,142]. Our group has demonstrated that, in male mice, this improvement may be due, in part, to a maintenance of fiber cross sectional area (fCSA) and a preferential preservation of type IIa (fast-oxidative) fibers [7]. A separate but fundamental part of movement is the ability of skeletal muscle to transmit force to avoid contraction-induced injury [143] – a primary driver of sarcopenia [144]. The dystrophin-associated glycoprotein complex (DGC) is largely responsible for protecting skeletal muscle from contraction induced injury as is seen in Duchenne's muscular dystrophy (DMD; Bloch et al. 2004; Worton 1995). In 2011, Ramaswamy et. al, beautifully demonstrated that there is a 30% reduction in lateral force transmission in *mdx mice* and in old rats where dystrophin levels have decreased [147]. Interestingly, in 2021 Fujikura et. al, found that in a rat model of DMD, feeding a KD rich in medium chain triglycerides rescued the dystrophic phenotype [77]. Yet, whether a KD affects dystrophin levels in otherwise healthy old muscle has yet to be explored.

In the present study, the ability of histone acetylation to mimic the benefits seen with a KD were explored. This was accomplished by putting animals on either an

isocaloric (11.2 kcal/day) control (CD) or KD, and further dividing the groups into those receiving an intraperitoneal injection of vehicle (VEH) or scriptaid (SCRIPT) for 28 consecutive days. This resulted in four groups: CD VEH, CD SCRIPT, KD VEH, and KD SCRIPT. After the intervention, skeletal muscle specific acetylation levels, muscle mass and function, cognitive behavior, muscle fCSA, DGC protein levels, autophagy, mitophagy, and mitochondrial biogenesis and mass were determined. We originally hypothesized that the CD SCRIPT group would show improved skeletal muscle mitochondrial biogenesis and function similar to that seen in the KD VEH group but, the KD SCRIPT group would not show an additive benefit of the two interventions.

Methods

Animal Husbandry

Female C57BL/6JN mice were obtained from the NIA Aged Rodent Colony at 22-months of age. Mice were housed in polycarbonate cages in a HEPA filtered room with controlled temperature (22–24°C) and humidity (40– 60%). Mice were maintained on a 12-hour light-dark cycle and health checks were performed daily. Health screens were completed on sentinel mice, which were housed on the same rack and exposed to bedding from the study mice. All tests (MHV, Sendai, PVM, MPV, MVM, M.pul and arth, TMEV [GDVII], Ectro, EDIM, MAD1 and 2, LCM, Reo-3, MNV) were negative throughout the study. All animal protocols were approved by the UC Davis Institutional Animal Care and Use Committee and were in accordance with the NIH guidelines for the Care and Use of Laboratory Animals.

Experimental Diets

Mice were group housed until they reached the age of 23 when they were randomly assigned to a control (CD) or a protein-matched ketogenic (KD) diet and all mice were provided 11.2 kcal/day of CD or KD for the duration of the study. This amount was selected to match the measured chow food intake during the acclimatization period. The CD contained (% of total kcal) 10% protein, 74% carbohydrate, and 16% fat. The KD contained 10% protein, <0.5% carbohydrate, and 89.5% fat. Diets were made in-house. The CD was a modified AIN93G diet with a lower protein content to match the KD. Table 1 provides a detailed description of the diet composition. Mineral mix TD.94046 was used for the CD and TD.98057 was used for the KD to avoid carbohydrate carriers in the mix.

Table 1: Composition of the experimental diets		
	Control	**Ketogenic**
Energy density (kcal/g)	3.8	6.7
kcal/day	11.2	11.2
Ingredients	**g/kg diet**	
Casein	111	191
DL-methionine	1.5	2.7
Corn starch	490	--
Maltodextrin	132	--
Sucrose	100	--
Mineral mix TD.94046	35	--
Mineral mix TD.98057	--	24
Vitamin mix TD.40060	10	18
Soybean oil	70	70
Lard	0	582
Calcium phosphate dibasic	--	19.3
Calcium carbonate	--	8.2
Cellulose	48	85
Potassium phosphate monobasic	2.4	--
TBHQ	0.014	0.126

Intraperitoneal injections

Injections of Scriptaid (Sigma Aldrich: 287383-59-9) or Vehicle (5% DMSO diluted in 1X PBS) were made fresh daily at a concentration of 1mg·kg^{-1} body weight as previously described [42]. The intervention lasted 28 consecutive days and each injection was administered during the animal's light cycle at 4pm PST immediately preceding their feeding time.

Mouse behavior tests

A series of behavior tests were performed at 23 months of age. All tests were conducted in the light cycle.

Y maze spontaneous alternation test

The Y maze was used to assess short-term working memory. The apparatus consisted of a white acrylic Y-shaped maze. Each arm was 35 x 8 x 15 cm (L x H x W) in dimension and was separated by a 120° angle. Mice were placed in the center of the maze and allowed to explore for 6 minutes. Videos were recorded and movement of the mice was tracked using the Ethovision XT15 software (Noldus, Wageningen, the Netherlands). A complete arm entry was defined when the center point of the mouse travelled to the distal side of the arm (more than 1/3 of the arm length) and returned to the center of the maze. An alternation occurs when the mouse enters three different arms consecutively. The percent alternation was calculated as ((number of alternations) ÷ (number of total arm entries - 2)) x 100%.

Open field test

The open field test was conducted in a 40 x 40 x 40 cm white plastic box to evaluate mice's general locomotor activity level, anxiety, and willingness to explore. Mice were placed at the corner of the arena and videos were recorded and analyzed for 15 minutes using the Enthovision XT15 software (Noldus, Wageningen, the Netherlands). A 25x25 cm middle square was defined as the center zone.

Novel object recognition test (NOR)

The novel object recognition test was conducted to evaluate recognition memory. This test was performed in the same apparatus as the open field test, which was also used as the acclimation session for the NOR. The familiarization session was conducted the

morning following the open field test. During this session, two identical objects were placed in the arena, and mice were allowed to explore for 10 minutes. In the novel object session, performed 6 hours after the familiarization session, one of the old objects was replaced with a novel object (the novel side was randomized among mice), and the test was performed over 10 minutes. A small orange cone and a cell culture flask (filled with sand) with similar height were used as the objects and were randomly assigned as the old or novel object. A mouse was considered as exploring an object if the nose of the mouse was pointed toward the object and was within 2 cm from the object. Time exploring each object was manually scored using two stopwatches. These data were gathered using two separate blinded individuals and their times were averaged to produce the numbers reported in the manuscript.

Grid wire hang test

The wire hang was used to measure skeletal muscle endurance. Briefly, mice were placed on a stainless-steel wire mesh screen (1 mm wires and 1x1 cm grids) raised 40 cm above the bottom of a plastic box. Soft towels were placed at the bottom of the box to cushion the fall. Upon placing the mice on the top of the screen, the screen was slightly shaken to ensure a firm grip of the mice, and then inverted such that the mice hang on the wires using all four limbs. Time till the mice fell was recorded. If the maximal hanging time did not exceed 180 seconds, mice were given another trial (maximum of 3 trials) after resting in the home cage for approximately 30 minutes. Maximal hanging impulse was computed as (maximum hanging time (s) x body weight (kg) x 9.8 $N \cdot kg^{-1}$).

Grip strength

Mice were encouraged to grab and pull on a single metal bar attached to an Imada push-pull force scale (PS-500N, Northbrook, IL). Mice were given two rounds of three trials each and the maximum grip strength was used to gauge skeletal muscle strength.

Rotarod

Rotarod testing was used to determine motor coordination and balance. The test was conducted on a RotaRod Rotamex (Columbus Instruments, Columbus, OH, USA). Once the mice were placed on the rod, the rod started rotating at 4 rpm and accelerated at 1 rpm/6 seconds to a maximum of 40 rpm. Mice were tested for 3 trials each day for 2 days. The latency to fall and the speed at fall were recorded.

Blood ketone measurement

Blood β-hydroxybutyrate levels were measured using a Precision Xtra glucose and ketone monitoring system (Abbott, Chicago, IL, USA) through a tail nick either 3 hours postprandial or following a 12-hour overnight fast.

Euthanasia and Tissue Collection

Three days after the last behavior test, mice were euthanized under isoflurane anesthesia. Liver, heart, hippocampus, cortex, quadriceps, soleus, gastrocnemius (GTN), and tibialis anterior muscles were collected and snap frozen in liquid nitrogen for biochemical analysis or in liquid nitrogen cooled isopentane for histological analysis. All tissues were then stored at -80˚C until further processing.

Tissue homogenization and western blotting

Gastrocnemius tissue was powdered on dry ice using a hammer and pestle. Two scoops of powder were then aliquoted into 1.5 mL Eppendorf tubes and homogenized in 250 µL of solaro lysis buffer [1M Tris, pH 7.5, 1M sucrose, 1mM EDTA, 1mM EGTA, 1% Triton X-100, and 1X protease inhibitor complex]. The solution was set on a shaker for 60 minutes at 4°C, spun down at 8,000g for 10 minutes, supernatants were transferred to new Eppendorf tubes and protein concentrations were determined using the DC protein assay (Bio-Rad, Hercules, CA). Equal aliquots of 300 µg of protein were diluted in 4X Laemmli sample buffer (LSB) (final volume 200uL) and boiled for 5 minutes at 100°C. 10µL of protein sample was loaded onto a Criterion TGX Stain-Free Precast Gel and run for 45 minutes at a constant voltage of 200V. Proteins were then transferred to an Immobilon-P PVDF membrane, after it was activated in methanol and equilibrated in transfer buffer, at a constant voltage of 100V for 30 minutes. Membranes were blocked in 1% Fish Skin Gelatin (FSG) in TBST (Tris-buffered saline w/ 0.1% Tween) and incubated overnight at 4°C with the appropriate primary antibody diluted in TBST at 1:1,000. The next day, membranes were washed with TBST for 5 minutes, and successively incubated at room temperature with peroxidase-conjugated secondary antibodies in a 0.5% Nonfat Milk TBST solution at 1:10,000. Bound antibodies were detected using a chemiluminescence HRP substrate detection solution (Millipore, Watford, UK). Band quantification was determined using BioRad Image Lab Software. Antibodies used were as followed: Total oxidative phosphorylation (abcam MS604-300), PGC1alpha (ab54481), p-AMPKthr172 (cs2531S), KAT1 (ab194296), KAT3 (sc365219), FABP1 (KAT4) (ab171739), PINK1(sc517353). LC3BI:II (cs2775S), ATG7 (cs8558S).

KBHB (PTM-1201), acetylated lysine (cs9481S), Sirtuin 3 (cs5490S). dystrophin (sc-365954), α-sarcoglycan (sc-271321).

Immunohistochemistry (IHC) for Cross Sectional Area

Gastrocnemius (GTN) muscle samples were collected from mice, mounted on a flat cork, and snap frozen in liquid nitrogen cooled isopentane. Using a Leica CM3050 S cryostat, 10μM cross-sections of the gastrocnemius muscle were obtained and mounted on glass slides. The microscope slides were then fixed in a bath of cold acetone and incubated at -30 C for five minutes. The tissues were gated using a hydrophobic pen and were washed three times in a solution of 1X PBS and 0.1% of Tween (PBST) in five-minute intervals. The tissues were then blocked in a solution of 60μL mouse on mouse (MOM) solution and 2.5mL 1X PBST for an hour and then washed three times in intervals of five minutes. A 5% Natural Goat Serum solution was made in PBST and used to block the tissues again for 30 minutes. The tissues were left for overnight incubation at 4˚C in a primary antibody solution of Sigma Rabbit anti laminin at a concentration of 1:500. Following three five-minute intervals of PBST washes, the tissues were incubated at room temperature for an hour with a mixture the following secondary antibody and its respective dilution: 1:200 of RB 647 (Sigma L9393). After the final three washes in PBST, slides were mounted with ProLong Gold Antifade Mountant no DAPI sealed with a glass cover slip and stored at -30˚C until imaging.

IHC Imaging and Quantification

The sections were imaged at x20 magnification using a Leica DMi8 microscope and the Leica Application Suite X. The images obtained were analyzed and quantified using ImageJ and MATLAB's SMASH program as previously described [148].

Statistical analysis

All values are expressed as mean ± SEM p values <0.05 considered significant (* $p<0.05$, ** $p<0.01$, *** $p<0.001$). All analyses were performed using GraphPad Prism 8.1 (GraphPad Software Inc., San Diego, CA). For biochemical and behavior tests, comparisons between the groups were conducted using a 2-way ANOVA. Outlier tests were conducted on each data set.

Results

Administration of Scriptaid Lowers β-Hydroxybutyrate Levels in the Fasted State, and Increases Grip Strength, Without Affecting Learning and Memory

23-month-old female mice were put on a 11.2 kcal/day control (CD) or ketogenic diet (KD) for 28 days and daily injected with either Vehicle (VEH) or Scriptaid (SCRIPT) just prior to feeding (Figure 3.1A). Throughout the intervention, groups showed no differences in body weight (Figure 3.1B). There was a main effect of diet on elevating fed β-hydroxybutyrate (BHB) levels. Interestingly, in the fasting state there was a main effect of diet and a significant interaction between a KD and SCRIPT. A KD alone increased fasted BHB levels ($p<0.01$), whereas the combination of a KD and SCRIPT did not increase fasted BHB levels (Figure 3.1B).

To assess functional behavior measures, we conducted the 4-limb wire hang, rotarod, and forelimb grip strength tests (Figure 3.1D-G). Wire hang ($p=0.04$) and max hanging impulse ($p=0.05$) showed a significant effect of scriptaid injection with both dietary groups responding adversely to $HDAC_i$ treatment (Figure 3.1D&E). Rotarod performance was unchanged between intervention groups (Figure 3.1F). Conversely, grip strength was significantly increased in the KD fed groups (diet; $p=0.0063$) when compared to CD fed animals (Figure 3.1F). To assess anxiety related behavior, short-term memory, and object memory, the open field, y maze and novel object recognition tests were conducted, respectively. The open field and novel object assays showed no changes with treatment (Figure 3.1H&K). Y Maze performance showed a strong trend for a main effect of scriptaid administration (injection; $p=0.06$). Lastly, there was a

tendency for KD fed animals to increase distance moved in the open field assay (Figure 3.1I; p=0.10).

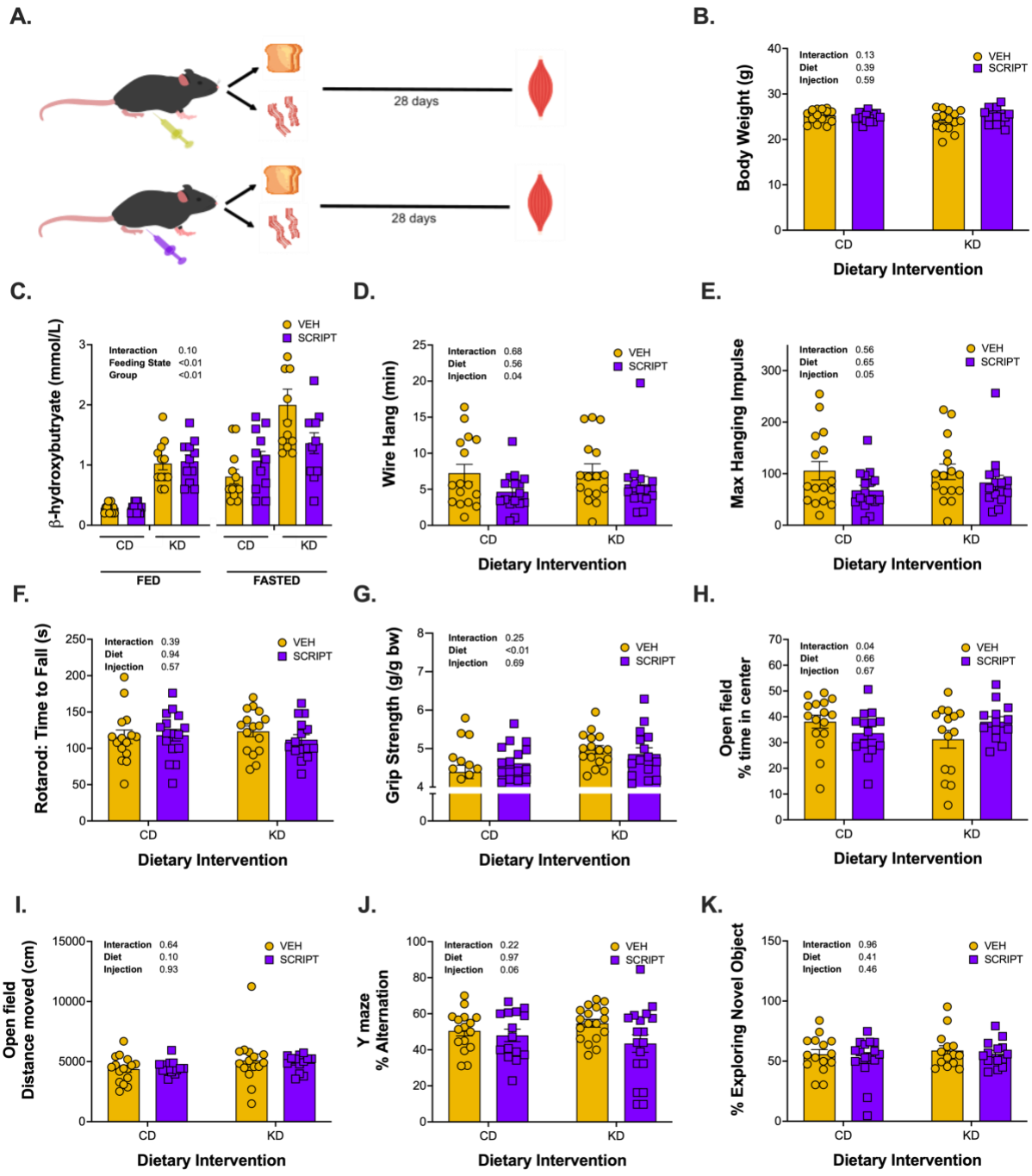
A.
28 days
28 days
B.
Body Weight (g)
Interaction 0.13
Diet 0.39
Injection 0.59
VEH
SCRIPT
CD
KD
Dietary Intervention
C.
β-hydroxybutryate (mmol/L)
Interaction 0.10
Feeding State <0.01
Group <0.01
FED
FASTED
D.
Wire Hang (min)
Interaction 0.68
Diet 0.56
Injection 0.04
E.
Max Hanging Impulse
Interaction 0.56
Diet 0.65
Injection 0.05
F.
Rotarod: Time to Fall (s)
Interaction 0.39
Diet 0.94
Injection 0.57
G.
Grip Strength (g/g bw)
Interaction 0.25
Diet <0.01
Injection 0.69
H.
Open field
% time in center
Interaction 0.04
Diet 0.66
Injection 0.67
I.
Open field
Distance moved (cm)
Interaction 0.64
Diet 0.10
Injection 0.93
J.
Y maze
% Alternation
Interaction 0.22
Diet 0.97
Injection 0.06
K.
% Exploring Novel Object
Interaction 0.96
Diet 0.41
Injection 0.46

One-month KD has Limited Effect on Body/Tissue Mass while Increasing Muscle Mitochondrial Mass

To understand the global effect of a KD ± SCRIPT, body and tissue mass of the liver, heart, gastrocnemius, soleus, quadriceps, and tibialis anterior muscles were taken. There was no difference in body mass, and only a trend towards increased quadricep muscle mass in the CD SCRIPT group when compared to their VEH counterparts (Supplemental Figure 3.1).

Acetylated and β-hydroxybutyrylated lysine (βHB-Lysine) moieties were measured in the GTN muscle via western blotting and found to be significantly higher in the KD VEH group, ~83% and ~45% respectfully (Figure 3.2A & B). As an estimate of mitochondrial mass, one protein from each of the oxidative phosphorylation complexes were measured. These proteins showed a noticeable, but insignificant increase, in the CD SCRIPT group while the KD VEH group increased these complexes significantly with significant interaction effect in the KD SCRIPT group ($p<0.01$) (Figure 3.2C).

Mitochondrial Mass Regulation

To begin to establish how mitochondrial mass was regulated by SCRIPT or a KD, markers of mitochondrial biogenesis were measured. PGC-1α protein levels showed a tendency to increase with SCRIPT and a strong trend to increase in the KD VEH group ($p=0.06$). When combined, a significant interaction effect ($p=0.016$) was found that mimicked the change in mitochondrial mass (Figure 3.2D). Levels of Sirtuin 3 (SIRT3) remained unchanged across all groups (Figure 3.2E). Kynurenine aminotransferase (KYAT) proteins I, III, and IV were unchanged across all groups (Figure 3.2F-H).

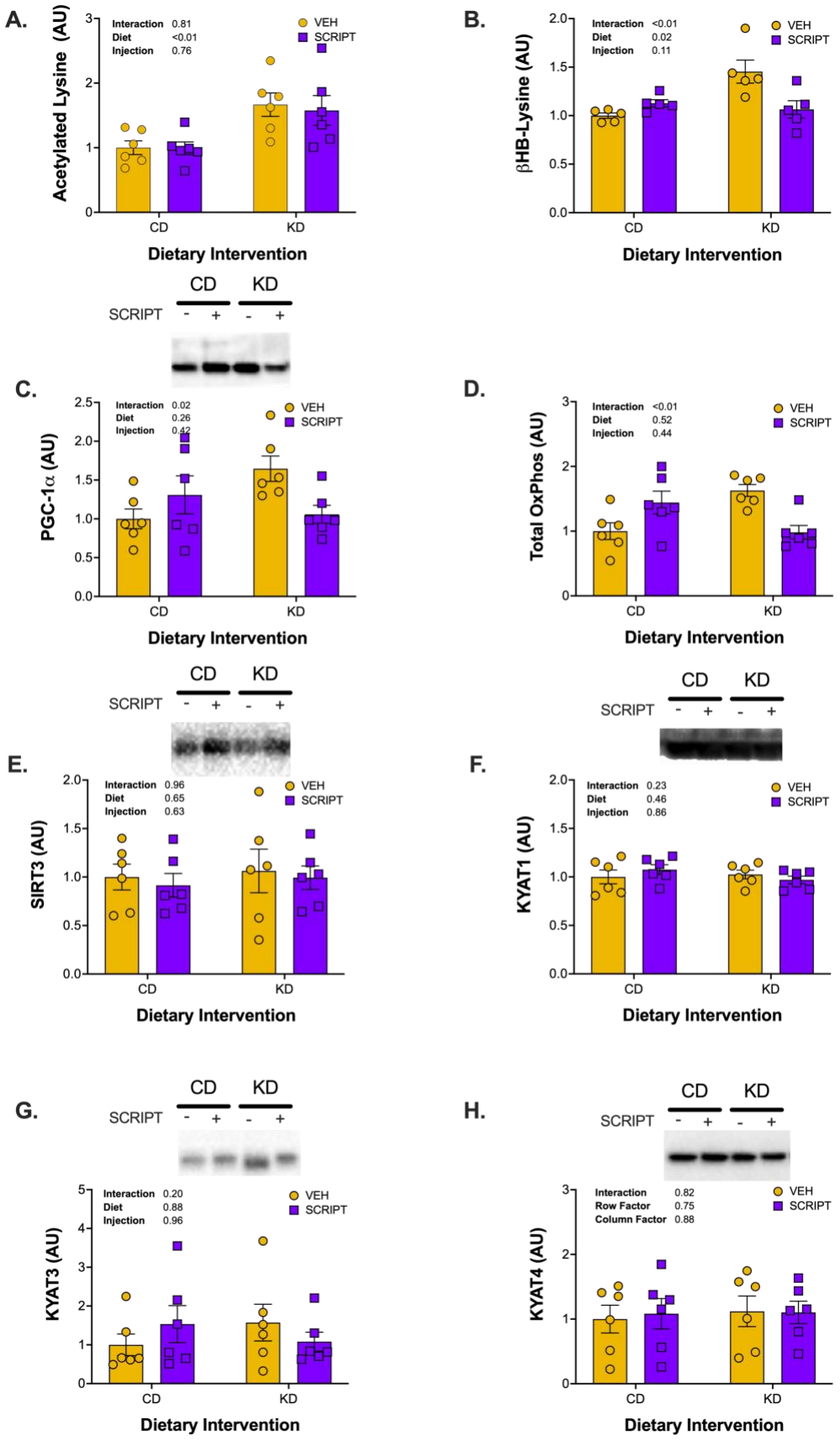
A.
Acetylated Lysine (AU)
Interaction 0.81
Diet <0.01
Injection 0.76
VEH
SCRIPT
CD
KD
Dietary Intervention
B.
βHB-Lysine (AU)
Interaction <0.01
Diet 0.02
Injection 0.11
VEH
SCRIPT
CD
KD
Dietary Intervention
CD KD
SCRIPT - + - +
C.
PGC-1α (AU)
Interaction 0.02
Diet 0.26
Injection 0.42
VEH
SCRIPT
CD
KD
Dietary Intervention
D.
Total OxPhos (AU)
Interaction <0.01
Diet 0.52
Injection 0.44
VEH
SCRIPT
CD
KD
Dietary Intervention
CD KD
SCRIPT - + - +
E.
SIRT3 (AU)
Interaction 0.96
Diet 0.65
Injection 0.63
VEH
SCRIPT
CD
KD
Dietary Intervention
CD KD
SCRIPT - + - +
F.
KYAT1 (AU)
Interaction 0.23
Diet 0.46
Injection 0.86
VEH
SCRIPT
CD
KD
Dietary Intervention
CD KD
SCRIPT - + - +
G.
KYAT3 (AU)
Interaction 0.20
Diet 0.88
Injection 0.96
VEH
SCRIPT
CD
KD
Dietary Intervention
CD KD
SCRIPT - + - +
H.
KYAT4 (AU)
Interaction 0.82
Row Factor 0.75
Column Factor 0.88
VEH
SCRIPT
CD
KD
Dietary Intervention
CD KD
SCRIPT - + - +

Phosphorylation of AMPK at the Thr172 site showed a main effect of diet (p=0.02), with a KD increasing phosphorylation of this site (Figure 3.3A). AMPK's direct target, ULK (Ser^{555} site) showed a significant effect of diet (p< 0.01), with a KD increasing phosphorylation (Figure 3.3B). Interestingly, the effect of SCRIPT on ULK phosphorylation was opposite to that of the effect of SCRIPT on AMPK phosphorylation. p62 levels also showed a main effect of diet (diet; p=0.02, Figure 3.3C), increasing on a KD. Neither the LC3BII:I ratio nor Beclin1 protein were different between intervention groups (Figure 3.3D, E). To understand mitochondrial specific autophagy (mitophagy), PINK1 protein levels were quantified. PINK1 levels showed a significant effect of diet (p=0.05), with a KD increasing PINK1, and injection, with SCRIPT decreasing PINK1(injection; p=0.01, Figure 3.3F).

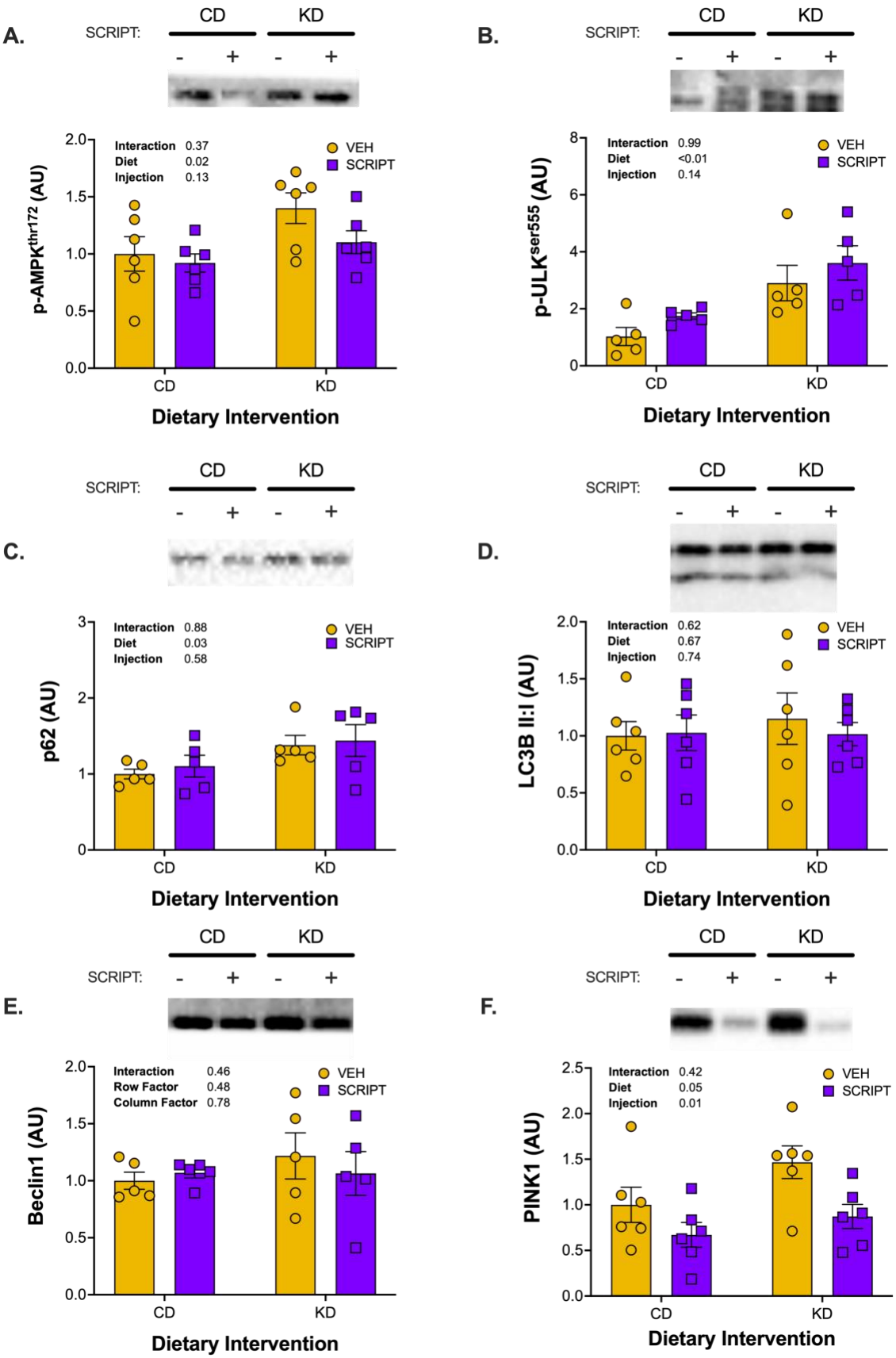
A.
SCRIPT:
CD
KD
- + - +
p-AMPK^{thr172} (AU)
Interaction 0.37
Diet 0.02
Injection 0.13
VEH
SCRIPT
Dietary Intervention
B.
p-ULK^{ser555} (AU)
Interaction 0.99
Diet <0.01
Injection 0.14
C.
p62 (AU)
Interaction 0.88
Diet 0.03
Injection 0.58
D.
LC3B II:I (AU)
Interaction 0.62
Diet 0.67
Injection 0.74
E.
Beclin1 (AU)
Interaction 0.46
Row Factor 0.48
Column Factor 0.78
F.
PINK1 (AU)
Interaction 0.42
Diet 0.05
Injection 0.01

A Ketogenic Diet Increases Dystrophin-Associated Glycoprotein Complex Proteins

To determine how muscle strength was improved by diet (Figure 3.1G), we determined fiber size and force transfer protein levels. Fiber cross sectional area (fCSA) plotted against fiber number (%) showed no statistical differences between intervention groups (Figure 4A&B). Minimum and maximum feret's diameter, along with mean fCSA (μm^2) were not statistically different between interventions. However, there was a trend for the KD to decrease fCSA and max feret's diameter (diet effect: p=0.11, p=0.10) and KD SCRIPT to maintain fCSA when compared to the KD VEH group (Figure 3.4C-E). Dystrophin was unchanged in the CD SCRIPT and KD SCRIPT animals but increased 2-fold in the KD VEH (diet; p=0.07) group when compared to the CD VEH group resulting in a strong trend of diet and injection interaction (p=0.05, Figure 3.4F). α-Sarcoglycan protein showed a moderate but insignificant in the KD VEH group (~55%; Figure 3.4G) and the pattern of expression matched dystrophin. Lastly, levels of micro-RNA 31 (mir31), a regulator of dystrophin translation, were unchanged at the time of measurement (Figure 3.4H).

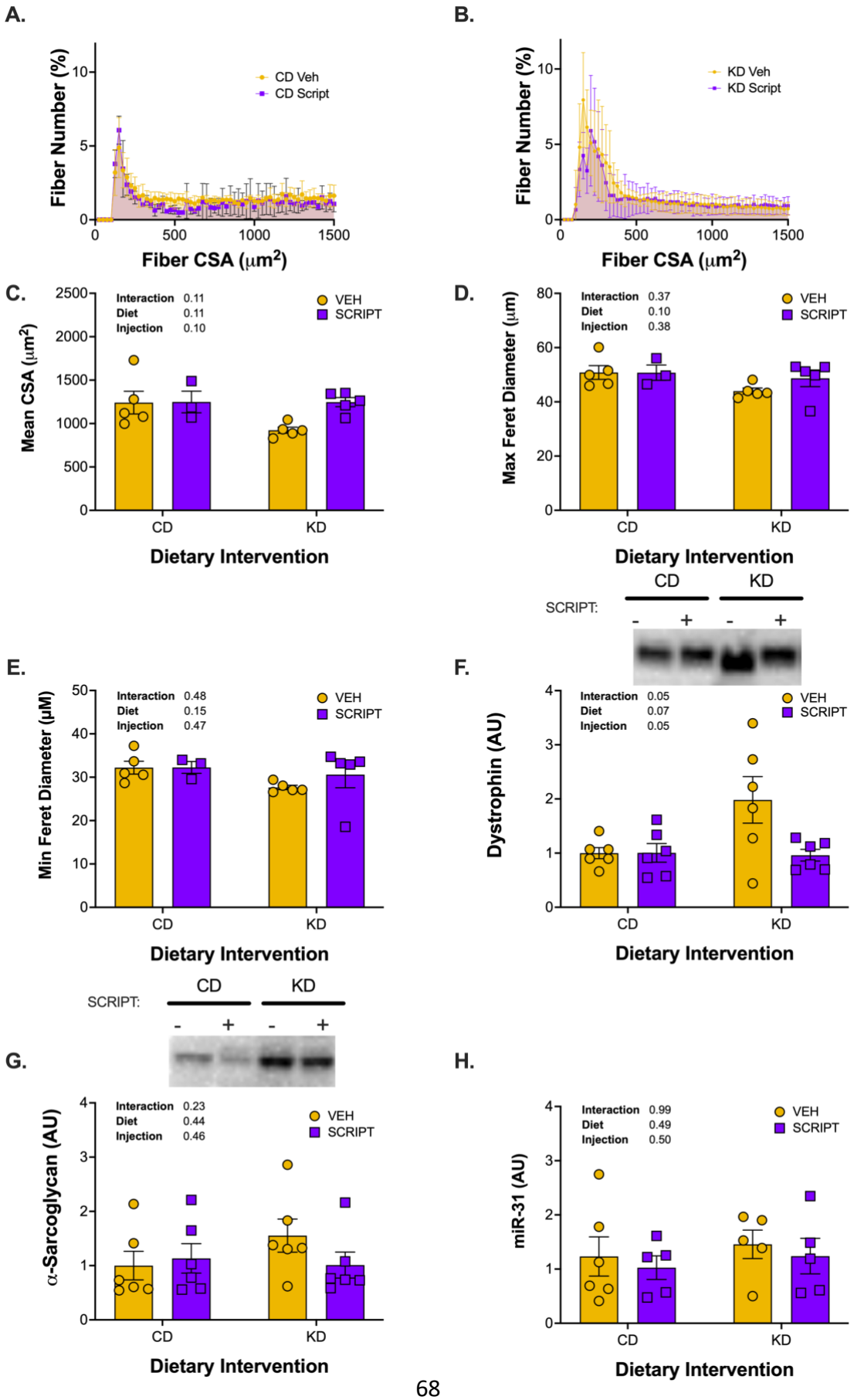
A.
Fiber Number (%)
CD Veh
CD Script
Fiber CSA (μm²)
B.
KD Veh
KD Script
C.
Mean CSA (μm²)
Interaction 0.11
Diet 0.11
Injection 0.10
VEH
SCRIPT
CD
KD
Dietary Intervention
D.
Max Feret Diameter (μm)
Interaction 0.37
Diet 0.10
Injection 0.38
E.
Min Feret Diameter (μM)
Interaction 0.48
Diet 0.15
Injection 0.47
F.
SCRIPT:
Dystrophin (AU)
Interaction 0.05
Diet 0.07
Injection 0.05
G.
α-Sarcoglycan (AU)
Interaction 0.23
Diet 0.44
Injection 0.46
H.
miR-31 (AU)
Interaction 0.99
Diet 0.49
Injection 0.50

Discussion

The objective of this study was to determine whether a 28 consecutive day treatment with histone deacetylase inhibitor scriptaid, could elicit some of the musculoskeletal benefits seen with an isocaloric (11.2 kcal/day) ketogenic diet (KD) in 23-month-old female mice. To accomplish this, we used a cross sectional study design with four experimental groups, a control diet fed group given daily intraperitoneal (IP) injections of a vehicle (CD VEH), a CD with daily scriptaid injections (CD SCRIPT), a ketogenic diet (KD) fed group given vehicle (KD VEH), or a KD group treated with scriptaid (KD SCRIPT). We hypothesized that there would be a modest increase in mitochondrial mass through PGC-1α in the CD SCRIPT group but, a larger effect in the KD VEH group, and no additive benefit by combining a KD and SCRIPT. Consistent with our original hypothesis, scriptaid treated mice were marginally stronger and had more mitochondrial mass than vehicle animals. Contrary to our hypothesis, the KD SCRIPT group showed lower BHB levels, and a tendency for lower mitochondrial mass, strength, and dystrophin levels than the KD VEH group. Further, the mechanism of mitochondrial regulation may differ between a KD and SCRIPT. SCRIPT blunted markers of mitophagy, whereas a KD showed signs of mitochondrial biogenesis through increased AMPK and PGC-1α. Lastly, the ability of a KD to increase strength may be more due to improved force transfer proteins, namely dystrophin, rather than an increase in fCSA.

Thus far, the literature on the impact of a KD on healthy old female mice is lacking, with most work in diseased models or young male mice [149–151]. To address this gap in knowledge, we recently demonstrated that a 2-month KD intervention in middle aged female mice improved mitochondrial biogenesis, increased kynurenine

aminotransferase (KYAT) protein levels in skeletal muscle, decreased circulating levels of the potential neurotoxin kynurenine, and improved cognitive function [152]. Interestingly, male mice that have undergone the same 2-month KD intervention showed no neurocognitive benefits in middle age [6]. Here we report a one-month KD in 23-month-old female mice shows no improvements in cognitive behavior (Figure3.1G-J) nor KYAT proteins (Figure 3.2F-H), suggesting that a one-month KD intervention is not sufficient, that 23-month-old animals are too old to adapt, or a combination of both factors. Scriptaid injections also failed to improve cognitive function (Figure 3.1H-K) in either the CD SCRIPT or KD SCRIPT groups indicating that 4 weeks of HDAC inhibition does not significantly affect neurocognitive function in old female mice.

Our previously published data suggested that the greatest physiological response to a KD is an increase in acetylated lysine in both male and female mice [6,152]. Together with the fact that Shimazu and colleagues showed that BHB can function as an HDAC inhibitor [141], these data suggested that a KD may work through HDAC inhibition. In support of this hypothesis, Gaur and colleagues showed that the HDAC inhibitor scriptaid increased mitochondrial protein, lipid oxidation, and fatigue resistance in young male mice through disruption of the HDAC corepressor complex [42]. To directly test the role of HDAC inhibition in the adaptation to a KD, we combine a KD +/- SCRIPT in old mice. A KD increased acetylation in the gastrocnemius (GTN) muscle by ~2-fold (Figure 3.2A). In line with our hypothesis, the significant increase in acetylation levels in the GTN muscle of the KD fed animals is associated with a significant increase in mitochondrial oxidative phosphorylation (OxPhos) protein levels. Contradictory to our hypothesis, when a KD is coupled with SCRIPT there is a failure for GTN muscle to

increase mitochondrial mass (Figure 2C). The pattern of OxPhos levels best mimicked the circulating ketone (Figure 1C) and protein BHBylation. These data suggest that BHB may directly increase mitochondrial mass independent of acetylation.

Increased phosphorylation and activation of the AMP-activated protein kinase at the threonine 172 (pAMPK^{thr172}) site is important in the regulation of fat metabolism, through the phosphorylation of ACC and activation of CPT-1 [153] and regulation of PGC-1α expression [154]. Consistent with previous work, the current results show that a KD significantly increases pAMPK^{thr172} (Figure 3.3A). Contrary to our previous work in young male mice, SCRIPT did not increase PGC-1α, indicating that females respond differently than males, that the animals were too old to benefit from this treatment, or a combination of both factors led to a different physiological outcome (Figure 3.2D; Gaur et al. 2016). The KD VEH group tended to increase in PGC-1α while this effect was prevented by SCRIPT (interaction; p=0.016, Figure 3.2D). Like OxPhos protein and AMPK phosphorylation, PGC1α levels mirror fasted BHB levels (Figure 3.1C). Resultingly, the lack of increase in PGC1α may be due to the lower fasted BHB levels in plasma (Figure 3.1C). Interestingly, higher levels of BHB (5mM) are needed to increase mitochondrial content in C2C12 muscle cells [155]. Though further work on the role of BHB is needed, the current experiment suggests that inhibition of class IIa HDACs blunts the ability of female mice to increase circulating BHB levels, suggesting that scriptaid either inhibits ketone production in the liver or increases the rate of oxidation of ketones in the periphery.

Protein content is primarily controlled by the balance between synthesis and degradation. To date, the understanding of whether histone acetylation regulates protein

degradation has yet to be addressed in skeletal muscle or aging. In the current work, we used a KD or SCRIPT to begin addressing this question. The autophagic system is responsible for generating double membrane vesicles that engulf portions of the cytoplasm, organelles, glycogen, and protein aggregates [156,157]. Within skeletal muscle, the importance of autophagy has been well documented across species. In mice, knocking autophagy gene 7 (ATG7) out of muscle induces a sarcopenic phenotype accompanied with a significant decline in force production [158]—an important implication as a decline in strength is a strong predictor of all-cause mortality [16]. In C. *elegans*, inhibition of ATG8 in the body-wall reduces lifespan, whereas overexpressing it significantly increases lifespan [159,160]. Exercise, increases autophagy, mitochondrial mass, skeletal muscle integrity, neurocognitive behavior, and healthspan [161–164]. Previously, McGee et. al demonstrated that suppression of class IIa HDACs induced by exercise, increases the phosphorylation of pAMPK. pAMPK^{thr172} has been shown to regulate autophagy in in both yeast and mammalian cells [165,166]. To assess AMPKs contribution to autophagy (beyond mitochondrial biogenesis) in skeletal muscle, phosphorylation of its direct target pULK1^{ser555} [167] was measured. SCRIPT tended to, and a KD significantly (diet; p=<0.01) increased ULK1 phosphorylation (Figure 3.3B). Other markers of autophagy, beclin1, p62, and the LC2BII:I ratio were unaffected by either diet or exercise. Interestingly, a marker of mitochondrial specific autophagy (mitophagy), PINK1 showed both a diet (increased) and injection (decreased) effect. The PTEN-induced putative kinase 1 (PINK1) is fundamental to the mitophagy process. PINK1 stabilizes the outer mitochondrial membrane (OMM) and recruits the E3-ubiquitin ligase Parkin to dysfunctional mitochondria. There are conflicting reports on the effect of

age on PINK1, with several studies indicating an increase in mitophagy within skeletal with age [168–170] and others reporting a decrease [21,171,172]. Interestingly, old mice that have undergone an endurance exercise protocol showed decreased in PINK1 protein levels [168] consistent with the effect of SCRIPT. The drop in PINK1 levels with SCRIPT, together with the increase in mitochondrial protein suggests that SCRIPT may be decreasing mitophagy. Therefore, scriptaid may induce exercise-like adaptations in skeletal muscle [42]. However, in order to better understand the role of SRIPT and a KD diet on mitophagy, additional studies are required.

The dystrophin-associated glycoprotein complex (DGC) is crucial to muscle function. Proteins within the DGC, such as dystrophin, α-sarcoglycan, and sarcospan, are essential to protect from shear stress, promote lateral force transfer, and reduce contraction-induced injury [143,147,173]. Our group, and others, have shown that aging skeletal muscle shows a significant decrease in dystrophin protein levels [147,174]. Our data suggests that a 1-month KD started late in life can increase dystrophin protein (Figure 3.4F). Similarly, α-sarcoglycan protein levels tended to increase in the KD VEH animals, whereas the response was blunted in both cases by co-administration of SCRIPT (Figure 3.4G&H). Fujikura and colleagues demonstrated that a KD rich in medium chain triglycerides rescued skeletal muscle phenotype and function in a rat model of Duchenne's muscular dystrophy [77]. Together, these data suggest that a KD can improve dystrophin protein levels and may decrease muscle injury. Interestingly, a KD increased forelimb grip strength despite a tendency to decrease fCSA and Ferret's diameter (Figure 3.4C-E). Like the increase in force transfer proteins, the improved force with a KD was lost with administration of SCRIPT. These data suggest that one

way that a KD may improve muscle function is by improving force transfer and decreasing contraction-induced muscle injury. These data provide an exciting avenue for future research regarding the use of a KD as a potential intervention to treat not only age-related loss in muscle function but also muscular dystrophies.

Conclusions

In conclusion, treatment with HDAC inhibitor scriptaid blunts ketone production in the fasted state when animals are fed a KD. The pattern of fasted BHB production is mimicked in the gastrocnemius' ability to enhance mitochondrial mass and biogenesis. Secondly, SCRIPT may increase mitochondrial mass by decreasing mitophagy in contrast to young male mice that show enhanced PGC-1α [42], indicating there is an age and/or sex dependent effect of scriptaid administration on skeletal muscle. Lastly, a one-month KD increased dystrophin levels in the muscles of old mice and the increase in dystrophin was better associated with the improved grip strength than changes in muscle fiber CSA. These data suggest that a KD may enhance lateral force transmission in skeletal muscle.

Author Contributions

K.B. and J.M.R contributed to conceptualization of the study. S.J.P., E.S.E, E.C., R.C. contributed to the data collection. S.J.P., E.S.E, and K.B., carried out the formal analysis. S.J.P. and K.B contributed to the manuscript. All authors approved the final manuscript.

Conflict of Interest

K. Baar and J. Ramsey has received funding to study ketogenic diets from the NIH. KB is a Scientific Advisor to KetoKind. Prof Baar has also received grants and donations from other nutritional companies such as PepsiCo, Bergstrom Nutrition, Ynsect, and GelTor.

Acknowledgements

This work was supported by a Program Project Grant (PO1 AG062817) from the NIH (USA). Lastly, the first author would like to thank the Los Angeles Lakers for winning the championship in the bubble during which the intervention was being conducted.

Figure legends

Figure 3.1. Administration of Scriptaid Blunts β-hydroxybutyrate Production in the Fasted State and a One-Month KD Increases Grip Strength. A) Schematic of experiment design. 23-month-old female C57Bl/6 were put on an isocaloric (11.2 kcal/day) control (CD) or ketogenic (KD) diet and given daily intraperitoneal injections of vehicle (VEH, gold) or scriptaid (SCRIPT; purple) for 28 consecutive days. B) Body weights over the course of the intervention. C) Blood β-hydroxybutyrate levels in the fed (3-hours post prandial) and fasted state (12-hours post prandial). D) Wire Hang, E) Max Hanging Impulse (calculated as MHI= (time x BW/9.8*1000)), F) Rotarod (time to fall in seconds), G) Grip Strength (Absolute Strength/body weight), H) Open filed (% Time in Center), I) Open Field Distance (cm), J) % Alteration in the Y-Maze, and K) Novel Object Recognition (% Time Exploring the novel object in the test session). Data is displayed as mean ± SEM (n=16-18/group) with symbols for every animal tested.

Figure 3.2. One-month KD Increases Mitochondrial Mass. Western blots for A) Acetylated Lysine, B) β-hydroxybutyrylation of Lysine (βHB-Lysine), C) Oxidative Phosphorylation Protein (Total OxPhos), D) PGC-1, E) Sirtuin 3 (SIRT3), F-H) Kynurenine Aminotransferase 1, 3, and 4 (KYAT1-4) from the GTN muscle were quantified following the one-month intervention. Data is displayed as mean ± SEM (n=5-6/group) with symbols for every animal tested.

Figure 3.3. Scriptaid May Inhibit Mitophagy**.** Western blots for A) phosphorylated AMP Kinase (p-AMPK^{thr172}), B) ULK1 phosphorylation at the serine^{555} site (p-ULK^{ser555}), C)

p62, D) LC3BII:I ratio, E) Beclin1, and F) PTEN-inducible putative kinase 1 (PINK1) from the GTN muscle were quantified following the one-month intervention. Data is displayed as mean ± SEM (n=5-6/group) with symbols for every animal tested.

Figure 3.4. 1-Month Ketogenic Diet Increases Dystrophin Not Cross-Sectional Area

A&B) Histograms of fiber cross-sectional area (CSA) of the GTN muscle plotted for the vehicle (yellow) and SCRIPT (purple) groups on a control (A) or KD (B). Mean measured C) cross-sectional area, D) Maximum Feret Diameter (μM), E) Minimum Feret Diameter (μM), and levels of F) dystrophin and G) α-sarcoglycan protein as well as H) micro-RNA 31 (miR-31) expression. Data is displayed as mean ± SEM (n=3-6/group) with symbols for every animal tested.

Supplementary Figure 3.1

A-F) Tissue weights of the heart (A), liver (B), gastrocnemius (C), tibialis anterior (D), soleus (E), and quadricep (F). Data is displayed as mean± SEM (n=16-18/group) with symbols for every animal collected.

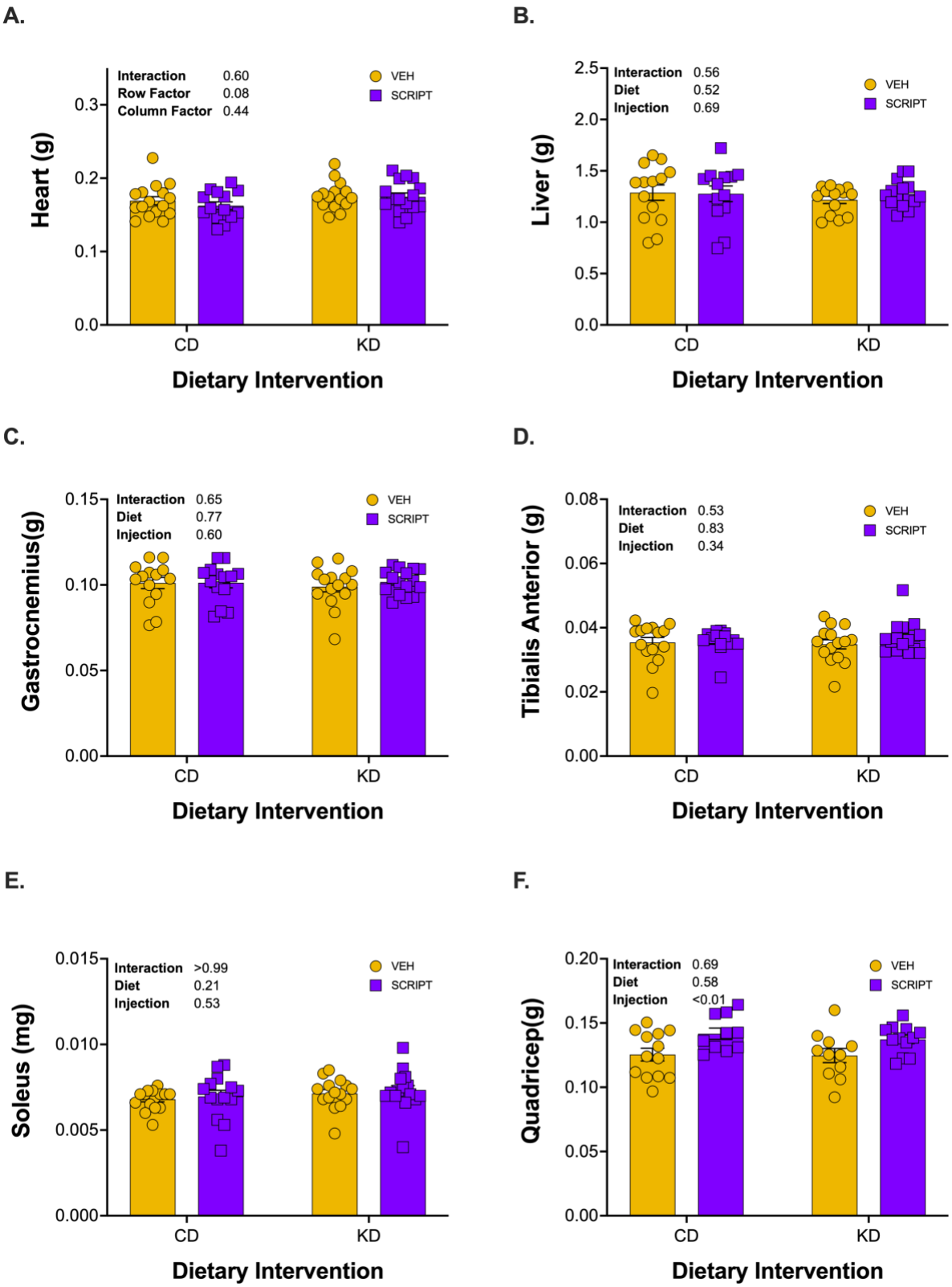
A.
Interaction 0.60
Row Factor 0.08
Column Factor 0.44
VEH
SCRIPT
Heart (g)
0.0
0.1
0.2
0.3
CD
KD
Dietary Intervention
B.
Interaction 0.56
Diet 0.52
Injection 0.69
VEH
SCRIPT
Liver (g)
0.0
0.5
1.0
1.5
2.0
2.5
CD
KD
Dietary Intervention
C.
Interaction 0.65
Diet 0.77
Injection 0.60
VEH
SCRIPT
Gastrocnemius(g)
0.00
0.05
0.10
0.15
CD
KD
Dietary Intervention
D.
Interaction 0.53
Diet 0.83
Injection 0.34
VEH
SCRIPT
Tibialis Anterior (g)
0.00
0.02
0.04
0.06
0.08
CD
KD
Dietary Intervention
E.
Interaction >0.99
Diet 0.21
Injection 0.53
VEH
SCRIPT
Soleus (mg)
0.000
0.005
0.010
0.015
CD
KD
Dietary Intervention
F.
Interaction 0.69
Diet 0.58
Injection <0.01
VEH
SCRIPT
Quadricep(g)
0.00
0.05
0.10
0.15
0.20
CD
KD
Dietary Intervention

<u>Chapter 4:</u> 2-month ketogenic diet preferentially alters skeletal muscle and augments cognitive function in middle aged female mice

This Chapter has been previously published in Aging Cell as:
Pathak, S.J., Z. Zhou, D. Steffen, T. Tran, Y. Ad, J.J. Ramsey, J.M. Rutkowsky, and K. Baar. 2-month ketogenic diet preferentially alters skeletal muscle and augments cognitive function in middle aged female mice. Aging Cell. 2022 Sep 23:e13706.

Abstract

The effect of a ketogenic diet (KD) on middle aged female mice is poorly understood as the majority of this work has been conducted in young female mice or diseased models. We have previously shown that an isocaloric KD started at middle age in male mice results in enhanced mitochondrial mass and function and cognitive behavior after being on diet for 14-months when compared to their control diet (CD) fed counterparts. Here, we aimed to investigate the effect of an isocaloric 2-month KD or CD on healthy 14-month-old female mice. At 16 months of age cognitive behavior tests were performed and then serum, skeletal muscle, cortex, and hippocampal tissues were collected for biochemical analysis. Two months on a KD resulted in enhanced cognitive behavior associated with anxiety, memory, and willingness to explore. The improved neurocognitive function was associated with increased PGC1α protein in the gastrocnemius (GTN) muscle and nuclear fraction. The KD resulted in a tissue specific increase in mitochondrial mass and kynurenine aminotransferase (KAT) levels in the GTN and soleus muscles, and increased kynurenic acid levels in serum. With KAT proteins being responsible for preventing kynurenine from entering the brain and being converted into quinolinic acid—a potent neurotoxin, this study provides a potential mechanism of how a KD may translate changes in skeletal muscle biochemistry into improved cognitive function in middle-aged female mice.

Key words: acetylation, skeletal muscle, mitochondria, cognitive behavior, Alzheimer's disease

Introduction

Over the last decade, there has been increased interest in the potential therapeutic benefits of a ketogenic diet (KD). Currently, there is little known about the impact of KDs in healthy middle-aged female mice. To date, female KD studies have primarily been completed in disease models and young mice [76,150,151]. In male mice, KDs initiated in middle age have increased health span and longevity. Interestingly, in males a KD preserves skeletal muscle mass, strength, and endurance as well as cognitive behavior [6,7]. By contrast, a recent study on the effect of a KD on female mice demonstrated a dramatic decrease in muscle mass and strength [76]. Whether this represents a sex difference in the response to a ketogenic diet, or simply an unpalatable, low methionine diet resulting in a starvation phenotype, remains to be determined.

The maintenance of musculoskeletal and neurocognitive function in male mice on a KD is in stark contrast to the normal decline that occurs with aging. The age-related loss of musculoskeletal and neurocognitive function are termed sarcopenia and age-associated cognitive decline, respectively. The decline in muscle mass and strength, is a predictor of all-cause mortality [175], whereas the incidence of neurocognitive diseases such as Alzheimer's double every 5 years between the ages of 65 and 90 [176]. Even with this high prevalence and the stark personal and economic cost, there are currently few treatment strategies to prevent or slow the progression of either sarcopenia or age-associated cognitive decline.

A decline of mitochondrial mass and function has been hypothesized to drive both sarcopenia and age-associated cognitive decline [176,177]. One intervention that has been shown to delay these conditions of aging is endurance exercise. Endurance exercise improves brain function through both a direct increase in brain-derived neurotrophic factor and the activation of mTORC1 in the brain [178], and an indirect conversion of kynurenine to kynurenic acid [12] by kynurenine aminotransferases (KAT) produced in muscle. Interestingly, the signals that increase KAT activity in muscle and promote the conversion of kynurenine to kynurenic acid, are the same as those activated by exercise and a KD to increase mitochondrial mass—increased peroxisome proliferator activated receptor (PPAR) and PPARγ coactivator 1α (PGC-1α) activity [7,179]. These data suggest that a KD may mimic exercise, increasing mitochondrial and KAT activity in muscle to improve both muscle and brain function. Since many individuals are unwilling or unable to exercise sufficiently to achieve these adaptations, interventions like a KD that mimic endurance exercise are desperately needed to improve physical and mental function with age.

Many dietary interventions that increase longevity in model organisms are thought to mimic aspects of endurance exercise. For example, caloric restriction [137], intermittent fasting [136], time restricted feeding [135], and a KD [7] increase mitochondrial mass and function. A KD, where fats are high and carbohydrates are limited, similar to fasting [45] and exercise [180] results in the production of ketones such as β-hydroxybutyrate (BHB) by the liver. BHB has been shown to increase lifespan in C. *elegans* [181]. In response to the rise in circulating BHB, there is an increase in acetylated protein levels—a post

translational modification that can alter gene expression and protein activity, stability, or localization. A similar shift in acetylation levels is seen following exercise—another stimulus that increases fat oxidation, mitochondrial biogenesis, and neurocognitive function [31,178]. Together, these data suggest that ketosis directly affects muscle and either directly or indirectly affects brain function in a way that may serve as an exercise mimetic.

Even though ketogenic diets have been proposed to improve aging, to date the majority of studies supporting this hypothesis have been performed in male mice. In contrast to the data from males, a recent study looking at the effect of a ketogenic diet on females demonstrated a dramatic decrease in muscle mass and strength [76]. Therefore, whether a KD is viable and beneficial in older females remains to be determined.

In the present study, the effect of a two-month isocaloric ketogenic diet was compared with a control diet in middle aged female C57BL/6JN mice (starting at 14 months-old). After two months on the diets, the effects on cognitive behavior, body mass, muscle mass and strength, tissue specific acetylation levels, KAT protein levels in muscle and liver, kynurenic acid in blood, and mitochondrial mass were determined. We hypothesized that a KD would increase acetylation levels, mitochondrial mass and KAT protein levels in a tissue specific manner resulting in an increase in KYNA and enhanced cognitive performance.

Methods

Animal Husbandry

Female C57BL/6JN mice were obtained from the NIA Aged Rodent Colony at 12 months of age. Mice were housed in polycarbonate cages in a HEPA filtered room with controlled temperature (22–24°C) and humidity (40– 60%). Mice were maintained on a 12-hour light-dark cycle and health checks were performed daily. Health screens were completed on sentinel mice, which were housed on the same rack and exposed to bedding from the study mice, every three months. All tests (MHV, Sendai, PVM, MPV, MVM, M.pul and arth, TMEV [GDVII], Ectro, EDIM, MAD1 and 2, LCM, Reo-3, MNV) were negative throughout the study. All animal protocols were approved by the UC Davis Institutional Animal Care and Use Committee and were in accordance with the NIH guidelines for the Care and Use of Laboratory Animals.

Experimental Diets

Mice were group housed and provided ad libitum access to a chow diet (LabDiet 5001; LabDiet, Saint Louis, MO, USA) until 14 months of age. Thereafter, mice were individually housed and randomly assigned to a control (CD) or a protein-matched ketogenic (KD) diet and all mice were provided 11.2 kcal/day of CD or KD for the duration of the study. This amount was selected to match the measured chow food intake during the acclimatization period. The CD contained (% of total kcal) 10% protein, 74% carbohydrate, and 16% fat. The KD contained 10% protein, <0.5% carbohydrate, and 89.5% fat. Diets were made in-house. The CD was a modified AIN93G diet with a lower protein content to match the KD. Table 1 provides a detailed description of the diet

composition. Mineral mix TD.94046 was used for the CD and TD.98057 was used for the KD to avoid carbohydrate carriers in the mix.

Table 1: Composition of the experimental diets

	Control	Ketogenic
Energy density (kcal/g)	3.8	6.7
kcal/day	11.2	11.2
Ingredients	**g/kg diet**	
Casein	111	191
DL-methionine	1.5	2.7
Corn starch	490	--
Maltodextrin	132	--
Sucrose	100	--
Mineral mix TD.94046	35	--
Mineral mix TD.98057	--	24
Vitamin mix TD.40060	10	18
Soybean oil	70	70
Lard	0	582
Calcium phosphate dibasic	--	19.3
Calcium carbonate	--	8.2
Cellulose	48	85
Potassium phosphate monobasic	2.4	--
TBHQ	0.014	0.126

Blood ketone measurement

Blood β-hydroxybutyrate level was measured using a Precision Xtra glucose and ketone monitoring system (Abbott, Chicago, IL, USA) through a tail nick either 3 hours postprandial or following a 12-hour overnight fast.

Body composition

Body composition was evaluated using NMR relaxometry (EchoMRI-100H, EchoMRI LLC, Houston, TX, USA) after 2 months of diet intervention.

Mouse behavior tests

A series of behavior tests were performed at 16 months of age. All tests were conducted in the light cycle.

Barnes maze

The Barnes maze was used to assess spatial learning and memory. The maze was a white round plastic disk (92 cm diameter) with twenty holes (5 cm diameter) evenly distributed on the periphery. A black escape box equipped with a step and filled with a layer of fresh bedding was attached underneath one of the holes. The maze was raised 80 cm above the floor, and an overhead LED light source was used to illuminate the maze (700 lux). Different images were placed around the maze to be used as visual cues. In training trials, mice were placed in the middle of the maze and covered under a black bucket. The light was switched on 10 seconds later and the bucket was immediately lifted. Mice were allowed to explore the maze for 3 minutes or until they entered the escape box through the target hole. Mice were directed to the target hole and gently nudged into the escape box if they did not enter within 3 minutes. The light was switched off once the mouse was inside the box and the mouse was returned to the home cage after 1 minute. Mice were trained with 3 trials per day for 3 days with an inter trial interval of 15-20 minutes. On the fourth day (probe day), the escape box was removed, and mice were allowed to explore for 2 minutes. Videos were recorded and analyzed using the Ethovision XT15 software (Noldus, Wageningen, the Netherlands).

Y maze spontaneous alternation test

The Y maze was used to assess short-term working memory. The apparatus consisted of a white acrylic Y-shaped maze. Each arm was 35 x 8 x 15 cm (L x H x W) in

dimension and was separated by a 120° angle. Mice were placed in the center of the maze and allowed to explore for 6 minutes. Videos were recorded and movement of the mice was tracked using the Ethovision XT15 software (Noldus, Wageningen, the Netherlands). A complete arm entry was defined when the center point of the mouse travelled to the distal side of the arm (more than 1/3 of the arm length) and returned to the center of the maze. An alternation occurs when the mouse enters three different arms consecutively. The percent alternation was calculated as ((number of alternations) ÷ (number of total arm entries - 2)) x 100%.

Open field test

The open field test was conducted in a 40 x 40 x 40 cm white plastic box to evaluate mice's general locomotor activity level, anxiety, and willingness to explore. Mice were placed at the corner of the arena and videos were recorded and analyzed for 15 minutes using the Enthovision XT15 software (Noldus, Wageningen, the Netherlands). A 25x25 cm middle square was defined as the center zone.

Novel object recognition test (NOR)

The novel object recognition test was conducted to evaluate recognition memory. This test was performed in the same apparatus as the open field test, which was also used as the acclimation session for the NOR. The familiarization session was conducted the morning following the open field test. During this session, two identical objects were placed in the arena, and mice were allowed to explore for 10 minutes. In the novel object session, performed 6 hours after the familiarization session, one of the old objects was replaced with a novel object (the novel side was randomized among mice),

and the test was performed over 10 minutes. A small orange cone and a cell culture flask (filled with sand) with similar height were used as the objects and were randomly assigned as the old or novel object. A mouse was considered as exploring an object if the nose of the mouse was pointed toward the object and was within 2 cm from the object. Time exploring each object was manually scored using two stopwatches.

Elevated plus maze

The elevated plus maze was used to assess anxiety related behavior of the mice. The apparatus consisted of a plastic plus-shaped maze with two open arms (30 cm L x 6cm W x 1 cm H) and closed arms (30 cm L x 6cm W x 20 cm H) with a square center zone (6 cm x 6 cm). The maze was elevated 70 cm from the floor. Mice were placed on the center zone, facing an open arm, and were allowed to explore the maze for 5 minutes. Videos were recorded and analyzed with the Ethovision XT15 software (Noldus, Wageningen, the Netherlands). Time on open arms was defined when the center point of the mouse traveled beyond 4.5 cm from the start of the arm.

Rearing test

Mice were placed into a clear acrylic cylinder (15 cm diameter) and videos were recorded for 5 minutes to estimate their exploratory behavior. The videos were manually scored, and a “rear” was defined as the mouse putting the forepaws on the side of the cylinder.

Grid wire hang test

The wire hang was used to measure skeletal muscle endurance. Briefly, mice were placed on a stainless-steel wire mesh screen (1 mm wires and 1x1 cm grids) raised 40 cm above the bottom of a plastic box. Soft towels were placed at the bottom of the box

to cushion the fall. Upon placing the mice on the top of the screen, the screen was slightly shaken to ensure a firm grip of the mice, and then inverted such that the mice hang on the wires using all four limbs. Time till the mice fell was recorded. If the maximal hanging time did not exceed 180 seconds, mice were given another trial (maximum of 3 trials) after resting in the home cage for approximately 30 minutes. Maximal hanging impulse was computed as (maximum hanging time (s) x body weight (kg) x 9.8 $N \cdot kg^{-1}$).

Grip strength

Mice were encouraged to grab and pull on a single metal bar attached to an Imada push-pull force scale (PS-500N, Northbrook, IL). Mice were given two rounds of three trials each and the maximum grip strength was used to gauge skeletal muscle strength.

Rotarod

Rotarod testing was used to determine motor coordination and balance. The test was conducted on a Rota Rod Rotamex (Columbus Instruments, Columbus, OH, USA). Once the mice were placed on the rod, the rod started rotating at 4 rpm and accelerated at 1 rpm/6 seconds to a maximum of 40 rpm. Mice were tested for 3 trials each day for 2 days. The latency to fall and the speed at fall were recorded.

Euthanasia and Tissue Collection

Three days after the last behavior test, mice were euthanized under isoflurane anesthesia. Serum, liver, heart, hippocampus, cortex, quadriceps, soleus, gastrocnemius (GTN), and tibialis anterior muscles were collected and snap frozen in liquid nitrogen for biochemical analysis or in liquid nitrogen cooled isopentane for histological analysis. All tissues were then stored at -80˚C until further processing.

Tissue homogenization and western blotting

Gastrocnemius, brain, and liver tissue were powdered on liquid nitrogen using a hammer and pestle. Two scoops of powder were then aliquoted into 1.5 mL Eppendorf tubes and homogenized in 250 µL of sucrose lysis buffer [1M Tris, pH 7.5, 1M sucrose, 1mM EDTA, 1mM EGTA, 1% Triton X-100, and 1X protease inhibitor complex]. The solution was set on a shaker for 60 minutes at 4°C, spun down at 8,000g for 10 minutes, supernatants were transferred to new Eppendorf tubes and protein concentrations were determined using the DC protein assay (Bio-Rad, Hercules, CA). Equal aliquots of 500 µg of protein were diluted in 4X Laemmli sample buffer (LSB) (final volume 200uL) and boiled for 5 minutes at 100°C. 10µL of protein sample was loaded onto a Criterion TGX Stain-Free Precast Gel and run for 45 minutes at a constant voltage of 200V. Proteins were then transferred to an Immobilon-P PVDF membrane, after it was activated in methanol and equilibrated in transfer buffer, at a constant voltage of 100V for 30 minutes. Membranes were blocked in 1% Fish Skin Gelatin (FSG) in TBST (Tris-buffered saline w/ 0.1% Tween) and incubated overnight at 4°C with the appropriate primary antibody diluted in TBST at 1:1,000. The next day, membranes were washed with TBST for 5 minutes, and successively incubated at room temperature with peroxidase-conjugated secondary antibodies in a 0.5% Nonfat Milk TBST solution at 1:10,000. Bound antibodies were detected using a chemiluminescence HRP substrate detection solution (Millipore, Watford, UK).Band quantification was determined using BioRad Image Lab Software. Antibodies used were as followed: Total Oxidative Phosphorylation (abcam MS604-300), PGC1alpha (ab54481), p-AMPKthr172 (CS2531S), KAT1 (ab194296), KAT3 (sc365219), FABP1 (KAT4) (ab171739),

PINK1(sc517353). LC3BI:II (cs2775S), ATG7 (cs8558S). KBHB (PTM-1201), acetylated lysine (cs9481S), acetylated p300/CBP (cs4771), acetylated p53 (cs2570), Sirtuin 1 (cs9475S), Sirtuin 3 (cs5490S), IRE1α (cs3294), BiP (cs3183S), CHOP (cs2895S), SOD2 (sc137254), phosphorylated eif2alpha (cs3398).

Nuclear Isolation

Cytosolic and nuclear protein fractions were extracted from frozen GTN muscles following homogenization using a glass-on-glass Dounce homogenizer in Buffer A (5mM KCl, 10mM Tris-HCL pH 7.4, 0.1% Triton X, 1.5 mM $MgCl_2$, protease inhibitor complex). Samples were centrifuged at 1800xg for 5 minutes and the supernatant was transferred to new tubes and labeled Cytosolic Fraction. The pellet from initial centrifugation was washed in Buffer A three times with subsequent centrifugation at 1000xg for 15 minutes. Following the third centrifugation, the supernatant was discarded, and the pellet was submerged in 80µL of NET buffer (20mM HEPES pH7.9, 1.5 mM $MgCl_2$, 0.5mM NaCl, 0.2 mM EDTA, 20% Glycerol, 1% Triton-x 100, protease inhibitor) and sonicated for 10 seconds. The resuspended pellet was centrifuged at 10,000xg for 5 minutes and the resulting pellet was transferred to a new tube and labeled Nuclear Fraction.

Enzyme-Linked Immunosorbent Assay (ELISA)

Kynurenic acid levels were measured using collected serum samples. The ELISA was carried out per the manufacturers protocol (MBS7256170, MyBioSource, San Diego, CA).

Total RNA and Gene Expression

Total RNA was isolated from frozen GTN muscle powder using Norgen Biotek Animal Tissue RNA Purification Kit (Cat # 25700; Ontario, Canada) according to manufacturer's

instructions. RNA quality and quantity were measured by spectrophotometry (Epoch Microplate Spectrophotometer, BioTek Instruments., Winooski, VT). Following isolation, 1 ug RNA was reverse transcribed to cDNA using a cDNA synthesis mix (MultiScribe RT, 10x RT buffer, 10x Random Primers, dNTPs, RNase inhibitor; Applied Biosystems, Foster City, CA). Real time qPCR (CFX384 Touch Real-Time PCR Detection System; BidRad, Hercules, CA) was performed with each sample amplified in triplicate using SYBR green as the fluorescent reporter (BioRad, Hercules, CA; PCRbio.com, Wayne, Pennsylvania). Expression of Ppargc1a, Sirt1, Tfam, and Mfn1 (Invitrogen, ThermoFisher, Waltham, WA) was determined using $2^{-\Delta\Delta Ct}$ method with B2m (IDT, Coralville, IA) as housekeeping control. Results are presented relative to average ΔCt of the control group.

Statistical analysis

All values are expressed as mean ± SEM p values <0.05 considered significant (* p<0.05, ** p<0.01, *** p<0.001). All analyses were performed using GraphPad Prism 8.1 (GraphPad Software Inc., San Diego, CA). For behavior tests, comparisons between the CD and KD group were conducted using an un-paired t-test or a non-parametric Man-Whitney test. Outliers were excluded following a ROUT test. Gene expression data ($2^{-\Delta\Delta Ct}$) was normally distributed with no outliers and analyzed with an un-paired t test with Welch's correction.

Results

Isocaloric feeding of a KD produced higher β-hydroxybutyrate levels without alterations in body weight in middle-aged female mice.

Female mice on a KD exhibited significantly elevated levels of postprandial and fasting blood BHB levels compared to mice fed the CD (Figure 4.1A). Both the CD and KD mice gained weight over the course of the study (CD: +1.93 g, KD: +2.54 g), but there was no significant difference in body weight between diet groups at any time point (Figure 4.1B). Interestingly, there was a trend toward increased percent body fat mass in KD mice (p=0.06, Figure 4.1C) compared to CD mice, and this might contribute to the slightly higher (not significant) body weight observed in the KD group. Mass of the gastrocnemius (GTN), quadricep (QUAD), and soleus (SOL) muscle showed no differences between the two groups, while the tibialis anterior (TA) trended towards significance in the KD fed mice (p=0.065) (Table 4.2). Lastly, there was a small but significant decrease in liver weight amongst KD fed animals (Table 4.2).

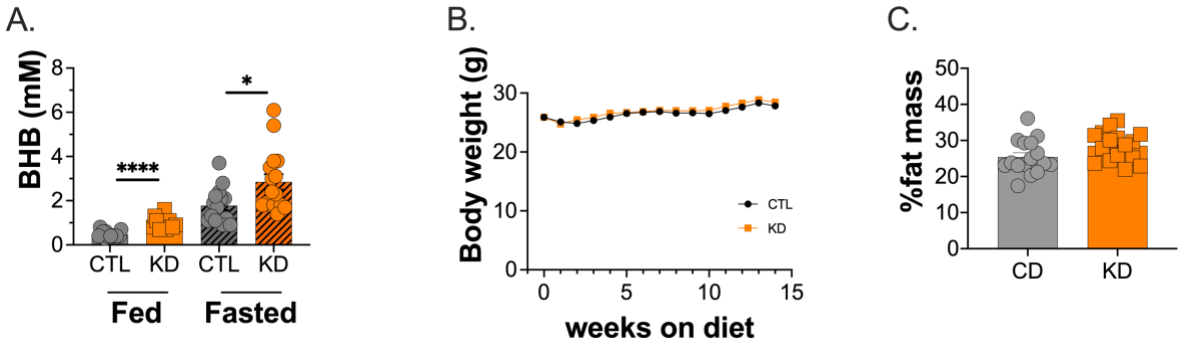

A 2-month KD increased exploratory behavior and some measures of locomotor activity in healthy middle-aged female mice.

Female KD mice were more active in the rearing tests (Figure 4.1D), consistent with an increased locomotor activity and willingness to explore. The total distance travelled on the Y maze and elevated plus maze was also significantly increased in female mice fed a KD (Figure 4.1E and 4.1F), although no difference was observed in the open field test (Figure 4.1G).

Although the percent time spent in the center region of the open field, a measure of anxiety, was not altered with a 2-month KD (Figure 1H), there was a trend for increased time on the open arms of the elevated plus maze (p=0.07, Figure 4.1I), consistent with reduced anxiety on the elevated plus maze or increased willingness to explore the open arms.

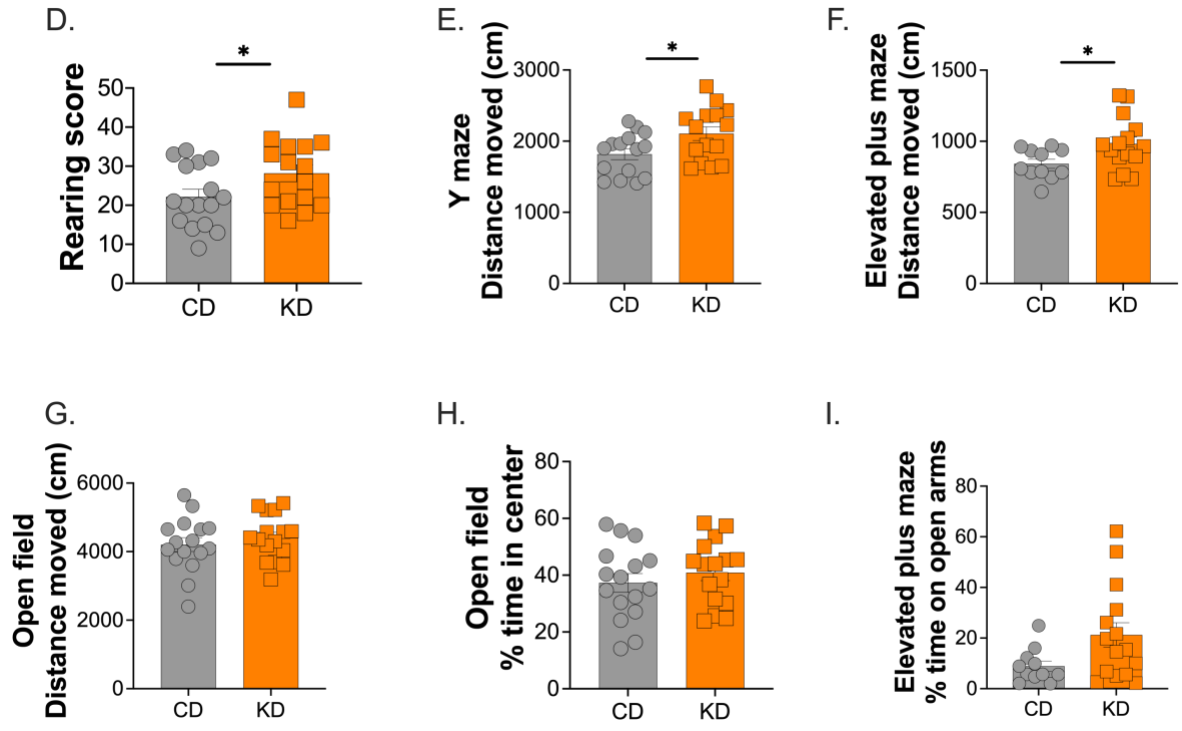

The 2-month KD did not impact performance in grip strength (Figure 4.1J), grid wire hang (Figure 4.1K), or rotarod (Figure 4.1L). These results suggested that neither motor coordination nor strength/endurance were altered in healthy middle-aged female mice fed a short-term KD.

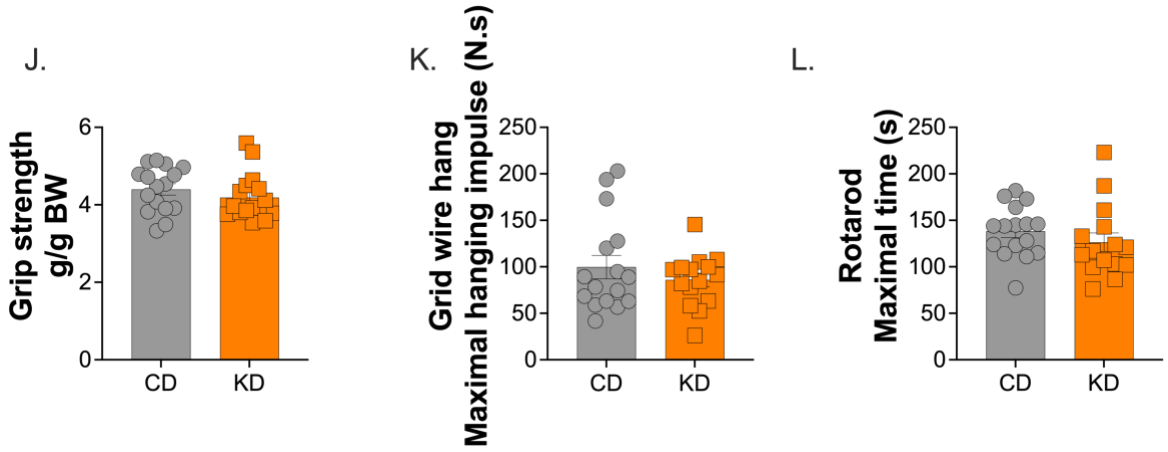

Spatial learning and memory were improved in female mice after 2 months on a KD, but no changes in recognition memory or short-term working memory were observed.

A significant increase in time spent in the target quadrant (Figure 4.1M) and a strong trend toward a decreased latency to find the target hole (p=0.06, Figure 4.1N) in the Barnes maze probe trial were observed in female KD mice, suggesting improved spatial learning. Neither short-term working memory measured through the Y-maze spontaneous test (Figure 4.1O) nor recognition memory evaluated using the novel object recognition test (Figure 4.1P) was impacted by 2 months of a KD.

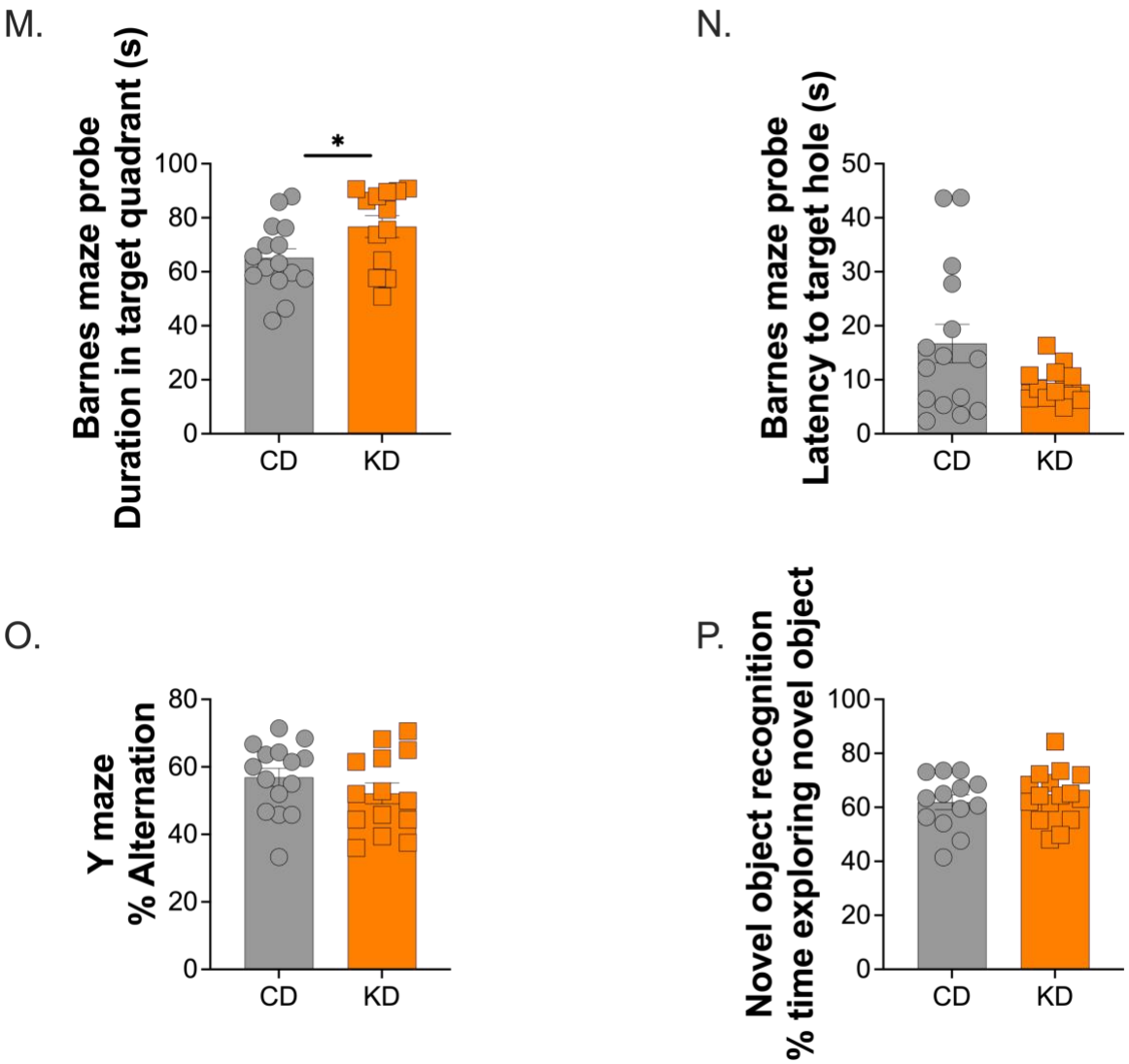

Increased Acetylation within the Liver is Not Associated with Mitochondrial Biogenesis

Acetylated and β-hydroxybutyrylated lysine (βHB-Lysine) moieties were measured via western blotting and found to be significantly increased, by 70% and 25% respectively, in female KD mice when compared to controls (Figure 4.2A &B). Acetylation of the acetyl transferase p300/CBP was 2-fold higher (Figure 4.2C) with its direct target p53 showing similar increases (Figure 4.2D) in the KD mice. There was no change in SIRT1 or SIRT3 protein in the liver as a result of the diet (Figure 4.2E). The phosphorylation of AMPK at Thr172 was also unchanged (Figure 4.2F). As an estimate of mitochondrial

mass, proteins in the oxidative phosphorylation pathway were measured. Only proteins from complex IV were increased in the liver of female mice on a KD (Figure 4.2G). There were no significant changes in markers of the integrated stress response, IRE1α, BIP, CHOP, p-eIF2α, and SOD2 (Figure 4.2I & H) between diet groups, indicating that the diet was well tolerated in female mice, irrespective of the decreased liver weight. There was no difference in kynurenine aminotransferase levels (Figure 4.2J-L).

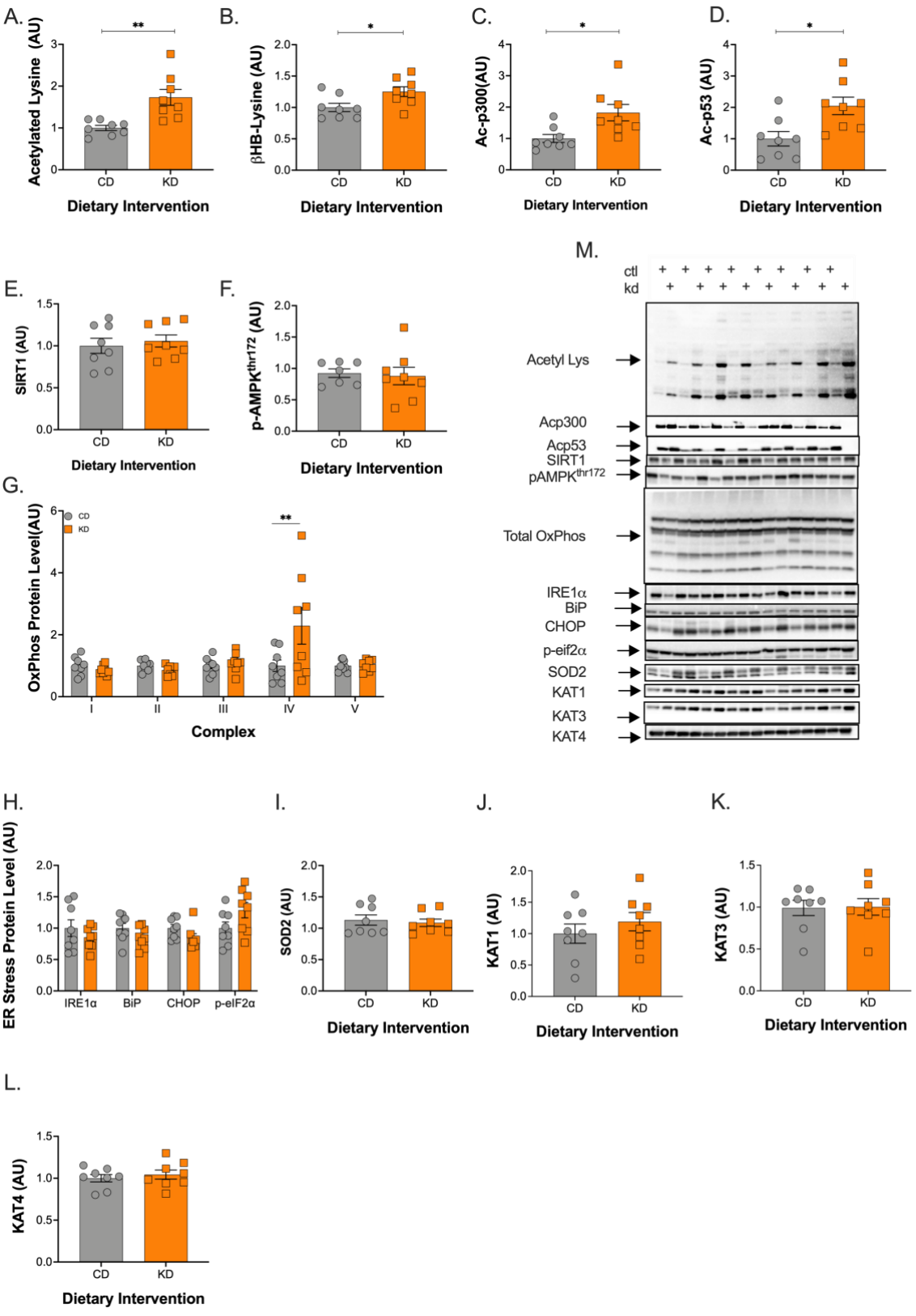
A.
Acetylated Lysine (AU)
Dietary Intervention
CD
KD
B.
βHB-Lysine (AU)
C.
Ac-p300(AU)
D.
Ac-p53 (AU)
E.
SIRT1 (AU)
F.
p-AMPKthr172 (AU)
G.
OxPhos Protein Level(AU)
Complex
I
II
III
IV
V
M.
ctl
kd
Acetyl Lys
Acp300
Acp53
SIRT1
pAMPKthr172
Total OxPhos
IRE1α
BiP
CHOP
p-eif2α
SOD2
KAT1
KAT3
KAT4
H.
ER Stress Protein Level (AU)
IRE1α
BiP
CHOP
p-eIF2α
I.
SOD2 (AU)
J.
KAT1 (AU)
K.
KAT3 (AU)
L.
KAT4 (AU)

Increased Acetylation within the Gastrocnemius is Associated with Mitochondrial Biogenesis and Increased KAT Levels

To understand how different sets of highly metabolically active tissues are impacted by the ketogenic diet— acetylation levels and mitochondrial mass was also determined in the gastrocnemius (GTN) muscle. Similar to the liver, acetylated lysine, βHB-lysine, and ac-p300/CBP increased in female KD mice compared with their control counterparts (Figure 4.3A-C). Ac-p53 protein levels also tended to increase (p=0.0726) on a KD (Figure 4.3D). SIRT1 showed a strong trend to increase (p=.0734), whereas SIRT3 increased significantly (Figure 4.3D &F) in the KD mice. ER stress markers were unchanged in the GTN (Figure 4.3G) with the exception of phosphorylation of eIF2α which increased 2-fold in female KD mice (Figure 4.3G).

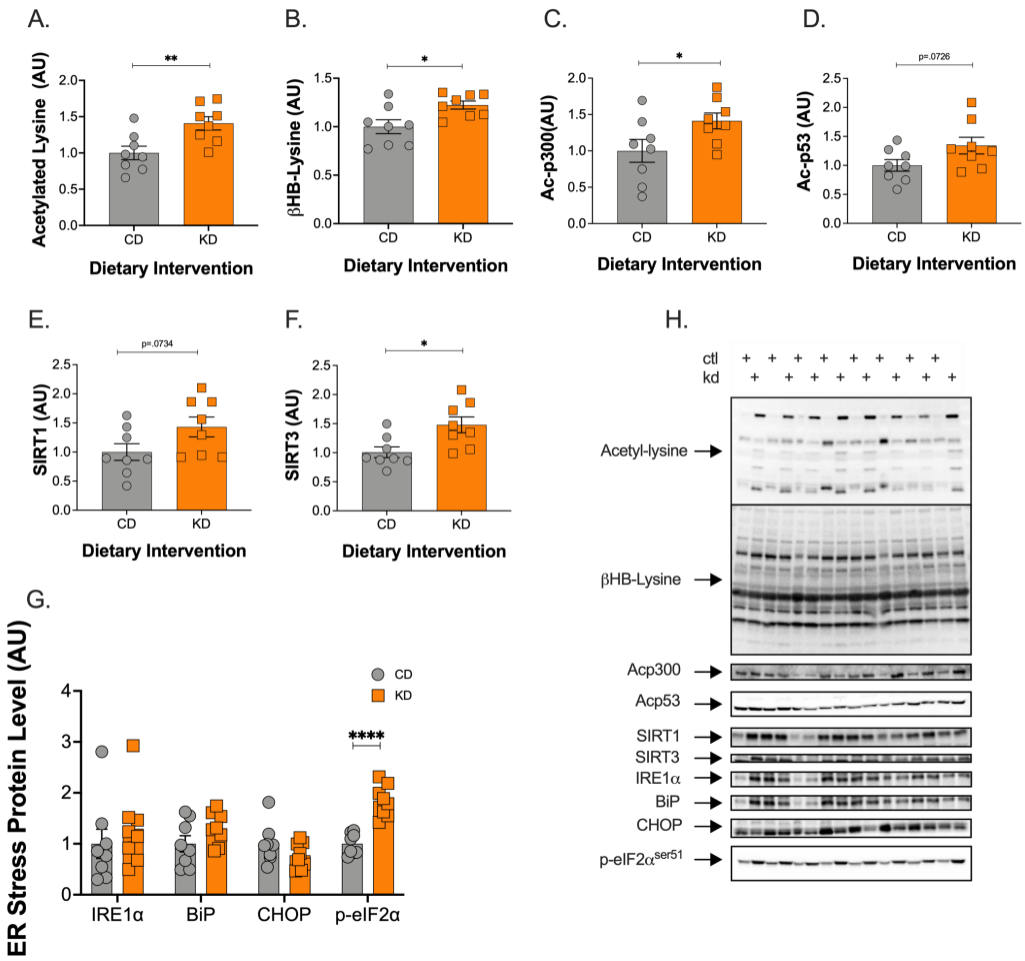

Total OxPhos levels were quantified in the GTN muscle. Proteins within complexes I/III/IV/V increased significantly in the female KD mice, whereas complex II showed a strong tendency (p=.0625) to increase (Figure 4.4A). In the GTN, both total PGC-1α and p-AMPK^{thr172} were significant higher in the KD fed animals (Figure 4.4C & D). Additionally, female KD mice showed significantly greater nuclear localization of PGC-1α (Figure 4.4E). KAT1 and KAT4 increased on a KD, whereas KAT3 remained unchanged (Figure 4.4G-I). Concomitant with the increase in KAT protein in muscle, plasma kynurenic acid tended to increase on a KD (Figure 4.4J). Since PGC-1α has been implicated in controlling mitochondrial autophagy (mitophagy), PINK1, LC3B II:I

and ATG7 proteins were quantified and there were no differences between the diet groups (data not shown).

Selected Mitochondrial Gene Expression is Unchanged in Skeletal Muscle

Despite an increase of total and nuclear PGC-1α protein (Figure 4.4C & E), there was no difference in the expression of *Ppargc1a* in the GTN between the control and ketogenic diet groups (Figure 4.4B). This may suggest that post-translational modifications underlie the increase in total and nuclear PGC-1α. As with PGC-1α, there was no difference in expression of *Sirt1* or genes downstream of PGC-1α (*Tfam* and *Mfn1*) between the diet groups (Figure 4.4B).

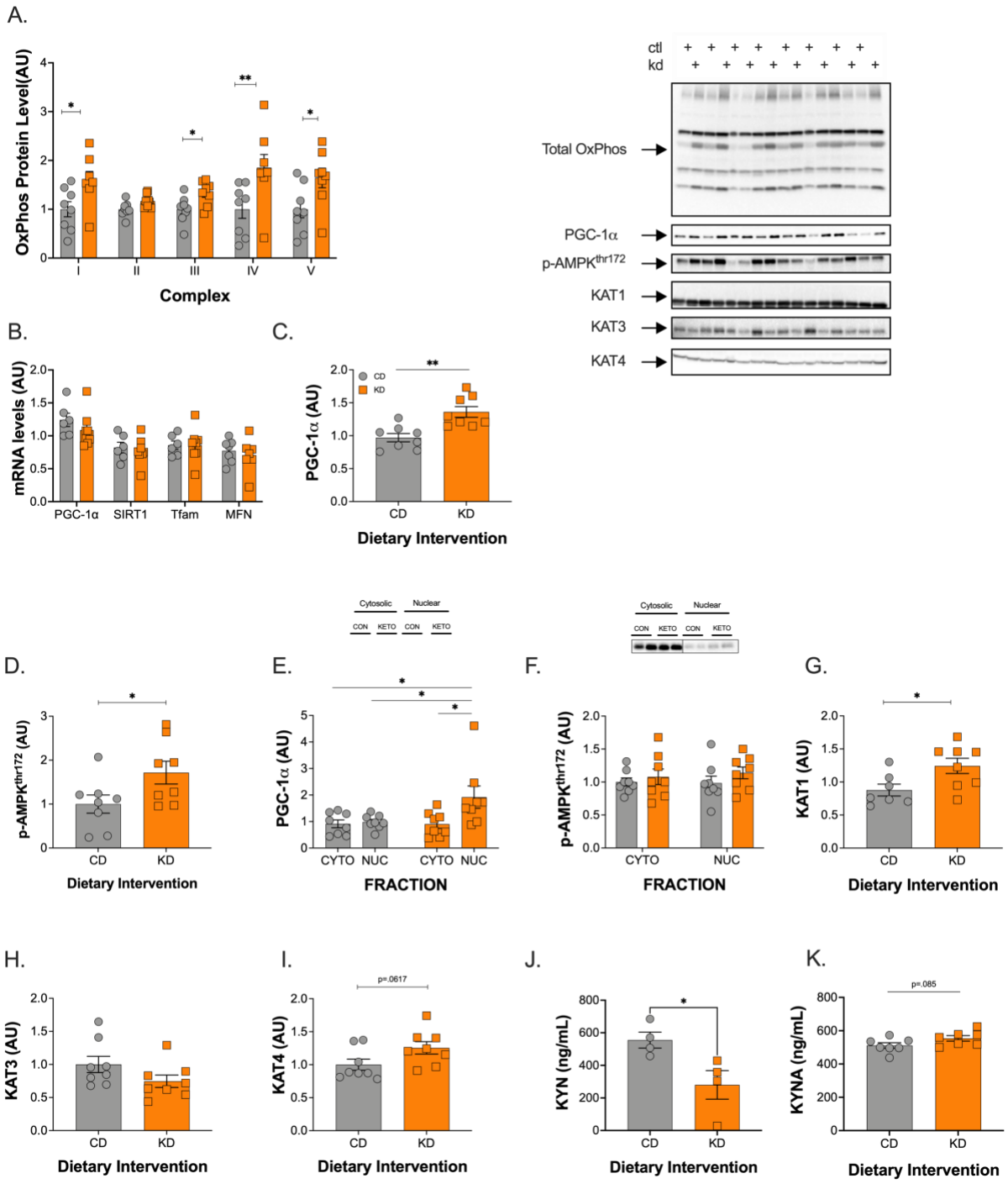

KAT4 specifically increases in response to a KD in Soleus Muscle

To understand how a KD effects skeletal muscle with differing fiber type composition, the soleus muscles from the mice were prepared for western blot analysis. As expected, levels of acetylated lysine increased significantly in the KD fed mice when compared to

controls (Figure 4.5A). There was no increase in PGC-1α (Figure 4.5B) SIRT1 or 3 (Figure 4.5C) in the more oxidative soleus muscle. Unlike the GTN muscle, KAT4 was the only KAT protein to significantly increase in the soleus while, KAT1 significantly decreased (Figure 4.5C-E), suggesting muscle-specific adaptations of different KAT isoforms.

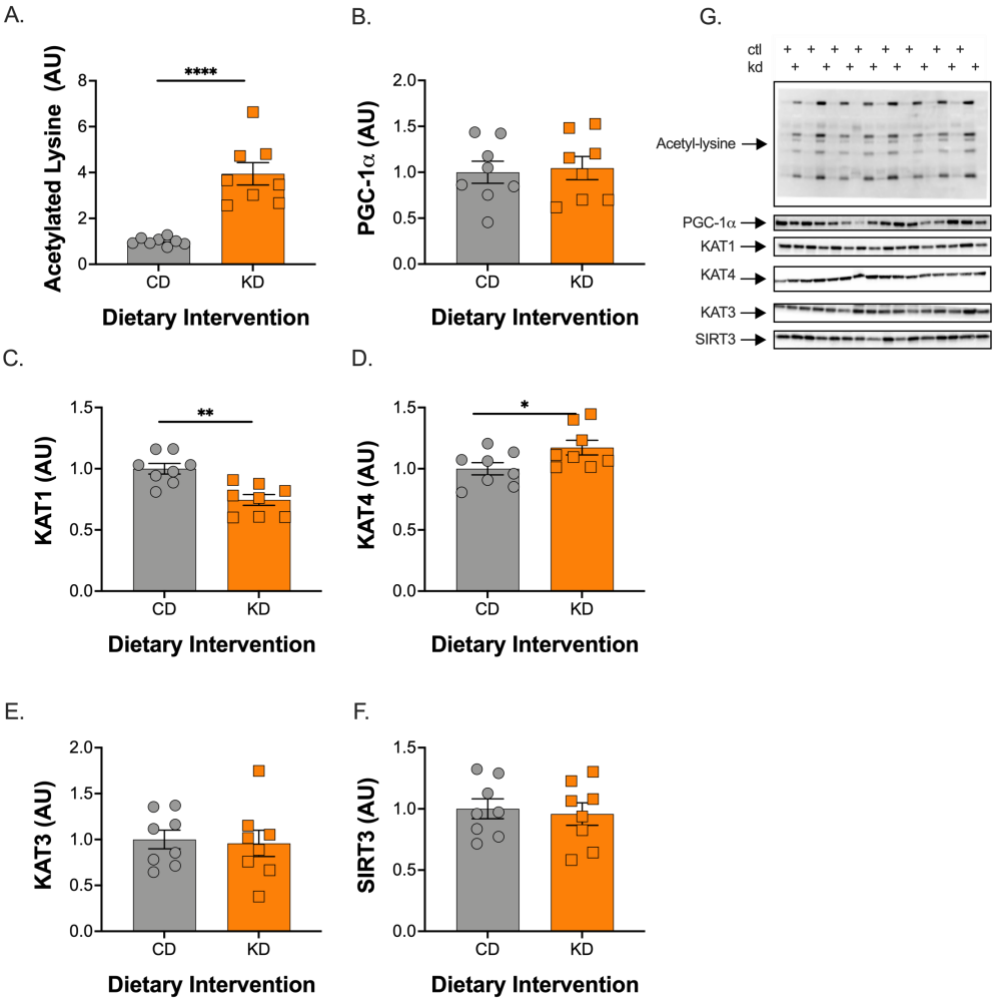

Changes in Cognitive Behavior Occur Irrespective of Changes in Brain Acetylation and Mitochondrial OxPhos Protein Levels

In the cortex, there was no change in acetylated proteins between female control and KD mice, whereas in hippocampal tissue there was a strong trend towards a decrease

in protein acetylation (p=0.0575) (Figure 4.6A & E). Further, no changes were seen in BHB-lysine levels between the groups (Figure 4.6B & F). Lastly, representative OxPhos proteins in both the cortex and hippocampus were unchanged by a 2-month KD (Figure 4.6C & G).

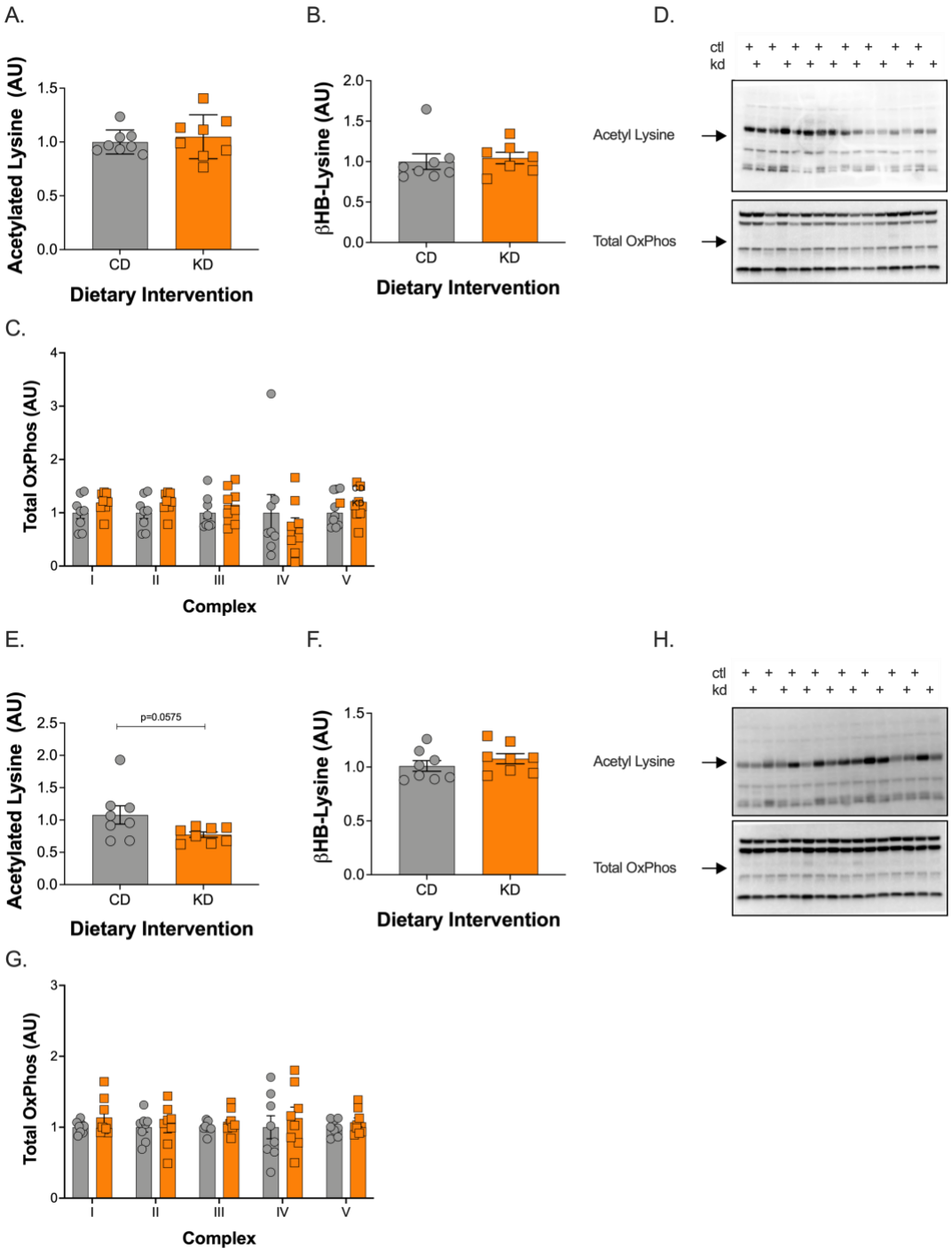

Discussion

The objective of this study was to determine whether a ketogenic diet (KD) negatively affected muscle mass and function in female mice. A secondary goal was to determine the neurocognitive effect of a short-term ketogenic diet in middle aged mice. Our data on 14-month-old female mice that were on 2 months of a 11.2 kcal/day control or KD, shows that a KD is well tolerated in female mice and preferentially alters skeletal muscle metabolism leading to increased acetylation of lysine residues, mitochondrial mass, and kynurenine aminotransferase (KAT) levels. Further, these changes in muscle function occurred in concert with a concomitant increase in kynurenic acid in the blood and improvement in neurocognitive behavior related to memory and anxiety.

Thus far, studies on KD fed female mice have produced equivocal results regarding body weight maintenance. Previous reports include an increase [151,182], decrease [76,150], or unchanged [183] body weight. Nakao and colleagues had recently reported that a KD can induce severe weight loss and skeletal muscle atrophy in young female mice [76]. Here we show that middle-aged female mice on an isocaloric KD maintain body weight, muscle mass and muscle function much the same as male mice [6,41,77]. It is important to note, the KD used by Nakao and colleagues was low in protein and may have been deficient in methionine, which has been shown to be a primary cause of body weight and lean mass loss observed on low-protein KDs [184].

Treatments that shift metabolism, such as caloric restriction, exercise, and a KD, enhance mitochondrial mass and activity and extend life span [6,185,186]. Common amongst these three interventions is an increase in acetylation—an important post

translational modification. The removal of the positive charges within histones decreases their interaction with negatively charged DNA, resulting in more open chromatin and increased transcriptional activity [26]. In non-histone proteins, the charge change can result in a change in shape that alters the location, activity, or stability of the protein [4]. We have previously demonstrated that in response to a KD there is an ~6-fold increase in acetylated lysine levels in liver tissue in male mice [6]. Here, we measured a smaller ~2-fold increase in acetylated lysine in the livers of female mice following 2 months on a KD (Figure 4.2A). There were no signs of mitochondrial biogenesis in the liver in response to the increase in acetylation, except for a small but significant rise in complex IV (Figure 4.2G). This is consistent with recent findings published by our group, showing that male mice on a KD for 1-month had no difference in liver mitochondrial complex I activities, whereas a significant change in complex IV activity was observed [41].

In line with our hypothesis that a KD would increase acetylation levels, mitochondrial mass and KAT protein levels, mitochondrial mass increased in the GTN muscle of middle aged female mice. The effects of a KD on acetylation and mitochondrial mass and activity mirrors those of male mice on a KD [6] or those treated with the HDAC inhibitor scriptaid, including increased fat oxidation, mitochondrial mass and fatigue resistance in skeletal muscle [42]. These results suggest that acetylation may be an important mediator of a KD. In support of this hypothesis, the increased mitochondrial mass on a KD was associated with greater acetylation of histone acetyltransferase protein (HAT) p300 and its direct target p53 within the gastrocnemius (GTN) muscle [187]. Acetylation of p300 on the 17 lysine residues within its regulatory domain stimulates

acetyltransferase activity and enhances the ability to interact with target proteins [80,82]. The importance of p300 in skeletal muscle was recently demonstrated in mice with a skeletal muscle-specific knockout of p300 who showed decreased grip strength and rotarod performance without histological evidence of disease [83]. Together, these data suggest that p300 may be a candidate for future studies regarding the KD and muscle function with age. One way that a KD could mediate the effects of p300 in skeletal muscle is through opening chromatin around myogenic regulatory factor protein (MyoD) binding sites [188]. Since these sites are crucial for skeletal muscle development, function, and regeneration, KD-dependent increases in p300 activity could underlie some of the benefits of the diet on muscle mass and function with age. It is important to note that no differences were seen in grip strength, wire hang, or rotarod performance between the diet groups. This finding is similar to what we see with 1 month of a KD in middle aged male mice [6]. By contrast, grip strength and wire hang improved in 26-month-old male mice who had been on a KD for 14 months, suggesting that the functional benefits of the diet may be more pronounced in older animals where loss of strength and endurance is normally observed. The acetylation of p53, which is fundamental for its activity, complex assembly and therefore its cellular effects [58], was increased in the GTN muscle of female mice, as previously demonstrated in male mice [6]. Active p53 can move to mitochondria where it stabilizes mtDNA and prevents mtDNA damage [59]. Whole body knockout (KO) of p53 results in a decline in mitochondrial protein content, aerobic capacity, and mtDNA [61], suggesting that p53 may be an important determinant of mitochondrial content and activity. However, using a muscle-specific KO, Stocks and colleagues showed that p53 was not essential for mitochondrial density or activity in

muscle [65]. The dispensable nature of p53 in muscle is further supported by muscle-specific KO of sirtuin (SIRT) 1, which deacetylates p53. In SIRT1 mKO mice, acetylated p53 increases significantly and yet neither baseline, nor exercise training-induced increases in, mitochondrial mass and activity were impaired [33]. This likely is due to the redundancy of signaling pathways that can regulate mitochondrial mass and activity; however, with ageing, it is possible that some of these signals are lost, increasing the necessity for p53.

An increased reliance on fat oxidation also increases adenosine monophosphate (AMP) levels and the phosphorylation of AMP-activated protein kinase at the threonine 172 (pAMPK^{thr172}) site which, in turn regulates fat metabolism through the phosphorylation of ACC and activation of CPT-1 [153] and PGC-1α [154]. Our results show, a KD increases both pAMPK^{thr172} and PGC-1α in the GTN muscle of female mice (Figure 4B&C) and increases PGC-1α in the nuclear fraction (Figure 4H). Within the soleus muscle we observed no difference in levels of PGC-1α which, is likely attributed to the fact that it is a more oxidative muscle at baseline in middle-aged mice. Beyond its role in mitochondrial biogenesis and promoting fat oxidation, PGC-1α is required for the exercise-induced increase in kynurenine aminotransferase (KAT) proteins in skeletal muscle [12]. KAT proteins are responsible for converting kynurenine (KYN), a byproduct of tryptophan metabolism, to kynurenic acid (KYNA), which cannot cross the blood brain barrier [189]. When KYN does enter the brain, it is metabolized into quinolinic acid, a potent neurotoxin [190]. Thus, the conversion of KYN to KYNA is crucial to preventing a variety of inflammatory brain diseases including, Huntington's Disease, Alzheimer's Disease, motor neuron diseases, major psychiatric disorders, and HIV-associated

neurocognitive disorders [191]. Like exercise, a KD increased KAT protein in skeletal muscle and not the liver. Specifically, KAT1 and KAT4 showed a significant increase and strong trend in the GTN muscle, respectively (Figure 4.4D&E), whereas KAT4 protein levels alone increased in the soleus muscle (Figure 4.5D). These results differ somewhat from exercise, since exercise increases expression of all three of the KAT enzymes (1, 3, and 4) in the mouse GTN [12]. Importantly, the increase in KAT levels resulting from exercise training are dependent on PGC-1α [12], suggesting that the increase in KAT protein on a KD may result from the greater level of PGC-1α. The increase in KAT protein on a KD was associated with a strong trend to increase KYNA levels in the serum (Figure 4.4G), providing a potential mechanism for the improved neurocognitive function on a KD.

Although the effects of KDs on motor function and cognition have been studied in diseased or very young female rodent models [150,151,192], little has been done to evaluate these functions in healthy middle aged female mice fed a KD. Our data show that some measures of locomotor activity, including rearing count and distance covered on the Y maze and elevated plus maze were significantly increased with a KD. Since the total movement in the open field, a simple arena consisting of a minimal compartment for the mice to explore, was not altered, the increase in activity in Y and elevated plus maze scores might be predominantly driven by the stimulation of exploratory behavior, rather than an elevation in overall movement. Muscle motor strength and coordination was not impacted by a short-term KD in middle aged female mice, and this is consistent with our previous finding in middle aged male mice [6].

Although short-term working memory evaluated using the Y maze or recognition memory measured by novel object test were not altered with the diet, long-term spatial learning memory assessed with the Barnes maze was improved in middle aged female mice fed a KD for 2 months. This suggests that in female mice a short-term KD might preferentially impact the hippocampus where long-term spatial learning memory is centered. Much of the mechanistic focus of the beneficial effects of a KD on cognitive behavior have been hypothesized to occur downstream of improved mitochondrial mass and function within the brain. Interestingly, the improved neurocognitive function observed in female mice on a short-term KD occurred independent of measurable changes in acetylation or mitochondrial mass within the hippocampus and cortex. This finding could reflect the fact that we did not look at specific regions or cell types within the hippocampus [193] or that the effect on neurocognitive function occurs downstream of a global change in metabolism as a result of the KD. Since improvement in recognition memory was observed in aged male mice on a long-term KD [6], more studies also need to be done to determine whether a long-term KD would benefit short-term working or recognition memory in aged female mice.

Summary

The data presented here demonstrate that a 2-month ketogenic diet with sufficient protein fed to middle aged female mice is well tolerated and improves neurocognitive function concomitant with improved muscle mitochondrial mass and function. The improved mitochondrial mass and function in skeletal muscle may result from changes in protein acetylation and PGC-1α activity. Another potential effect of the increase in PGC-1α is an increase in kynurenine aminotransferases within muscle and a

subsequent rise in kynurenic acid in the blood. The rise in kynurenic acid, and its inability to cross the blood brain barrier and be converted into the neurotoxin quinolinic acid, is one potential mechanism for the improved neurocognitive function on a KD. However, it is clear that further work is needed to directly test this hypothesis.

Acknowledgements

This work was supported by a Program Project Grant (PO1 AG062817) from the NIH (USA). YA by training grant 2T35OD010956-21. The authors would like to thank Viviana Vazquez and Audrey Evangelista for assistance with the feedings of the mice over the two-month intervention.

Author Contributions

J.J.R., K.B., S.P., Z.Z., J.M.R., contributed to conceptualization of the study. S.J.P., D.S., Z.Z., Y.A, T.T, J.M.R., contributed to the data collection. S.J.P., Z.Z., D.S and K.B., carried out the formal analysis. S.J.P., Z.Z., D.S., K.B, J.M.R., and J.J.R contributed the manuscript. All authors approved the final manuscript.

Data Availability Statement:

Raw Data were generated at UC Davis. Derived data supporting the findings of this study are available from KB on request.

Conflict of Interest

K. Baar has received funding to study ketogenic diets from NIH and is a Scientific Advisor to KetoKind. Prof Baar has also received grants and donations from other nutritional companies such as PepsiCo, Bergstrom Nutrition, Ynsect, and GelTor.

Figure legends

Figure 4.1. Blood ketone levels, body weight, fat mass and motor and cognitive behavior test results after 2 months of a KD (n=16).

(A) 3-hour postprandial and 12-hour fasted blood β-hydroxybutyrate levels in middle-aged female fed a control (CD) or ketogenic diet (KD). (B) Body weight of female mice fed an isocaloric CD or KD. (C) Percent fat mass measured using NMR relaxometry. (D) Rearing score: number of wall-contact rears. Total distance travelled in (E) Y maze, (F) elevated plus maze, and (G) open field. Percent time spent (H) in center region of the open field and (I) on the open arms of the elevated plus maze. (J) Grip strength test: relative maximum force exerted on the meter. (K) Grid wire hang: maximum hanging impulse. (L) Rotarod: maximum time on the rod. (M) Time spent in the target quadrant and (N) latency to find the target hole in the Banes maze probe trial. (O) Percent alternation in the Y maze spontaneous alternation test. (P) Percent time exploring the novel object in the novel object recognition time. $*p < 0.05$. All values are presented as mean ± SEM.

Figure 4.2. Increased acetylation in liver is not associated with mitochondrial biogenesis after 2-months on a ketogenic diet **(n=8).** Quantification of A) acetylated lysine, B) BHB-lysine, C) acetylated p300, D) acetylated p53, E) SIRT1, F) phosphorylated $AMPK^{thr172}$, G) total oxidative phosphorylation, H) IRE1, BiP, CHOP, and phosphorylated eIF2α, I)SOD2, J) KAT1, K) KAT3 and L) KAT4. M) Representative images for all western blot data are shown. CD= control and KD= ketogenic diet animals. * $p<0.05$, ** $p<0.01$. All values are presented as mean ± SEM.

Figure 4.3: Acetylation and mitochondrial mass increase in response to a 2-month KD in gastrocnemius muscle **(n=8).** Quantification of A) acetylated lysine, B) BHB-lysine, C) acetylated p300, D) acetylated p53, E) SIRT1, F) SIRT3, and G) total oxidative phosphorylation. H) Representative images for all graphs. CD= control and KD= ketogenic diet animals. * $p<0.05$, ** $p<0.01$, *** $p<0.001$, **** $p<<0.0001$. All values are presented as mean ± SEM.

Figure 4.4. A 2-month KD increases mitochondrial proteins and KAT1 in Gastrocnemius Muscle **(n=8).** Quantification of: A) total OxPhos, B) PGC-1α, C) phosphorylated $AMPK^{thr172}$, D) KAT1, E) KAT3, F) KAT4, G) Kynurenic acid serum levels, H&I) Nuclear levels of: J) qRT-PCR of: PGC-1α, SIRT1, Tfam, Mitfusion1 mRNA, and K) representative images for all western blot data is shown. CD= control and KD= ketogenic diet animals. * $p<0.05$, ** $p<0.01$. All values are presented as mean ± SEM.

Figure 4.5: A 2-month KD increases acetylation and KAT4 levels in soleus muscle **(n=8).** Quantification of: A) acetylated lysine, B) PGC-1alpha, C) KAT1, D) KAT3, E) KAT4, and F) SIRT3. CD= control and KD= ketogenic diet animals.* $p<0.05$, ** $p<0.01$, **** $p<<0.0001$. All values are presented as mean ± SEM.

Figure 4.6: Improvements in cognitive behavior are independent of Acetylation or Mitochondrial Levels in the Cortex and Hippocampus **(n=8).** Quantification of cortex A) acetylated lysine, B) BHB-lysine, and C) Total Oxphos western blot data is shown. Levels of hippocampal D) acetylated lysine, E) BHB-lysine, and F) Total Oxphos

western blot data is shown, and G) representative western blot data is shown. CD= control and KD= ketogenic diet animals. All values are presented as mean ± SEM.

Tissue	*Control Diet (g)*	*Ketogenic Diet (g)*
Liver	1.093 ± .0469*	0.9432 ± .08265
Heart	0.1458 ± 0.0059	0.1434 ± 0.0042
Quadricep	0.1600 ± 0.0046	0.1622 ± 0.0045
Tibialis Anterior	0.03611± 0.0025	0.04151 ± 0.0010 ‡
Gastrocnemius	0.1270 ± 0.0019	0.1238 ± 0.0015
Soleus	0.007.913 ± 0.0003	0.007.875 ± 0.0003
*All values are presented as mean ± SEM. * p<0.05,* ‡ p<0.1		

Table 4.2: Tissue weights after 2 months on a Control Diet or Ketogenic Diet.

Chapter 5: General Discussion

Background

Since its development in 1924, the ketogenic diet (KD) has been widely studied as a treatment for neurocognitive disorders (i.e., epilepsy—for which it was created, Alzheimer's Disease, Parkinson's, etc.). More recently, the ability of a KD to impact other organ systems has been noted. In 2017, our group was the first to demonstrate the ability of an isocaloric (11.2kcal/day) KD started at middle-age to improve neurocognitive and musculoskeletal function, and extend lifespan 13.6% in male mice when compared to a control diet (CD)[6]. As reported by Roberts and colleagues, the greatest biochemical change in response to a KD was a ~4-fold increase in proteins containing acetylated lysines. Concomitant with the increase in acetylated lysine levels, male mice showed significant increases in the master regulator of mitochondrial biogenesis, the peroxisome proliferator activated-receptor gamma coactivation -1α (PGC-1α), and a preservation of fast-oxidative (type IIA) fiber cross sectional area (fCSA) in skeletal muscle when compared to CD fed animals—topics I explain in detail in **chapter 1** [7,194]. Based on this background, in this dissertation I investigated the effects of manipulating acetylation either pharmaceutically or with diet (a KD) on skeletal muscle biochemistry, functionality, and neurocognitive behavior across species, sex, and age. In this final chapter I will address the implications of the data I generated, discuss these results in a broader perspective, and address future directions for research.

Chapter 2: Regulation of acetylation to improve load-induced muscle hypertrophy

Muscle mass and strength are strong predictors of all-cause mortality in humans[195]. Lack of mass and functionality is also linked to poor post-surgery recovery and increases the risk of diabetes, heart-disease, and cancer[111]. Exercise is currently the only way to increase muscle mass and functionality. Therefore, understanding which mechanisms contribute to hypertrophy and discovering ways to augment hypertrophy at a given quantity of exercise can help inform

treatment options for those unable or unwilling to exercise at the intensity needed to achieve benefits.

Hamilton and colleague identified a number of molecular breaks that were hypothesized to limit muscle growth in response to heavy loading (i.e., synergist ablation)[120]. One of these was sirtuin 1, an NAD^+-dependent deacetylase (SIRT1). SIRT1 was hypothesized to limit growth through the deacetylation of TAF68, a component of the SL-1 transcription factor that drives the expression of rRNA of the 47S ribosomal subunit, leading to diminished rRNA transcription and ribosome biogenesis[122]. Since ribosomal mass is theorized to be required for muscle growth in response to synergist ablation[10], in **chapter 2** we tested the efficacy of a natural product inhibitor of SIRT1 to increase fiber cross sectional area (fCSA) in rats.

We identified more than 50 natural products that could inhibit SIRT1 activity more than 50% in an *in vitro* assay. When combined in the optimal manner, three of these natural products could increase fCSA in response to functional overload almost 10-fold better than a vehicle control. Contrary to our hypothesis, the SIRT1 inhibitor did not increase ribosome mass. Instead, we found that treatment decreased total RNA/mg of muscle and also decreased markers of rRNA expression. Our data indicates that inhibition of SIRT1 coupled with synergist ablation led to an increase in acetylation of ribosomal subunits, an increase in ribosome efficiency, and a concomitant increase in muscle fCSA (Figure 2.6A&B, Figure 2.2G).

Altogether, the data from **chapter 2** suggest that acetylation of ribosomal subunits may alter the translational efficiency, as previously seen in rat liver[11], rather than increasing ribosomal mass leading to greater muscle mass. Our findings provide a potential for exciting new therapeutics that may benefit the aging and athletic populations.

From my data in **chapter 2** a number of questions arise. First, my data indicate that one potential benefit of increased ribosomal acetylation is it's increased translational efficiency. To test this directly, I would use the translating ribosomal affinity purification (TRAP) technique in skeletal muscle allowing me to identify transcripts bound by the large ribosomal subunit from

actively translating ribosomes [196], to better understand translational regulation of the animals within our study. This will allow for a deeper understanding of how ribosomal acetylation effects skeletal muscle translation in response to a growth stimulus. As a validation of any potential results, I would use rats overexpressing and lacking acetyltransferase p300 in skeletal muscle, which is crucial for skeletal muscle functionality and for health- and life- span, to increase acetylated lysine residues[83]. Upon collection using the SUnSET method, I would determine protein synthesis via western blotting. Altogether these outlined experiments, will allow for a deeper understanding of how manipulating acetylation effects skeletal muscle translation.

Chapter 3: HDAC inhibitors decrease ketones and prevent the positive effects of a KD

As described in detail in the introduction of this chapter, a long-term KD has been shown to increase acetylation of histone and non-histone proteins with a concomitant increase in skeletal muscle and neurocognitive function in male mice[6]. However, this finding led to a series of questions: 1) To what degree does an acute KD benefit these physiological outcomes? 2) Does an acute KD benefit an already aged population? 3) Does an acute KD benefit female mice? 4) To what degree does histone acetylation play a role in these physiological benefits? These four listed questions were the motivation of the studies described in Chapter 3.

In 2016, Gaur and colleagues demonstrated that treatment with the HDAC inhibitor scriptaid for 28 days in young male mice led to increases in histone acetylation, lipid oxidation, fatigue resistance, and mitochondrial biogenesis[42]. Interestingly, these physiological changes mimic those seen with exercise[29,94,138]. In both cases there is an increased reliance on fatty acid oxidation, leading to more acetyl-coA production and lessening the need for glucose oxidation. Similar to scriptaid administration and exercise, a KD where fats are high and carbohydrates are limited, shifts metabolism towards fatty-acid oxidation and leads to production of the primary ketone β-hydroxybutyrate (BHB) from the liver. With elevated BHB levels in circulation achieved with a KD, there is an increase in both acetylated histone and nonhistone proteins. BHB, like

scriptaid, inhibits class I and IIa HDACs both *in vivo* and *in vitro*[140,197]. Together, these data suggest that a KD may be working through similar mechanisms as exercise and/or scriptaid to enhance mitochondrial biogenesis and skeletal muscle functionality.

The experiments in **chapter 3** were designed to test the role of inhibition of HDAC activity in the adaptations to a ketogenic diet. These experiments demonstrated first that the fasted BHB levels were modified by scriptaid administration. Specifically, fasted BHB levels in the animals getting both KD and SCRIPT were significantly lower than those getting a KD alone (Figure 3.1C). Interestingly, forelimb grip strength (Figure 3.1G), PGC-1α (Figure 3.2C), Total OxPhos (Figure 3.2D), and dystrophin (Figure 3.4F) levels follow the same pattern. We are the first to show that treatment with an HDAC inhibitor blunts the amount of BHB circulating in the fasted state. This suggests that either HDACs or their off targets are important in the production of ketones or block the uptake of ketones into target tissues. The fact that many of the important biochemical changes in muscle mirror BHB levels and not HDAC inhibition, suggests that high circulating BHB levels drive the biochemical and motor function benefits seen with an acute KD.

One of the key findings from this work was that a KD increased dystrophin protein. A KD rich in medium chain triglycerides has been shown to ameliorate the debilitating phenotype on Duchenne's Muscular Dystrophy (DMD) in rats[77]. However, whether the improvement in muscle function coincides with an increase in proteins within the dystrophin glycoprotein complex (DGC) remains to be determined. Future experiments should determine the effect of an acute KD in various animal models of muscular dystrophy. Feeding an isocaloric control (CD) or ketogenic (KD) for two-months to the CRISPR-Cas9 generated desminopathy model[198] and then measuring muscle force, contraction-induced injury, the levels of DGC related proteins, and fiber type specific cross sectional area would provide an initial assessment of the validity of using a KD to treat muscle diseases.

Chapter 4: Female mice show improved learning and memory concomitant with decreased KYN

Our group has previously reported that a KD for 14 months increases skeletal muscle functionality and neurocognitive function in male mice[6]. However, at the time the effect of a KD on female mice was largely unexplored. In 2019, Nakao et. al demonstrated that a KD in female mice induces skeletal muscle atrophy and results in a starvation like phenotype causing mortality after 7-days[149]. We felt that the diet used in this study may have been of limited palatability and deficient in methionine. This is crucial as methionine supplementation promotes normal metabolism of a KD in mice[199]. In **chapter 4** we fed middle-aged female mice control or ketogenic diets, with sufficient methionine levels, for 2 months and determined the effect on neurocognitive and musculoskeletal function. We found that female mice thrived on a KD. Like their male counterparts, their muscles showed higher acetylation, PGC-1α, mitochondrial mass, and kynurenine aminotransferase I and IV levels. These changes in muscle corresponded with decreases in circulating KYN and improved learning and memory.

To extend this work, it is important to determine whether the decrease in KYN results in less quinolinic acid (QA) in the brain. QA in different regions of the brain should therefore be directly measured in brain tissue using an enzyme linked immunosorbent assay (ELISA) following homogenization. Secondly, because the brain is the primary producer of QA from KYN[200], western blots of both cortex and hippocampus for cell death and inflammatory signaling cascades would provide useful insight[201]. The reported improvements in spatial learning memory, which is a primary function of the hippocampus, suggest that long-term potentiation is affected by a KD. A direct measure of this property should be preformed[202]. Lastly, since there are obvious differences in results between the middle-aged male and female mice on a KD, a lifespan study directly comparing the longevity effects of a KD on male and female mice is warranted.

Conclusion

In conclusion, this dissertation demonstrated that acetylation is an important regulator of muscle fiber cross-sectional area; that inhibiting HDACs alters either the production or use of ketones; that the positive neurocognitive effects of a KD may be driven by both decreasing circulating KYN (minor) and increasing BHB (major); The data show that muscle plays an important role both directly (through force production) and indirectly (through metabolizing fat and other substrates) affects both life- and health- span.

References

1. Reimers CD, Knapp G, Reimers AK. Does physical activity increase life expectancy? A review of the literature. *J Aging Res*. 2012;2012:243958. doi:10.1155/2012/243958
2. Sujkowski A, Bazzell B, Carpenter K, Arking R, Wessells RJ. Endurance exercise and selective breeding for longevity extend Drosophila healthspan by overlapping mechanisms. *Aging (Albany NY)*. 2015;7(8):535-552. doi:10.18632/aging.100789
3. Kelty TJ, Brown JD, Kerr NR, et al. RNA-sequencing and behavioral testing reveals inherited physical inactivity co-selects for anxiogenic behavior without altering depressive-like behavior in Wistar rats. *Neurosci Lett*. 2021;753. doi:10.1016/j.neulet.2021.135854
4. Christensen DG, Xie X, Basisty N, et al. Post-translational Protein Acetylation: An Elegant Mechanism for Bacteria to Dynamically Regulate Metabolic Functions . *Front Microbiol* . 2019;10:1604. https://www.frontiersin.org/article/10.3389/fmicb.2019.01604
5. McGee SL, Fairlie E, Garnham AP, Hargreaves M. Exercise-induced histone modifications in human skeletal muscle. *J Physiol*. 2009;587(Pt 24):5951-5958. doi:10.1113/jphysiol.2009.181065
6. Roberts MN, Wallace MA, Tomilov AA, et al. A Ketogenic Diet Extends Longevity and Healthspan in Adult Mice. *Cell Metab*. 2017;26(3):539-546.e5. doi:10.1016/j.cmet.2017.08.005
7. Wallace MA, Aguirre NW, Marcotte GR, et al. The ketogenic diet preserves skeletal muscle with aging in mice. *Aging Cell*. 2021;20(4). doi:10.1111/acel.13322
8. Stec MJ, Kelly NA, Many GM, Windham ST, Tuggle SC, Bamman MM. Ribosome biogenesis may augment resistance training-induced myofiber hypertrophy and is required for myotube growth in vitro. *Am J Physiol Endocrinol Metab*. 2016;310(8):E652-E661. doi:10.1152/ajpendo.00486.2015
9. Figueiredo VC, McCarthy JJ. Regulation of Ribosome Biogenesis in Skeletal Muscle Hypertrophy. *Physiology (Bethesda)*. 2019;34(1):30-42. doi:10.1152/physiol.00034.2018
10. Kirby TJ, Lee JD, England JH, Chaillou T, Esser KA, McCarthy JJ. Blunted hypertrophic response in aged skeletal muscle is associated with decreased ribosome biogenesis. *J Appl Physiol*. 2015;119(4):321-327. doi:10.1152/japplphysiol.00296.2015
11. Liew CC, Gornall AG. Acetylation of ribosomal proteins. I. Characterization and properties of rat liver ribosomal proteins. *J Biol Chem*. 1973;248(3):977-983.
12. Agudelo LZ, Femenía T, Orhan F, et al. Skeletal muscle PGC-1α1 modulates kynurenine metabolism and mediates resilience to stress-induced depression. *Cell*. 2014;159(1):33-45. doi:10.1016/j.cell.2014.07.051

13. Liu P, Hao Q, Hai S, Wang H, Cao L, Dong B. Sarcopenia as a predictor of all-cause mortality among community-dwelling older people: A systematic review and meta-analysis. *Maturitas*. 2017;103:16-22. doi:10.1016/j.maturitas.2017.04.007
14. Janssen I, Shepard DS, Katzmarzyk PT, Roubenoff R. *The Healthcare Costs of Sarcopenia in the United States*. Vol 52.; 2004.
15. Nilwik R, Snijders T, Leenders M, et al. The decline in skeletal muscle mass with aging is mainly attributed to a reduction in type II muscle fiber size. *Exp Gerontol*. 2013;48(5):492-498. doi:10.1016/j.exger.2013.02.012
16. Newman AB, Kupelian V, Visser M, et al. Strength, but not muscle mass, is associated with mortality in the health, aging and body composition study cohort. *Journals Gerontol - Ser A Biol Sci Med Sci*. 2006;61(1):72-77. doi:10.1093/gerona/61.1.72
17. Landi F, Cruz-Jentoft AJ, Liperoti R, et al. Sarcopenia and mortality risk in frail olderpersons aged 80 years and older: Results from iLSIRENTE study. *Age Ageing*. 2013;42(2):203-209. doi:10.1093/ageing/afs194
18. Short KR, Vittone JL, Bigelow ML, Proctor DN, Nair KS. Age and aerobic exercise training effects on whole body and muscle protein metabolism. *Am J Physiol Endocrinol Metab*. 2004;286(1):E92-101. doi:10.1152/ajpendo.00366.2003
19. Welle S, Bhatt K, Shah B, et al. Reduced amount of mitochondrial DNA in aged human muscle. *J Appl Physiol*. 2003;94:1479-1484. doi:10.1152/japplphysiol.01061.2002.-Mus
20. Crane JD, Devries MC, Safdar A, Hamadeh MJ, Tarnopolsky MA. The effect of aging on human skeletal muscle mitochondrial and intramyocellular lipid ultrastructure. *Journals Gerontol - Ser A Biol Sci Med Sci*. 2010;65(2):119-128. doi:10.1093/gerona/glp179
21. Joseph AM, Adhihetty PJ, Buford TW, et al. The impact of aging on mitochondrial function and biogenesis pathways in skeletal muscle of sedentary high- and low-functioning elderly individuals. *Aging Cell*. 2012;11(5):801-809. doi:10.1111/j.1474-9726.2012.00844.x
22. Conley KE, Jubrias S, Esselman P. Oxidative Capacity and Ageing in Human Muscle. *J Physiol*. 2000;526.1:203-210.
23. Luukkonen PK, Dufour S, Lyu K, et al. Effect of a ketogenic diet on hepatic steatosis and hepatic mitochondrial metabolism in nonalcoholic fatty liver disease. *Proc Natl Acad Sci U S A*. 2020;117(13):7347-7354. doi:10.1073/pnas.1922344117
24. Lee RC, Wang Z, Heo M, Ross R, Janssen I, Heymsfield SB. Total-body skeletal muscle mass: development and cross-validation of anthropometric prediction models. *Am J Clin Nutr*. 2000;72(3):796-803. doi:10.1093/ajcn/72.3.796
25. Evans M, Cogan KE, Egan B. Metabolism of ketone bodies during exercise and training: physiological basis for exogenous supplementation. *J Physiol*. 2017;595(9):2857-2871. doi:10.1113/JP273185
26. Reinke H, Hörz W. Histones are first hyperacetylated and then lose contact with the activated PHO5 promoter. *Mol Cell*. 2003;11(6):1599-1607. doi:10.1016/s1097-2765(03)00186-2
27. Zhao J, Herrera-Diaz J, Gross DS. Domain-wide displacement of histones by

activated heat shock factor occurs independently of Swi/Snf and is not correlated with RNA polymerase II density. *Mol Cell Biol*. 2005;25(20):8985-8999. doi:10.1128/MCB.25.20.8985-8999.2005
28. Chandy M, Gutiérrez JL, Prochasson P, Workman JL. SWI/SNF displaces SAGA-acetylated nucleosomes. *Eukaryot Cell*. 2006;5(10):1738-1747. doi:10.1128/EC.00165-06
29. McGee SL, Fairlie E, Garnham AP, Hargreaves M. Exercise-induced histone modifications in human skeletal muscle. *J Physiol*. 2009;587(24):5951-5958. doi:10.1113/jphysiol.2009.181065
30. Overmyer KA, Evans CR, Qi NR, et al. Maximal oxidative capacity during exercise is associated with skeletal muscle fuel selection and dynamic changes in mitochondrial protein acetylation. *Cell Metab*. 2015;21(3):468-478. doi:10.1016/j.cmet.2015.02.007
31. Holloszy JO, Smith EK, Vining M, Adams S. Effect of voluntary exercise on longevity of rats. *J Appl Physiol*. 1985;59(3):826-831. doi:10.1152/jappl.1985.59.3.826
32. Holloszy JO. Biochemical adaptations in muscle. Effects of exercise on mitochondrial oxygen uptake and respiratory enzyme activity in skeletal muscle. *J Biol Chem*. 1967;242(9):2278-2282. doi:10.1016/S0021-9258(18)96046-1
33. Philp A, MacKenzie MG, Belew MY, et al. Glycogen Content Regulates Peroxisome Proliferator Activated Receptor-∂ (PPAR-∂) Activity in Rat Skeletal Muscle. *PLoS One*. 2013;8(10):e77200. https://doi.org/10.1371/journal.pone.0077200
34. Kersten S, Seydoux J, Peters JM, Gonzalez FJ, Desvergne B, Wahli W. Peroxisome proliferator-activated receptor alpha mediates the adaptive response to fasting. *J Clin Invest*. 1999;103(11):1489-1498. doi:10.1172/JCI6223
35. Dressel U, Allen TL, Pippal JB, Rohde PR, Lau P, Muscat GEO. The peroxisome proliferator-activated receptor beta/delta agonist, GW501516, regulates the expression of genes involved in lipid catabolism and energy uncoupling in skeletal muscle cells. *Mol Endocrinol*. 2003;17(12):2477-2493. doi:10.1210/me.2003-0151
36. Pawlak M, Lefebvre P, Staels B. Molecular mechanism of PPARα action and its impact on lipid metabolism, inflammation and fibrosis in non-alcoholic fatty liver disease. *J Hepatol*. 2015;62(3):720-733. doi:10.1016/j.jhep.2014.10.039
37. Phua WW, Wong MX, Liao Z, Tan NS. An aPPARent Functional Consequence in Skeletal Muscle Physiology via Peroxisome Proliferator-Activated Receptors. *Int J Mol Sci* . 2018;19(5). doi:10.3390/ijms19051425
38. Ehrenborg E, Krook A. Regulation of Skeletal Muscle Physiology and Metabolism by Peroxisome Proliferator-Activated Receptor δ. *Pharmacol Rev*. 2009;61(3):373 LP - 393. doi:10.1124/pr.109.001560
39. Peters SJ, St Amand TA, Howlett RA, Heigenhauser GJ, Spriet LL. Human skeletal muscle pyruvate dehydrogenase kinase activity increases after a low-carbohydrate diet. *Am J Physiol*. 1998;275(6):E980-6. doi:10.1152/ajpendo.1998.275.6.E980
40. Stellingwerff T, Spriet LL, Watt MJ, et al. Decreased PDH activation and glycogenolysis during exercise following fat adaptation with carbohydrate restoration. *Am J Physiol Endocrinol Metab*. 2006;290(2):E380-8.

doi:10.1152/ajpendo.00268.2005
41. Zhou Z, Hagopian K, López-Domínguez JA, et al. A ketogenic diet impacts markers of mitochondrial mass in a tissue specific manner in aged mice. *Aging (Albany NY)*. 2021;13(6):7914-7930. doi:10.18632/aging.202834
42. Gaur V, Connor T, Sanigorski A, et al. Disruption of the Class IIa HDAC Corepressor Complex Increases Energy Expenditure and Lipid Oxidation. *Cell Rep*. 2016;16(11):2802-2810. doi:10.1016/j.celrep.2016.08.005
43. Akimoto T, Sorg BS, Yan Z. Real-time imaging of peroxisome proliferator-activated receptor-gamma coactivator-1alpha promoter activity in skeletal muscles of living mice. *Am J Physiol Cell Physiol*. 2004;287(3):C790-6. doi:10.1152/ajpcell.00425.2003
44. Zhong R, Miao R, Meng J, Wu R, Zhang Y, Zhu D. Acetoacetate promotes muscle cell proliferation via the miR-133b/SRF axis through the Mek-Erk-MEF2 pathway. *Acta Biochim Biophys Sin (Shanghai)*. 2021;53(8):1009-1016. doi:10.1093/abbs/gmab079
45. Newman JC, Verdin E. β-Hydroxybutyrate: A Signaling Metabolite. *Annu Rev Nutr*. 2017;37:51-76. doi:10.1146/annurev-nutr-071816-064916
46. Wang D-F, Helquist P, Wiech NL, Wiest O. Toward Selective Histone Deacetylase Inhibitor Design: Homology Modeling, Docking Studies, and Molecular Dynamics Simulations of Human Class I Histone Deacetylases. *J Med Chem*. 2005;48(22):6936-6947. doi:10.1021/jm0505011
47. Huang T-Y, Linden MA, Fuller SE, et al. Combined effects of a ketogenic diet and exercise training alter mitochondrial and peroxisomal substrate oxidative capacity in skeletal muscle. *Am J Physiol Metab*. 2021;320(6):E1053-E1067. doi:10.1152/ajpendo.00410.2020
48. Partsalaki I, Karvela A, Spiliotis BE. Metabolic impact of a ketogenic diet compared to a hypocaloric diet in obese children and adolescents. *J Pediatr Endocrinol Metab*. 2012;25(7-8):697-704. doi:10.1515/jpem-2012-0131
49. McGee SL, van Denderen BJW, Howlett KF, et al. AMP-activated protein kinase regulates GLUT4 transcription by phosphorylating histone deacetylase 5. *Diabetes*. 2008;57(4):860-867. doi:10.2337/db07-0843
50. Abdelmegeed MA, Kim SK, Woodcroft KJ, Novak RF. Acetoacetate activation of extracellular signal-regulated kinase 1/2 and p38 mitogen-activated protein kinase in primary cultured rat hepatocytes: role of oxidative stress. *J Pharmacol Exp Ther*. 2004;310(2):728-736. doi:10.1124/jpet.104.066522
51. Puigserver P, Rhee J, Lin J, et al. Cytokine stimulation of energy expenditure through p38 MAP kinase activation of PPARgamma coactivator-1. *Mol Cell*. 2001;8(5):971-982. doi:10.1016/s1097-2765(01)00390-2
52. Saleem A, Carter HN, Iqbal S, Hood DA. Role of p53 Within the Regulatory Network Controlling Muscle Mitochondrial Biogenesis. *Exerc Sport Sci Rev*. 2011;39(4). https://journals.lww.com/acsm-essr/Fulltext/2011/10000/Role_of_p53_Within_the_Regulatory_Network.6.aspx
53. Bartlett JD, Close GL, Drust B, Morton JP. The emerging role of p53 in exercise metabolism. *Sports Med*. 2014;44(3):303-309. doi:10.1007/s40279-013-0127-9
54. Saleem A, Adhihetty PJ, Hood DA. Role of p53 in mitochondrial biogenesis and apoptosis in skeletal muscle. *Physiol Genomics*. 2009;37(1):58-66.

doi:10.1152/physiolgenomics.90346.2008
55. Donahue RJ, Razmara M, Hoek JB, Knudsen TB. Direct influence of the p53 tumor suppressor on mitochondrial biogenesis and function. *FASEB J Off Publ Fed Am Soc Exp Biol*. 2001;15(3):635-644. doi:10.1096/fj.00-0262com
56. Park J-H, Zhuang J, Li J, Hwang PM. p53 as guardian of the mitochondrial genome. *FEBS Lett*. 2016;590(7):924-934. doi:10.1002/1873-3468.12061
57. Matoba S, Kang J-G, Patino WD, et al. p53 regulates mitochondrial respiration. *Science*. 2006;312(5780):1650-1653. doi:10.1126/science.1126863
58. Tang Y, Zhao W, Chen Y, Zhao Y, Gu W. Acetylation is indispensable for p53 activation. *Cell*. 2008;133(4):612-626. doi:10.1016/j.cell.2008.03.025
59. Liang S-H, Clarke MF. Regulation of p53 localization. *Eur J Biochem*. 2001;268(10):2779-2783. doi:https://doi.org/10.1046/j.1432-1327.2001.02227.x
60. Peterson CM, Johannsen DL, Ravussin E. Skeletal muscle mitochondria and aging: a review. *J Aging Res*. 2012;2012:194821. doi:10.1155/2012/194821
61. Lebedeva MA, Eaton JS, Shadel GS. Loss of p53 causes mitochondrial DNA depletion and altered mitochondrial reactive oxygen species homeostasis. *Biochim Biophys Acta - Bioenerg*. 2009;1787(5):328-334. doi:https://doi.org/10.1016/j.bbabio.2009.01.004
62. Saleem A, Hood DA. Acute exercise induces tumour suppressor protein p53 translocation to the mitochondria and promotes a p53-Tfam-mitochondrial DNA complex in skeletal muscle. *J Physiol*. 2013;591(14):3625-3636. doi:10.1113/jphysiol.2013.252791
63. Park J-Y, Wang P-Y, Matsumoto T, et al. p53 improves aerobic exercise capacity and augments skeletal muscle mitochondrial DNA content. *Circ Res*. 2009;105(7):705-712, 11 p following 712. doi:10.1161/CIRCRESAHA.109.205310
64. Saleem A, Carter HN, Hood DA. p53 is necessary for the adaptive changes in cellular milieu subsequent to an acute bout of endurance exercise. *Am J Physiol Cell Physiol*. 2014;306(3):C241-9. doi:10.1152/ajpcell.00270.2013
65. Stocks B, Dent JR, Joanisse S, McCurdy CE, Philp A. Skeletal Muscle Fibre-Specific Knockout of p53 Does Not Reduce Mitochondrial Content or Enzyme Activity . *Front Physiol* . 2017;8:941. https://www.frontiersin.org/article/10.3389/fphys.2017.00941
66. Kowald A, Kirkwood TB. A network theory of ageing: the interactions of defective mitochondria, aberrant proteins, free radicals and scavengers in the ageing process. *Mutat Res*. 1996;316(5-6):209-236. doi:10.1016/s0921-8734(96)90005-3
67. Drake JC, Wilson RJ, Laker RC, et al. Mitochondria-localized AMPK responds to local energetics and contributes to exercise and energetic stress-induced mitophagy. *Proc Natl Acad Sci U S A*. 2021;118(37). doi:10.1073/pnas.2025932118
68. Yang X, Xue P, Yuan M, et al. SESN2 protects against denervated muscle atrophy through unfolded protein response and mitophagy. *Cell Death Dis*. 2021;12(9):805. doi:10.1038/s41419-021-04094-9
69. Archer SL. Mitochondrial Dynamics — Mitochondrial Fission and Fusion in Human Diseases. *N Engl J Med*. 2013;369(23):2236-2251. doi:10.1056/NEJMra1215233
70. Balan E, Schwalm C, Naslain D, Nielens H, Francaux M, Deldicque L. Regular

Endurance Exercise Promotes Fission, Mitophagy, and Oxidative Phosphorylation in Human Skeletal Muscle Independently of Age . *Front Physiol* . 2019;10:1088. https://www.frontiersin.org/article/10.3389/fphys.2019.01088
71. Sebastián D, Hernández-Alvarez MI, Segalés J, et al. Mitofusin 2 (Mfn2) links mitochondrial and endoplasmic reticulum function with insulin signaling and is essential for normal glucose homeostasis. *Proc Natl Acad Sci*. 2012;109(14):5523 LP - 5528. doi:10.1073/pnas.1108220109
72. Mishra P, Varuzhanyan G, Pham AH, Chan DC. Mitochondrial Dynamics is a Distinguishing Feature of Skeletal Muscle Fiber Types and Regulates Organellar Compartmentalization. *Cell Metab*. 2015;22(6):1033-1044. doi:10.1016/j.cmet.2015.09.027
73. Santra S, Gilkerson RW, Davidson M, Schon EA. Ketogenic treatment reduces deleted mitochondrial DNAs in cultured human cells. *Ann Neurol*. 2004;56(5):662-669. doi:10.1002/ana.20240
74. Ahn Y, Sabouny R, Villa BR, et al. Aberrant Mitochondrial Morphology and Function in the BTBR Mouse Model of Autism Is Improved by Two Weeks of Ketogenic Diet. *Int J Mol Sci* . 2020;21(9). doi:10.3390/ijms21093266
75. Aapro M, Arends J, Bozzetti F, et al. Early recognition of malnutrition and cachexia in the cancer patient: a position paper of a European School of Oncology Task Force. *Ann Oncol*. 2014;25(8):1492-1499. doi:https://doi.org/10.1093/annonc/mdu085
76. Nakao R, Abe T, Yamamoto S, Oishi K. Ketogenic diet induces skeletal muscle atrophy via reducing muscle protein synthesis and possibly activating proteolysis in mice. *Sci Rep*. 2019;9(1). doi:10.1038/s41598-019-56166-8
77. Fujikura Y, Sugihara H, Hatakeyama M, Oishi K, Yamanouchi K. Ketogenic diet with medium-chain triglycerides restores skeletal muscle function and pathology in a rat model of Duchenne muscular dystrophy. *FASEB J Off Publ Fed Am Soc Exp Biol*. 2021;35(9):e21861. doi:10.1096/fj.202100629R
78. Rudolf R, Khan MM, Labeit S, Deschenes MR. Degeneration of Neuromuscular Junction in Age and Dystrophy . *Front Aging Neurosci* . 2014;6:99. https://www.frontiersin.org/article/10.3389/fnagi.2014.00099
79. Nilwik R, Snijders T, Leenders M, et al. The decline in skeletal muscle mass with aging is mainly attributed to a reduction in type II muscle fiber size. *Exp Gerontol*. 2013;48(5):492-498. doi:10.1016/j.exger.2013.02.012
80. Karanam B, Wang L, Wang D, et al. Multiple roles for acetylation in the interaction of p300 HAT with ATF-2. *Biochemistry*. 2007;46(28):8207-8216. doi:10.1021/bi7000054
81. Karanam B, Jiang L, Wang L, Kelleher NL, Cole PA. Kinetic and mass spectrometric analysis of p300 histone acetyltransferase domain autoacetylation. *J Biol Chem*. 2006;281(52):40292-40301. doi:10.1074/jbc.M608813200
82. Karukurichi KR, Wang L, Uzasci L, Manlandro CM, Wang Q, Cole PA. Analysis of p300/CBP histone acetyltransferase regulation using circular permutation and semisynthesis. *J Am Chem Soc*. 2010;132(4):1222-1223. doi:10.1021/ja909466d
83. Svensson K, LaBarge SA, Sathe A, et al. p300 and cAMP response element-binding protein-binding protein in skeletal muscle homeostasis, contractile function, and survival. *J Cachexia Sarcopenia Muscle*. 2020;11(2):464-477.

doi:10.1002/jcsm.12522
84. Vargas S, Romance R, Petro JL, et al. Efficacy of ketogenic diet on body composition during resistance training in trained men: a randomized controlled trial. *J Int Soc Sports Nutr*. 2018;15(1):31. doi:10.1186/s12970-018-0236-9
85. Jabekk PT, Moe IA, Meen HD, Tomten SE, Høstmark AT. Resistance training in overweight women on a ketogenic diet conserved lean body mass while reducing body fat. *Nutr Metab (Lond)*. 2010;7(1):17. doi:10.1186/1743-7075-7-17
86. Kaufman RJ, Davies M V, Pathak VK, Hershey JW. The phosphorylation state of eucaryotic initiation factor 2 alters translational efficiency of specific mRNAs. *Mol Cell Biol*. 1989;9(3):946-958. doi:10.1128/mcb.9.3.946-958.1989
87. Thomsen HH, Rittig N, Johannsen M, et al. Effects of 3-hydroxybutyrate and free fatty acids on muscle protein kinetics and signaling during LPS-induced inflammation in humans: anticatabolic impact of ketone bodies. *Am J Clin Nutr*. 2018;108(4):857-867. doi:10.1093/ajcn/nqy170
88. Paoli A, Grimaldi K, D'Agostino D, et al. Ketogenic diet does not affect strength performance in elite artistic gymnasts. *J Int Soc Sports Nutr*. 2012;9(1):34. doi:10.1186/1550-2783-9-34
89. Zinn C, Wood M, Williden M, Chatterton S, Maunder E. Ketogenic diet benefits body composition and well-being but not performance in a pilot case study of New Zealand endurance athletes. *J Int Soc Sports Nutr*. 2017;14(1):22. doi:10.1186/s12970-017-0180-0
90. Kephart WC, Pledge CD, Roberson PA, et al. The Three-Month Effects of a Ketogenic Diet on Body Composition, Blood Parameters, and Performance Metrics in CrossFit Trainees: A Pilot Study. *Sport (Basel, Switzerland)*. 2018;6(1):1. doi:10.3390/sports6010001
91. Burke LM, Ross ML, Garvican-Lewis LA, et al. Low carbohydrate, high fat diet impairs exercise economy and negates the performance benefit from intensified training in elite race walkers. *J Physiol*. 2017;595(9):2785-2807. doi:10.1113/JP273230
92. Greene DA, Varley BJ, Hartwig TB, Chapman P, Rigney M. A Low-Carbohydrate Ketogenic Diet Reduces Body Mass Without Compromising Performance in Powerlifting and Olympic Weightlifting Athletes. *J Strength Cond Res*. 2018;32(12). https://journals.lww.com/nsca-jscr/Fulltext/2018/12000/A_Low_Carbohydrate_Ketogenic_Diet_Reduces_Body.10.aspx
93. Heikura IA, Burke LM, Hawley JA, et al. A Short-Term Ketogenic Diet Impairs Markers of Bone Health in Response to Exercise . *Front Endocrinol* . 2020;10:880. https://www.frontiersin.org/article/10.3389/fendo.2019.00880
94. Romijn JA, Coyle EF, Sidossis LS, et al. Regulation of endogenous fat and carbohydrate metabolism in relation to exercise intensity and duration. *Am J Physiol*. 1993;265(3 Pt 1):E380-91. doi:10.1152/ajpendo.1993.265.3.E380
95. Holloway GP, Bezaire V, Heigenhauser GJF, et al. Mitochondrial long chain fatty acid oxidation, fatty acid translocase/CD36 content and carnitine palmitoyltransferase I activity in human skeletal muscle during aerobic exercise. *J Physiol*. 2006;571(Pt 1):201-210. doi:10.1113/jphysiol.2005.102178
96. Bradley NS, Snook LA, Jain SS, Heigenhauser GJF, Bonen A, Spriet LL. Acute

endurance exercise increases plasma membrane fatty acid transport proteins in rat and human skeletal muscle. *Am J Physiol Endocrinol Metab*. 2012;302(2):E183-9. doi:10.1152/ajpendo.00254.2011
97. SHAW DM, MERIEN F, BRAAKHUIS A, MAUNDER ED, DULSON DK. Effect of a Ketogenic Diet on Submaximal Exercise Capacity and Efficiency in Runners. *Med Sci Sport Exerc*. 2019;51(10). https://journals.lww.com/acsm-msse/Fulltext/2019/10000/Effect_of_a_Ketogenic_Diet_on_Submaximal_Exercise.19.aspx
98. Antonio Paoli A, Mancin L, Caprio M, et al. Effects of 30 days of ketogenic diet on body composition, muscle strength, muscle area, metabolism, and performance in semi-professional soccer players. *J Int Soc Sports Nutr*. 2021;18(1):62. doi:10.1186/s12970-021-00459-9
99. Cox PJ, Kirk T, Ashmore T, et al. Nutritional Ketosis Alters Fuel Preference and Thereby Endurance Performance in Athletes. *Cell Metab*. 2016;24(2):256-268. doi:10.1016/j.cmet.2016.07.010
100. Stubbs BJ, Cox PJ, Evans RD, et al. On the Metabolism of Exogenous Ketones in Humans . *Front Physiol* . 2017;8:848. https://www.frontiersin.org/article/10.3389/fphys.2017.00848
101. Ari C, Kovács Z, Juhasz G, et al. Exogenous Ketone Supplements Reduce Anxiety-Related Behavior in Sprague-Dawley and Wistar Albino Glaxo/Rijswijk Rats. *Front Mol Neurosci*. 2016;9:137. doi:10.3389/fnmol.2016.00137
102. Kesl SL, Poff AM, Ward NP, et al. Effects of exogenous ketone supplementation on blood ketone, glucose, triglyceride, and lipoprotein levels in Sprague–Dawley rats. *Nutr Metab (Lond)*. 2016;13(1):9. doi:10.1186/s12986-016-0069-y
103. Caminhotto R de O, Komino ACM, de Fatima Silva F, et al. Oral β-hydroxybutyrate increases ketonemia, decreases visceral adipocyte volume and improves serum lipid profile in Wistar rats. *Nutr Metab (Lond)*. 2017;14(1):31. doi:10.1186/s12986-017-0184-4
104. O'Malley T, Myette-Cote E, Durrer C, Little JP. Nutritional ketone salts increase fat oxidation but impair high-intensity exercise performance in healthy adult males. *Appl Physiol Nutr Metab*. 2017;42(10):1031-1035. doi:10.1139/apnm-2016-0641
105. Rodger S, Plews D, Laursen P, Driller M. The effects of an oral β-hydroxybutyrate supplement on exercise metabolism and cycling performance. *J Sci Cycl*. 2017;6(1 SE-):26-31. https://www.jsc-journal.com/index.php/JSC/article/view/304
106. Whitfield J, Burke LM, McKay AKA, et al. Acute Ketogenic Diet and Ketone Ester Supplementation Impairs Race Walk Performance. *Med Sci Sports Exerc*. 2021;53(4):776-784. doi:10.1249/MSS.0000000000002517
107. Srikanthan P, Karlamangla AS. Muscle Mass Index As a Predictor of Longevity in Older Adults. *Am J Med*. 2014;127:547-553. doi:10.1016/j.amjmed.2014.02.007
108. Ruiz JR, Sui X, Lobelo F, et al. Association between muscular strength and mortality in men: prospective cohort study. *Br Med J*. 2008;337:a439. doi:10.1136/bmj.a439
109. Rantanen T, Harris T, Leveille SG, et al. *Muscle Strength and Body Mass Index as Long-Term Predictors of Mortality in Initially Healthy Men*. Vol 55.; 2000.
110. Gariballa S, Alessa A. Impact of poor muscle strength on clinical and service

outcomes of older people during both acute illness and after recovery. *BMC Geriatr*. 2017;17(1). doi:10.1186/s12877-017-0512-6
111. Celis-Morales CA, Welsh P, Lyall DM, et al. Associations of grip strength with cardiovascular, respiratory, and cancer outcomes and all cause mortality: Prospective cohort study of half a million UK Biobank participants. *BMJ*. 2018;361. doi:10.1136/bmj.k1651
112. Nahin RL, Barnes PM, Stussman BJ. Expenditures on complementary health approaches: United States, 2012. *Natl Health Stat Report*. 2016;2016(95).
113. Cermak NM, Res PT, de Groot LC, Saris WH, van Loon LJ. Protein supplementation augments the adaptive response of skeletal muscle to resistance-type exercise training: a meta-analysis. *Am J Clin Nutr*. 2012;96:1454-1464. doi:10.3945/ajcn.112.037556
114. Baar K, Esser K. Phosphorylation of p70(S6k) correlates with increased skeletal muscle mass following resistance exercise. *Am J Physiol*. 1999;276:C120-C127.
115. Hong S, Zhao B, Lombard DB, Fingar DC, Inoki K. Cross-talk between sirtuin and mammalian target of rapamycin complex 1 (mTORC1) signaling in the regulation of S6 kinase 1 (S6K1) phosphorylation. *J Biol Chem*. 2014;289(19):13132-13141. doi:10.1074/jbc.M113.520734
116. Choudhary C, Kumar C, Gnad F, et al. Lysine acetylation targets protein complexes and co-regulates major cellular functions. *Science (80-)*. 2009;325(5942):834-840. doi:10.1126/science.1175371
117. Dickinson JM, Fry CS, Drummond MJ, et al. Mammalian Target of Rapamycin Complex 1 Activation Is Required for the Stimulation of Human Skeletal Muscle Protein Synthesis by Essential Amino Acids. *J Nutr*. 2011;141(5):856-862. doi:10.3945/jn.111.139485
118. Drummond MJ, Fry CS, Glynn EL, et al. Rapamycin administration in humans blocks the contraction-induced increase in skeletal muscle protein synthesis. *J Physiol*. 2009;587(7):1535-1546. doi:10.1113/jphysiol.2008.163816
119. Damas F, Phillips SM, Libardi CA, et al. Resistance training-induced changes in integrated myofibrillar protein synthesis are related to hypertrophy only after attenuation of muscle damage. *J Physiol*. 2016;594(18):5209-5222. doi:10.1113/JP272472
120. Hamilton DL, Philp A, MacKenzie MG, et al. Molecular brakes regulating mTORC1 activation in skeletal muscle following synergist ablation. *Am J Physiol - Endocrinol Metab*. 2014;307(4). doi:10.1152/ajpendo.00674.2013
121. Solomon JM, Pasupuleti R, Xu L, et al. Inhibition of SIRT1 catalytic activity increases p53 acetylation but does not alter cell survival following DNA damage. *Mol Cell Biol*. 2006;26(1):28-38. doi:10.1128/MCB.26.1.28-38.2006
122. Muth V, Nadaud S, Grummt I, Voit R. Acetylation of TAFI68, a subunit of TIF-IB/SL1, activates RNA polymerase I transcription. *EMBO J*. 2001;20(6):1353-1362. doi:10.1093/emboj/20.6.1353
123. Kirby TJ, Lee JD, England JH, et al. Blunted hypertrophic response in aged skeletal muscle is associated with decreased ribosome biogenesis. *J Appl Physiol*. 2015;119:321-327. doi:10.1152/japplphysiol.00296.2015.-The
124. Pandey KB, Rizvi SI. Plant polyphenols as dietary antioxidants in human health and disease. *Oxid Med Cell Longev*. 2009;2(5):270-278.

doi:10.4161/oxim.2.5.9498
125. Xiao S, Zhang M, Liang Y, Wang D. Celastrol synergizes with oral nifedipine to attenuate hypertension in preeclampsia: a randomized, placebo-controlled, and double blinded trial. *J Am Soc Hypertens*. 2017;11(9):598-603. doi:10.1016/j.jash.2017.07.004
126. Taub PR, Ramirez-Sanchez I, Ciaraldi TP, et al. Perturbations in skeletal muscle sarcomere structure in patients with heart failure and type 2 diabetes: Restorative effects of (-)-epicatechinrich cocoa. *Clin Sci*. 2013;125(8):383-389. doi:10.1042/CS20130023
127. Hodgson AB, Randell RK, Mahabir-Jagessar-T K, et al. Acute effects of green tea extract intake on exogenous and endogenous metabolites in human plasma. *J Agric Food Chem*. 2014;62(5):1198-1208. doi:10.1021/jf404872y
128. Jorgenson KW, Hornberger TA. The overlooked role of fiber length in mechanical load-induced growth of skeletal muscle. *Exerc Sport Sci Rev*. 2019;47(4):258-259. doi:10.1249/JES.0000000000000198
129. LIEW CC, GORNALL AG. Acetylation of Ribosomal Proteins in Regenerating Rat Liver. *Biochem Soc Trans*. 1973;1(4):994-995. doi:10.1042/bst0010994
130. Yang Y, Cimen H, Han MJ, et al. NAD+-dependent deacetylase SIRT3 regulates mitochondrial protein synthesis by deacetylation of the ribosomal protein MRPL10. *J Biol Chem*. 2010;285(10):7417-7429. doi:10.1074/jbc.M109.053421
131. Fenton TR, Gwalter J, Cramer R, Gout IT. S6K1 is acetylated at lysine 516 in response to growth factor stimulation. *Biochem Biophys Res Commun*. 2010;398(3):400-405. doi:10.1016/j.bbrc.2010.06.081
132. Fenton TR, Gwalter J, Ericsson J, Gout IT. Histone acetyltransferases interact with and acetylate p70 ribosomal S6 kinases in vitro and in vivo. *Int J Biochem Cell Biol*. 2010;42(2):359-366. doi:10.1016/j.biocel.2009.11.022
133. Das F, Maity S, Ghosh-Choudhury N, Kasinath BS, Choudhury GG. Deacetylation of S6 kinase promotes high glucose-induced glomerular mesangial cell hypertrophy and matrix protein accumulation. *J Biol Chem*. 2019;294(24):9440-9460. doi:10.1074/jbc.RA118.007023
134. Livak KJ, Schmittgen TD. Analysis of relative gene expression data using real-time quantitative PCR and the 2-ΔΔCT method. *Methods*. 2001;25(4):402-408. doi:10.1006/meth.2001.1262
135. Hatori M, Vollmers C, Zarrinpar A, et al. Time-Restricted Feeding without Reducing Caloric Intake Prevents Metabolic Diseases in Mice Fed a High-Fat Diet. *Cell Metab*. 2012;15(6):848-860. doi:https://doi.org/10.1016/j.cmet.2012.04.019
136. Weir HJ, Yao P, Huynh FK, et al. Dietary Restriction and AMPK Increase Lifespan via Mitochondrial Network and Peroxisome Remodeling. *Cell Metab*. 2017;26(6):884-896.e5. doi:10.1016/j.cmet.2017.09.024
137. Lanza IR, Zabielski P, Klaus KA, et al. Chronic caloric restriction preserves mitochondrial function in senescence without increasing mitochondrial biogenesis. *Cell Metab*. 2012;16(6):777-788. doi:10.1016/j.cmet.2012.11.003
138. Holloszy JO, Oscai LB. Effect of exercise on alpha-glycerophosphate dehydrogenase activity in skeletal muscle. *Arch Biochem Biophys*. 1969;130(1):653-656. doi:10.1016/0003-9861(69)90083-6

139. Johnson RH, Walton JL, Krebs HA, Williamson DH. POST-EXERCISE KETOSIS. *Lancet*. 1969;294(7635):1383-1385. doi:10.1016/S0140-6736(69)90931-3
140. Gregoretti I V, Lee Y-M, Goodson H V. Molecular evolution of the histone deacetylase family: functional implications of phylogenetic analysis. *J Mol Biol*. 2004;338(1):17-31. doi:10.1016/j.jmb.2004.02.006
141. Shimazu T, Hirschey MD, Newman J, et al. Suppression of oxidative stress by β-hydroxybutyrate, an endogenous histone deacetylase inhibitor. *Science (80-)*. 2013;339(6116):211-214. doi:10.1126/science.1227166
142. Barrea L, de Alteriis G, Muscogiuri G, et al. Impact of a Very Low-Calorie Ketogenic Diet (VLCKD) on Changes in Handgrip Strength in Women with Obesity. *Nutrients*. 2022;14(19). doi:10.3390/nu14194213
143. Lovering RM, De Deyne PG. Contractile function, sarcolemma integrity, and the loss of dystrophin after skeletal muscle eccentric contraction-induced injury. *Am J Physiol Cell Physiol*. 2004;286(2):C230-8. doi:10.1152/ajpcell.00199.2003
144. Manfredi TG, Fielding RA, O'Reilly KP, Meredith CN, Lee HY, Evans WJ. Plasma creatine kinase activity and exercise-induced muscle damage in older men. *Med Sci Sports Exerc*. 1991;23(9):1028-1034.
145. Bloch RJ, Reed P, O'Neill A, et al. Costameres mediate force transduction in healthy skeletal muscle and are altered in muscular dystrophies. *J Muscle Res Cell Motil*. 2004;25(8):590-592.
146. Worton R. Muscular dystrophies: diseases of the dystrophin-glycoprotein complex. *Science*. 1995;270(5237):755-756. doi:10.1126/science.270.5237.755
147. Ramaswamy KS, Palmer ML, van der Meulen JH, et al. Lateral transmission of force is impaired in skeletal muscles of dystrophic mice and very old rats. *J Physiol*. 2011;589(Pt 5):1195-1208. doi:10.1113/jphysiol.2010.201921
148. Smith LR, Barton ER. SMASH – semi-automatic muscle analysis using segmentation of histology: a MATLAB application. *Skelet Muscle*. 2014;4(1):21. doi:10.1186/2044-5040-4-21
149. Nakao R, Abe T, Yamamoto S, Oishi K. Ketogenic diet induces skeletal muscle atrophy via reducing muscle protein synthesis and possibly activating proteolysis in mice. *Sci Rep*. 2019;9(1):19652. doi:10.1038/s41598-019-56166-8
150. Van der Auwera I, Wera S, Van Leuven F, Henderson ST. A ketogenic diet reduces amyloid beta 40 and 42 in a mouse model of Alzheimer's disease. *Nutr Metab (Lond)*. 2005;2:28. doi:10.1186/1743-7075-2-28
151. Ruskin DN, Murphy MI, Slade SL, Masino SA. Ketogenic diet improves behaviors in a maternal immune activation model of autism spectrum disorder. *PLoS One*. 2017;12(2):e0171643. doi:10.1371/journal.pone.0171643
152. Pathak SJ, Zhou Z, Steffen D, et al. 2-month ketogenic diet preferentially alters skeletal muscle and augments cognitive function in middle aged female mice. *Aging Cell*. 2022;21(10):e13706. doi:10.1111/acel.13706
153. Hardie DG, Pan DA. Regulation of fatty acid synthesis and oxidation by the AMP-activated protein kinase. *Biochem Soc Trans*. 2002;30(6):1064-1070. doi:10.1042/bst0301064
154. Jäger S, Handschin C, St.-Pierre J, Spiegelman BM. AMP-activated protein kinase (AMPK) action in skeletal muscle via direct phosphorylation of PGC-1α. *Proc Natl Acad Sci*. 2007;104(29):12017 LP - 12022.

doi:10.1073/pnas.0705070104
155. Parker BA, Walton CM, Carr ST, et al. β-Hydroxybutyrate Elicits Favorable Mitochondrial Changes in Skeletal Muscle. *Int J Mol Sci*. 2018;19(8). doi:10.3390/ijms19082247
156. Levine B, Kroemer G. Autophagy in the Pathogenesis of Disease. *Cell*. 2008;132(1):27-42. doi:https://doi.org/10.1016/j.cell.2007.12.018
157. Mizushima N, Levine B, Cuervo AM, Klionsky DJ. Autophagy fights disease through cellular self-digestion. *Nature*. 2008;451(7182):1069-1075. doi:10.1038/nature06639
158. Masiero E, Agatea L, Mammucari C, et al. Autophagy is required to maintain muscle mass. *Cell Metab*. 2009;10(6):507-515. doi:10.1016/j.cmet.2009.10.008
159. Bai H, Kang P, Hernandez AM, Tatar M. Activin signaling targeted by insulin/dFOXO regulates aging and muscle proteostasis in Drosophila. *PLoS Genet*. 2013;9(11):e1003941. doi:10.1371/journal.pgen.1003941
160. Chang JT, Kumsta C, Hellman AB, Adams LM, Hansen M. Spatiotemporal regulation of autophagy during Caenorhabditis elegans aging. Zhang H, ed. *Elife*. 2017;6:e18459. doi:10.7554/eLife.18459
161. Salminen A, Vihko V. Autophagic response to strenuous exercise in mouse skeletal muscle fibers. *Virchows Arch B Cell Pathol Incl Mol Pathol*. 1984;45(1):97-106. doi:10.1007/BF02889856
162. Baar K, Wende AR, Jones TE, et al. Adaptations of skeletal muscle to exercise: Rapid increase in the transcriptional coactivator PGC-1. *FASEB J*. 2002;16(14). doi:10.1096/fj.02-0367com
163. Garcia-Valles R, Gomez-Cabrera MC, Rodriguez-Mañas L, et al. Life-long spontaneous exercise does not prolong lifespan but improves health span in mice. *Longev Heal*. 2013;2(1):14. doi:10.1186/2046-2395-2-14
164. Mandolesi L, Polverino A, Montuori S, et al. Effects of Physical Exercise on Cognitive Functioning and Wellbeing: Biological and Psychological Benefits. *Front Psychol*. 2018;9:509. doi:10.3389/fpsyg.2018.00509
165. Meley D, Bauvy C, Houben-Weerts JHPM, et al. AMP-activated protein kinase and the regulation of autophagic proteolysis. *J Biol Chem*. 2006;281(46):34870-34879. doi:10.1074/jbc.M605488200
166. Høyer-Hansen M, Bastholm L, Szyniarowski P, et al. Control of macroautophagy by calcium, calmodulin-dependent kinase kinase-beta, and Bcl-2. *Mol Cell*. 2007;25(2):193-205. doi:10.1016/j.molcel.2006.12.009
167. Egan DF, Shackelford DB, Mihaylova MM, et al. Phosphorylation of ULK1 (hATG1) by AMP-Activated Protein Kinase Connects Energy Sensing to Mitophagy. *Science (80-)*. 2011;331(6016):456-461. doi:10.1126/science.1196371
168. Goljanek-Whysall K, Soriano-Arroquia A, McCormick R, Chinda C, McDonagh B. miR-181a regulates p62/SQSTM1, parkin, and protein DJ-1 promoting mitochondrial dynamics in skeletal muscle aging. *Aging Cell*. 2020;19(4):e13140. doi:https://doi.org/10.1111/acel.13140
169. Yeo D, Kang C, Gomez-Cabrera MC, Vina J, Ji LL. Intensified mitophagy in skeletal muscle with aging is downregulated by PGC-1alpha overexpression in vivo. *Free Radic Biol Med*. 2019;130:361-368.

doi:https://doi.org/10.1016/j.freeradbiomed.2018.10.456
170. Chen CCW, Erlich AT, Crilly MJ, Hood DA. Parkin is required for exercise-induced mitophagy in muscle: impact of aging. *Am J Physiol Metab*. 2018;315(3):E404-E415. doi:10.1152/ajpendo.00391.2017
171. García-Prat L, Martínez-Vicente M, Perdiguero E, et al. Autophagy maintains stemness by preventing senescence. *Nature*. 2016;529(7584):37-42. doi:10.1038/nature16187
172. Gaugler M, Brown A, Merrell E, DiSanto-Rose M, Rathmacher JA, Reynolds TH. PKB signaling and atrogene expression in skeletal muscle of aged mice. *J Appl Physiol*. 2011;111(1):192-199. doi:10.1152/japplphysiol.00175.2011
173. Hughes DC, Marcotte GR, Baehr LM, et al. Alterations in the muscle force transfer apparatus in aged rats during unloading and reloading: impact of microRNA-31. *J Physiol*. 2018;596(14):2883-2900. doi:10.1113/JP275833
174. Hughes DC, Marcotte GR, Marshall AG, et al. Age-related Differences in Dystrophin: Impact on Force Transfer Proteins, Membrane Integrity, and Neuromuscular Junction Stability. *J Gerontol A Biol Sci Med Sci*. 2017;72(5):640-648. doi:10.1093/gerona/glw109
175. Metter EJ, Talbot LA, Schrager M, Conwit R. *Skeletal Muscle Strength as a Predictor of All-Cause Mortality in Healthy Men*. Vol 57.; 2002. https://academic.oup.com/biomedgerontology/article/57/10/B359/629964
176. Atamna H, Frey WH 2nd. Mechanisms of mitochondrial dysfunction and energy deficiency in Alzheimer's disease. *Mitochondrion*. 2007;7(5):297-310. doi:10.1016/j.mito.2007.06.001
177. Konopka AR, Sreekumaran Nair K. Mitochondrial and skeletal muscle health with advancing age. *Mol Cell Endocrinol*. 2013;379(1-2):19-29. doi:10.1016/j.mce.2013.05.008
178. Watson K, Baar K. mTOR and the health benefits of exercise. *Semin Cell Dev Biol*. 2014;36:130-139. doi:10.1016/j.semcdb.2014.08.013
179. Baar K, Wende AR, Jones TE, et al. Adaptations of skeletal muscle to exercise: rapid increase in the transcriptional coactivator PGC-1. *FASEB J Off Publ Fed Am Soc Exp Biol*. 2002;16(14):1879-1886. doi:10.1096/fj.02-0367com
180. Sleiman SF, Henry J, Al-Haddad R, et al. Exercise promotes the expression of brain derived neurotrophic factor (BDNF) through the action of the ketone body β-hydroxybutyrate. Elmquist JK, ed. *Elife*. 2016;5:e15092. doi:10.7554/eLife.15092
181. Edwards C, Canfield J, Copes N, Rehan M, Lipps D, Bradshaw PC. D-beta-hydroxybutyrate extends lifespan in C. elegans. *Aging (Albany NY)*. 2014;6(8):621-644. doi:10.18632/aging.100683
182. Holcomb LE, O'Neill CC, DeWitt EA, Kolwicz SCJ. The Effects of Fasting or Ketogenic Diet on Endurance Exercise Performance and Metabolism in Female Mice. *Metabolites*. 2021;11(6). doi:10.3390/metabo11060397
183. Wu X, Ding J, Xu X, et al. Ketogenic diet compromises vertebral microstructure and biomechanical characteristics in mice. *J Bone Miner Metab*. 2019;37(6):957-966. doi:10.1007/s00774-019-01002-2
184. Pissios P, Hong S, Kennedy AR, Prasad D, Liu F-F, Maratos-Flier E. Methionine and choline regulate the metabolic phenotype of a ketogenic diet. *Mol Metab*. 2013;2(3):306-313. doi:10.1016/j.molmet.2013.07.003

185. Mercken EM, Carboneau BA, Krzysik-Walker SM, de Cabo R. Of mice and men: The benefits of caloric restriction, exercise, and mimetics. *Ageing Res Rev*. 2012;11(3):390-398. doi:https://doi.org/10.1016/j.arr.2011.11.005
186. Weindruch R, Keenan KP, Carney JM, et al. Caloric Restriction Mimetics: Metabolic Interventions. *Journals Gerontol Ser A*. 2001;56(suppl_1):20-33. doi:10.1093/gerona/56.suppl_1.20
187. Lill NL, Grossman SR, Ginsberg D, DeCaprio J, Livingston DM. Binding and modulation of p53 by p300/CBP coactivators. *Nature*. 1997;387(6635):823-827. doi:10.1038/42981
188. Tapscott SJ. The circuitry of a master switch: Myod and the regulation of skeletal muscle gene transcription. *Development*. 2005;132(12):2685-2695. doi:10.1242/dev.01874
189. Fukui S, Schwarcz R, Rapoport SI, Takada Y, Smith QR. Blood-brain barrier transport of kynurenines: implications for brain synthesis and metabolism. *J Neurochem*. 1991;56(6):2007-2017. doi:10.1111/j.1471-4159.1991.tb03460.x
190. Cervenka I, Agudelo LZ, Ruas JL. Kynurenines: Tryptophan's metabolites in exercise, inflammation, and mental health. *Science*. 2017;357(6349). doi:10.1126/science.aaf9794
191. Guillemin GJ. Quinolinic acid, the inescapable neurotoxin. *FEBS J*. 2012;279(8):1356-1365. doi:https://doi.org/10.1111/j.1742-4658.2012.08485.x
192. Ruskin DN, Ross JL, Kawamura Jr M, Ruiz TL, Geiger JD, Masino SA. A ketogenic diet delays weight loss and does not impair working memory or motor function in the R6/2 1J mouse model of Huntington's disease. *Physiol Behav*. 2011;103(5):501-507. doi:10.1016/j.physbeh.2011.04.001
193. Levenson JM, O'Riordan KJ, Brown KD, Trinh MA, Molfese DL, Sweatt JD. Regulation of histone acetylation during memory formation in the hippocampus. *J Biol Chem*. 2004;279(39):40545-40559. doi:10.1074/jbc.M402229200
194. Pathak SJ, Baar K. Ketogenic Diets and Mitochondrial Function: Benefits for Aging But Not for Athletes. *Exerc Sport Sci Rev*. 2023;51(1). https://journals.lww.com/acsm-essr/Fulltext/2023/01000/Ketogenic_Diets_and_Mitochondrial_Function_.4.aspx
195. Srikanthan P, Karlamangla AS. Muscle mass index as a predictor of longevity in older adults. *Am J Med*. 2014;127(6):547-553. doi:10.1016/j.amjmed.2014.02.007
196. Zhou P, Zhang Y, Ma Q, et al. Interrogating translational efficiency and lineage-specific transcriptomes using ribosome affinity purification. *Proc Natl Acad Sci*. 2013;110(38):15395-15400. doi:10.1073/pnas.1304124110
197. Shimazu T, Hirschey MD, Newman J, et al. Suppression of oxidative stress by β-hydroxybutyrate, an endogenous histone deacetylase inhibitor. *Science*. 2013;339(6116):211-214. doi:10.1126/science.1227166
198. Langer HT, Mossakowski AA, Willis BJ, et al. Generation of desminopathy in rats using CRISPR-Cas9. *J Cachexia Sarcopenia Muscle*. 2020;11(5):1364-1376. doi:10.1002/jcsm.12619
199. Pissios P, Hong S, Kennedy AR, Prasad D, Liu FF, Maratos-Flier E. Methionine and choline regulate the metabolic phenotype of a ketogenic diet. *Mol Metab*. 2013;2(3):306-313. doi:10.1016/j.molmet.2013.07.003
200. Steiner J, Walter M, Gos T, et al. Severe depression is associated with increased

microglial quinolinic acid in subregions of the anterior cingulate gyrus: Evidence for an immune-modulated glutamatergic neurotransmission? *J Neuroinflammation*. 2011;8(1):94. doi:10.1186/1742-2094-8-94
201. la Cruz VP, Carrillo-Mora P, Santamaría A. Quinolinic Acid, an Endogenous Molecule Combining Excitotoxicity, Oxidative Stress and Other Toxic Mechanisms. *Int J Tryptophan Res*. 2012;5:1-8.
202. Sarvey JM, Burgard EC, Decker G. Long-term potentiation: studies in the hippocampal slice. *J Neurosci Methods*. 1989;28(1-2):109-124. doi:10.1016/0165-0270(89)90016-2